Chapter

4

Cell Coverage for Signal and Traffic

4.1 General Introduction

Cell coverage can be based on signal coverage or on traffic coverage. Signal coverage can be predicted by coverage prediction models and is usually applied to a start-up system. The task is to cover the whole area with a minimum number of cell sites. Since 100 percent cell coverage of an area is not possible, the cell sites must be engineered so that the holes are located in the no-traffic locations. The prediction model is a point-to-point model which is discussed in this chapter. We have to examine the service area as occurring in one of the following environments:

Human-made structures

In an open area

In a suburban area

In an urban area

Natural terrains

Over flat terrain

Over hilly terrain

Over water

Through foliage areas

The results generated from the prediction model will differ depending on which service area is used.

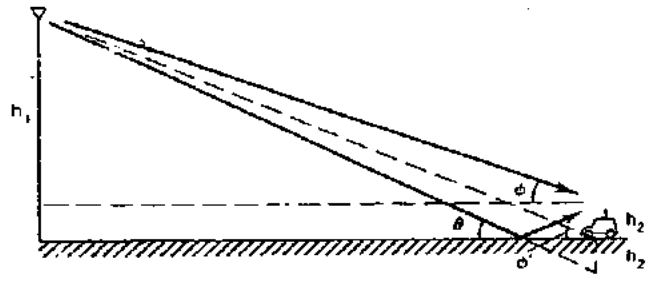

θ is the incident angle
ϕ is the elevation angle

Figure 4.1 A coordinate sketch in a flat terrain.

There are many field-strength prediction models in the literature.[1–28] They all provide more or less an area-to-area prediction. As long as 68 percent of the predicted values from a model are within 6 to 8 dB (one standard deviation) of their corresponding measured value, the model is considered a good one. However, we cannot use area-to-area prediction models for cellular system design because of the large uncertainty of the prediction.

The model being introduced here is the point-to-point prediction model which would provide a standard deviation from the predicted value of less than 3 dB. An explanation of this model appears in Refs. 23, 24, and 41. Many tools can be developed based upon this model, such as cell-site choosing, interference reduction, and traffic handling.

4.1.1 Ground incident angle and ground elevation angle

The ground incident angle and the ground elevation angle over a communication link are described as follows. The ground incident angle θ is the angle of wave arrival incidently pointing to the ground as shown in Fig. 4.1. The ground elevation angle ϕ is the angle of wave arrival at the mobile unit as shown in Fig. 4.1.

Example 4.1 In a mobile radio environment, the average cell-site antenna height is about 50 m, the mobile antenna height is about 3 m, and the communication path length is 5 km. The incident angle is (see Fig. 4.1)

$$\theta = \tan^{-1}\frac{50\text{ m} + 3\text{ m}}{5\text{ km}} = 0.61°$$

The elevation angle at the antenna of the mobile unit is

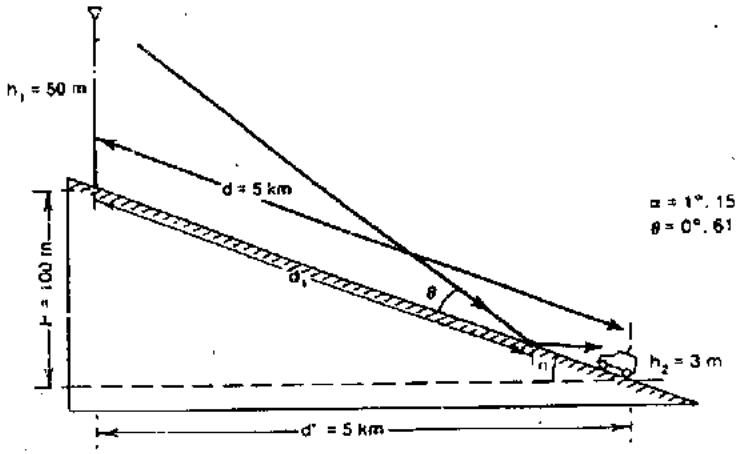

Figure 4.2 A coordinate sketch in a hilly terrain.

$$\phi = \tan^{-1}\frac{50\text{ m} - 3\text{ m}}{5\text{ km}} = 0.54°$$

The elevation angle at the location of the mobile unit is

$$\phi' = \tan^{-1}\frac{50\text{ m}}{5\text{ km}} = 0.57°$$

4.1.2 Ground reflection angle and reflection point

Based on Snell's law, the reflection angle and incident angle are the same. Since in graphical display we usually exaggerate the hilly slope and the incident angle by enlarging the vertical scale, as shown in Fig. 4.2, then as long as the actual hilly slope is less than 10°, the reflection point on a hilly slope can be obtained by following the same method as if the reflection point were on flat ground. Be sure that the two antennas (base and mobile) have been placed vertically, not perpendicular to the sloped ground. The reason is that the actual slope of the hill is usually very small and the vertical stands for two antennas are correct. The scale drawing in Fig. 4.2 is somewhat misleading; however, it provides a clear view of the situation.

Example 4.2 Let $h_1 = 50$ m, $h_2 = 3$ m, $d = 5$ km, and $H = 100$ m as shown in Fig. 4.2.

(a) Using the approximate method ($d \approx d' \approx 5$ km), the slope angle α of the hill is

$$\alpha = \tan^{-1}\frac{100\text{ m}}{5\text{ km}} = 1.14576°$$

the incident angle is

$$\theta = \tan^{-1}\frac{50\text{ m} + 3\text{ m}}{5\text{ km}} = 0.61$$

and the reflection point location from the cell-site antenna

$$d_1 = 50/\tan\theta = 4.717\text{ km}.$$

(*b*) Using the accurate method, the slope angle α of the hill is

$$\alpha = \tan^{-1}\frac{100\text{ m}}{\sqrt{(5\text{ km})^2 - (100\text{ m})^2}} = \tan^{-1}\frac{100}{4999} = 1.14599°$$

The incident angle θ and the reflection point location d_1 are the same as above.

4.2 Obtaining the Mobile Point-to-Point Model (Lee Model)

This mobile point-to-point model is obtained in three steps: (1) generate a standard condition, (2) obtain an area-to-area prediction model, (3) obtain a mobile point-to-point model using the area-to-area model as a base. The philosophy of developing this model is to try to separate two effects, one caused by the natural terrain contour and the other by the human-made structures, in the received signal strength.

4.2.1 A standard condition

To generate a standard condition and provide correction factors, we have used the standard conditions shown on the left side and the correction factors on the right side[10] of Table 4.1. The advantage of using these standard values is to obtain directly a predicted value in decibels above 1 mW expressed in dBM.

4.2.2 Obtain area-to-area prediction curves for human-made structures

The area-to-area prediction curves are different in different areas. In area-to-area prediction, all the areas are considered flat even though the data may be obtained from nonflat areas. The reason is that area-to-area prediction is an average process. The standard deviation of the average value indicates the degree of terrain roughness.

TABLE 4.1 Generating a Standard Condition

Standard condition	Correction factors*
At the Base Station	
Transmitted power P_t = 10 W (40 dBm)	$\alpha_1 = 10 \log \frac{P_t'}{10}$
Antenna height h_1 = 100 ft (30 m)	$\alpha_2 = 20 \log \frac{h_1'}{h_1}$
Antenna gain g_t = 6 dB/dipole	$\alpha_3 = g_{t2}' - 6$
At the Mobile Unit	
Antenna height, h_2 = 10 ft (3 m)	$\alpha_4 = 10 \log \frac{h_2'}{h_2}$
Antenna gain, g_m = 0 dB/dipole	$\alpha_5 = g_m'$

*All the parameters with primes are the new conditions.

Effect of the human-made structures. Since the terrain configuration of each city is different, and the human-made structure of each city is also unique, we have to find a way to separate these two. The way to factor out the effect due to the terrain configuration from the man-made structures is to work out a way to obtain the path loss curve for the area as if the area were flat, even if it is not. The path loss curve obtained on virtually flat ground indicates the effects of the signal loss due to solely human-made structures. This means that the different path loss curves obtained in each city show the different human-made structure in that city. To do this, we may have to measure signal strengths at those high spots and also at the low spots surrounding the cell sites, as shown in Fig. 4.3*a*. Then the average path loss slope (Fig. 4.3*b*), which is a combination of measurements from high spots and low spots along different radio paths in a general area, represents the signal received as if it is from a flat area affected only by a different local human-made structured environment. We are using 1-mi intercepts (or, alternatively, 1-km intercepts) as a starting point for obtaining the path loss curves.

Therefore, the differences in area-to-area prediction curves are due to the different man-made structures. We should realize that measurements made in urban areas are different from those made in suburban and open areas. The area-to-area prediction curve is obtained from the mean value of the measured data and used for future predictions in that area. Any area-to-area prediction model[1–28] can be used as a first step toward achieving the point-to-point prediction model.

One area-to-area prediction model which is introduced here[10] can be represented by two parameters. (1) the 1-mi (or 1-km) intercept point

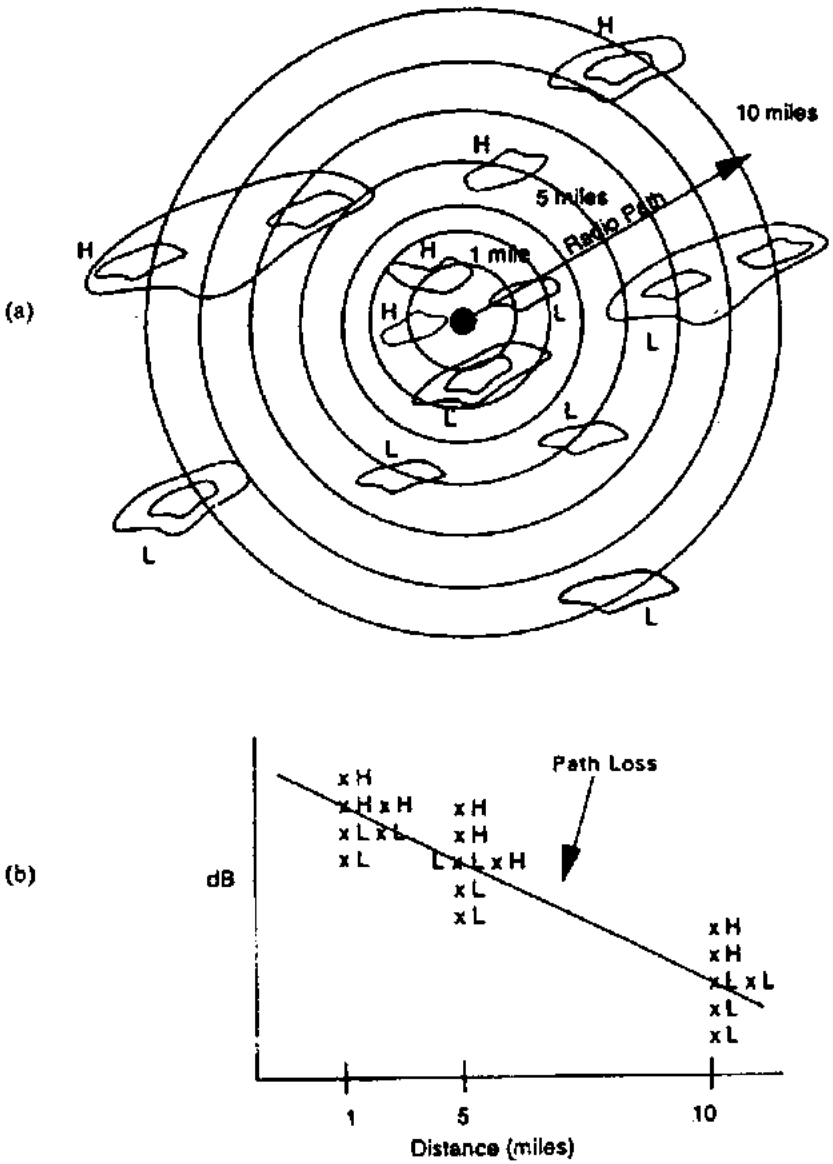

Figure 4.3 Propagation path loss curves for human-made structures. (*a*) For selecting measurement areas (*b*) path loss phenomenon.

and (2) the path-loss slope. The 1-mi intercept point is the power received at a distance of 1 mi from the transmitter. There are two general approaches to finding the values of the two parameters experimentally.

1. Compare an area of interest with an area of similar human-made structures which presents a curve such as that shown in Fig. 4.3c. The suburban area curve is a commonly used curve. Since all suburban areas in the United States look alike, we can use this curve for all suburban areas. If the area is not suburban but is similar to the city of Newark, then the curve for Newark should be used.

2. If the human-made structures of a city are different from the cities listed in Fig. 4.3c, a simple measurement should be carried out. Set up a transmitting antenna at the center of a general area. As long as the building height is comparable to the others in the area, the antenna location is not critical. Take six or seven measured data points around the 1-mi intercept and around the 10-mi boundary based on the high and low spots. Then compute the average of the 1 mi data points and of the 10 mi data points. By connecting the two values, the path-loss slope can be obtained. If the area is very hilly, then the data points measured at a given distance from the base station in different locations can be far apart. In this case, we may take more measured data points to obtain the average path-loss slope.

If the terrain of the hilly area is generally sloped, then we have to convert the data points that were measured on the sloped terrain to a fictitiously flat terrain in that area. The conversion is based on the effective antenna-height gain as[29]

$$\Delta G = \text{effective antenna-height gain} = 20 \log \frac{h_e}{h_1} \qquad (4.2\text{-}1)$$

where h_1 is the actual height and h_e is the effective antenna height at either the 1- or 10-mi locations. The method for obtaining h_e is shown in the following section.

3. An explanation of the path-loss phenomenon is as follows. The plotted curves shown in Fig. 4.3c have different 1-mi intercepts and different slopes. The explanation can be seen in Fig. 4.3*d*. When the base station antenna is located in the city, then the 1-mi intercept could be very low and the slope is flattened out, as shown by Tokey's curve. When the base station is located outside the city, the intercept could be much higher and the slope is deeper, as shown by the Newark curve. When the structures are uniformly distributed, depending on the density (average separation between buildings) s, the 1-mi intercept could be high or low, but the slope may also keep at 40 dB/dec.

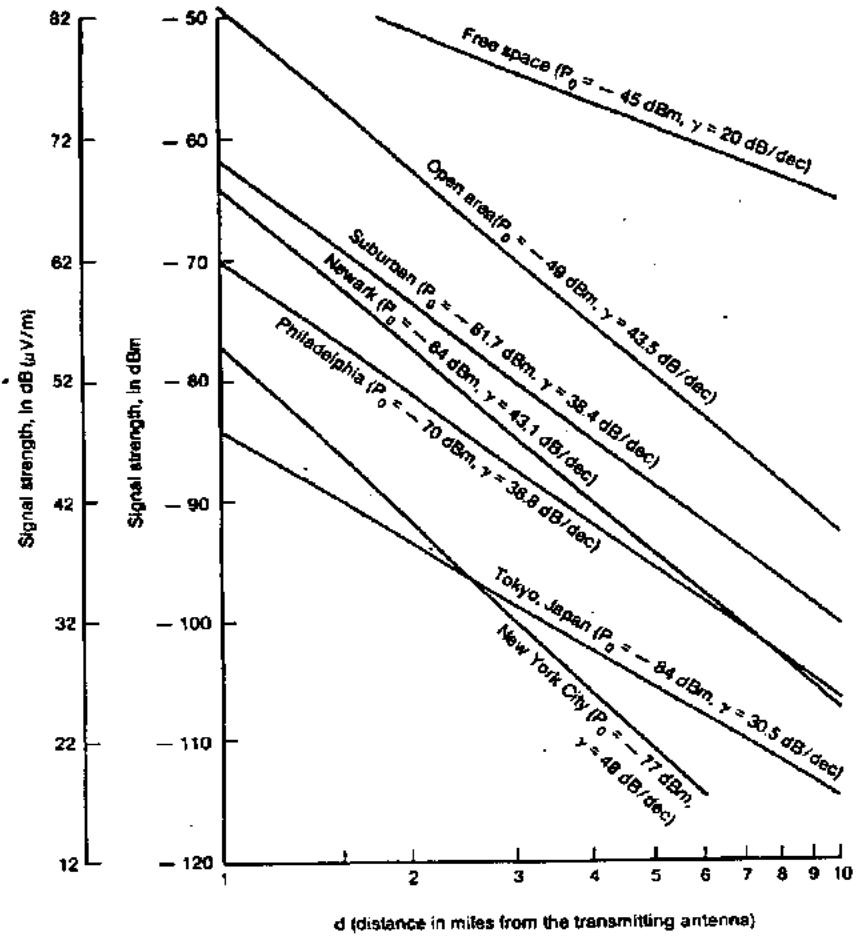

Figure 4.3 (c) Propagation path loss in different cities.

4.2.3 The phase difference between a direct path and a ground-reflected path

Based on a direct path and a ground-reflected path (see Fig. 4.4),

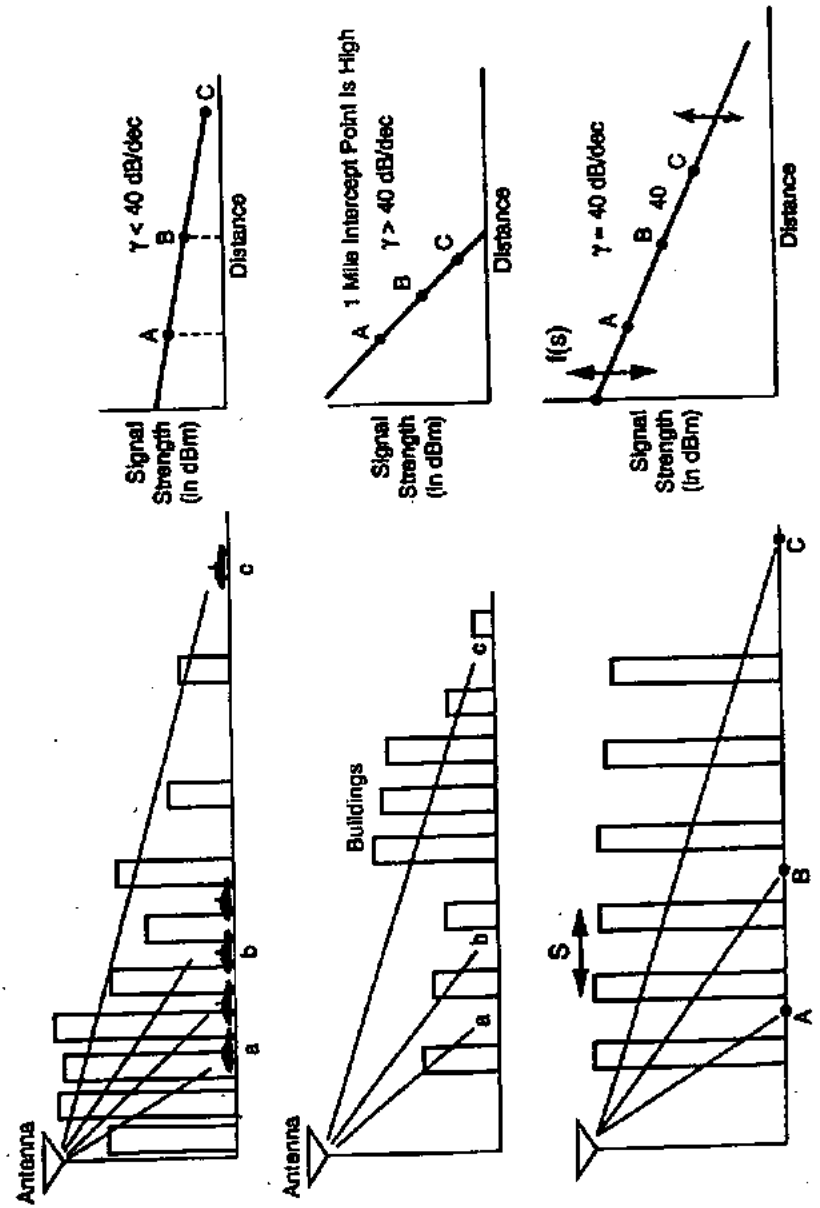

Figure 4.3 (*d*) Explanation of the path-loss phenomenon.

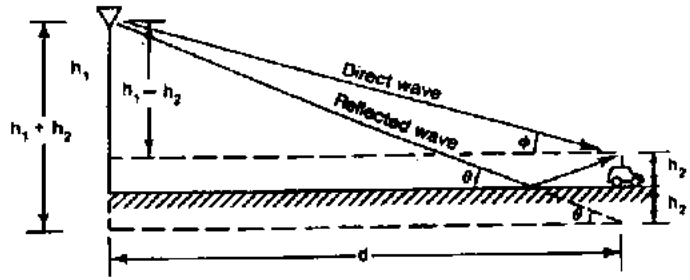

Figure 4.4 A simple model.

$$P_r = P_0 \left(\frac{1}{4\pi d/\lambda}\right)^2 \left|1 + a_v e^{j\Delta\phi}\right|^2 \tag{4.2-2}$$

where a_v = the reflection coefficient
$\Delta\phi$ = the phase difference between a direct path and a reflected path
P_0 = the transmitted power
d = the distance
λ = the wavelength

Equation (4.2-2) indicates a two-wave model which is used to understand the path-loss phenomenon in a mobile radio environment. It is not the model for analyzing the multipath fading phenomenon. In a mobile environemnt $a_v = -1$ because of the small incident angle of the ground wave caused by a relatively low cell-site antenna height.

Thus

$$P_r = P_0 \left(\frac{1}{4\pi d/\lambda}\right)^2 \left|1 - \cos\Delta\phi - j\sin\Delta\phi\right|^2$$

$$= P_0 \frac{2}{(4\pi d/\lambda)^2}(1 - \cos\Delta\phi) = P_0 \frac{4}{(4\pi d/\lambda)^2}\sin^2\frac{\Delta\phi}{2} \tag{4.2-3}$$

where
$$\Delta\phi = \beta\,\Delta d \tag{4.2-4}$$

and Δd is the difference, $\Delta d = d_1 - d_0$, from Fig. 4.4.

$$d_1 = \sqrt{(h_1 + h_2)^2 + d^2} \tag{4.2-5}$$

and
$$d_2 = \sqrt{(h_1 - h_2)^2 + d^2} \tag{4.2-6}$$

Since Δd is much smaller than either d_1 or d_2,

$$\Delta\phi = \beta\,\Delta d \approx \frac{2\pi}{\lambda}\frac{2h_1h_2}{d} \tag{4.2-7}$$

Then the received power of Eq. (4.2-3) becomes

$$P_r = P_0\frac{\lambda^2}{(4\pi)^2d^2}\sin^2\frac{4\pi h_1h_2}{\lambda d} \tag{4.2-8}$$

If $\Delta\phi$ is less than 0.6 rad, then $\sin(\Delta\phi/2) \approx \Delta\phi/2$, $\cos(\Delta\phi/2) \approx 1$ and Eq. (4.2-8) simplifies to

$$P_r = P_0\frac{4}{16\pi^2(d/\lambda)^2}\left(\frac{2\pi h_1h_2}{\lambda d}\right)^2 = P_0\left(\frac{h_1h_2}{d^2}\right)^2 \tag{4.2-9}$$

From Eq. (4.2-9), we can deduce two relationships as follows:

$$\Delta P = 40\log\frac{d_1}{d_2} \qquad \text{(a 40 dB/dec path loss)} \tag{4.2-10a}$$

$$\Delta G = 20\log\frac{h'_1}{h_1} \qquad \text{(an antenna height gain of 6 dB/oct)} \tag{4.2-10b}$$

where ΔP is the power difference in decibels between two different path lengths and ΔG is the gain (or loss) in decibels obtained from two different antenna heights at the cell site. From these measurements, the gain from a mobile antenna height is only 3 dB/oct, which is different from the 6 dB/oct for h'_1 shown in Eq. (4.2-10*b*). Then

$$\Delta G' = 10\log\frac{h'_2}{h_2} \qquad \text{(an antenna-height gain of 3 dB/oct)} \tag{4.2-10c}$$

Example 4.3 The distance d = 8 km. The antenna height at the cell site is 30 m, and at the mobile unit it is 3 m. Then the phase difference at 850 MHz is $\beta \cdot \Delta d$, or 0.4 rad, which is less than 0.6 rad. Therefore, Eq. (4.2-9) can be applied.

4.2.4 Why there is a constant standard deviation along a path-loss curve

When plotting signal strengths at any given radio-path distance, the deviation from predicted values is approximately 8 dB.[10,12] This standard deviation of 8 dB is roughly true in many different areas. The explanation is as follows. When a line-of-sight path exists, both the direct wave path and reflected wave path are created and are strong (see Fig. 4.2). When an out-of-sight path exists, both the direct wave path and the reflected wave path are weak. In either case, according to the theoretical model, the 40-dB/dec path-loss slope applies. The

difference between these two conditions is the 1-mi intercept (or 1-km intercept) point. It can be seen that in the open area, the 1-mi intercept is high. In the urban area, the 1-mi intercept is low. The standard deviation obtained from the measured data remains the same along the different path-loss curves regardless of environment.

Support for the above argument can also be found from the observation that the standard deviation obtained from the measured data along the predicted path-loss curve is approximately 8 dB. The explanation is that at a distance from the cell site, some mobile unit radio paths are line-of-sight, some are partial line-of-sight, and some are out-of-sight. Thus the received signals are strong, normal, and weak, respectively. At any distance, the above situations prevail. If the standard deviation is 8 dB at one radio-path distance, the same 8 dB will be found at any distance. Therefore a standard deviation of 8 dB is always found along the radio path as shown in Fig. 4.5. The standard deviation of 8 dB from the measured data near the cell site is due mainly to the close-in buildings around the cell site. The same standard deviation from the measured data at a distant location is due to the great variation along different radio paths.

4.2.5 The straight-line path-loss slope with confidence

As we described earlier, the path-loss curves are obtained from many different runs at many different areas. As long as the distances of the radio path from the cell site to the mobile unit are the same in different runs, the signal strength data measured at that distance would be used to calculate the mean value for the path loss at that distance. In the experimental data, the path-loss deviation is 8 dB across the distance from 1.6 to 15 km (1 to 10 mi) where the general terrain contours are not generally flat. Figure 4.5 depicts this. The path-loss curve is γ. The received power can be expressed as

$$P_r = P_0 - \gamma \log \frac{r}{r_0} \tag{4.2-11}$$

The slope γ is different in different areas, but it is always a straight line in a log scale. If $\gamma = 20$ is a free-space path loss, $\gamma = 40$ is a mobile path loss.

Confidence level.[31] A confidence level can only be applied to the path-loss curve when the standard deviation σ is known. In American suburban areas, the standard deviation $\sigma = 8$ dB. The values at any given distance over the radio path are concentrated close to the mean and

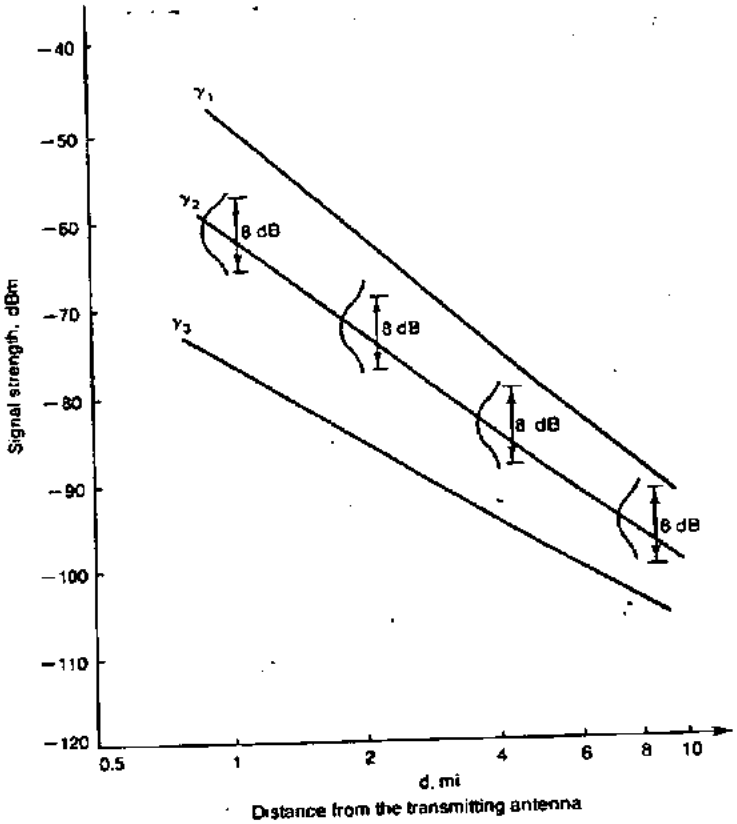

Figure 4.5 An 8-dB local mean spread.

have a bell-shaped (normal) distribution. The probability that 50 percent of the measured data are equal to or below a given level is

$$P(x \geq C) = \int_C^{\infty} \frac{1}{\sqrt{2\pi}\sigma} e^{-(x-A)^2/2\sigma^2} dx = 50\% \qquad (4.2\text{-}12)$$

where A is the mean level obtained along the path-loss slope, which is shown in Eq. (4.2-11) as

$$A = P_0 - \gamma \log \frac{r_1}{r_0}$$

Thus level A corresponds to the distance r_1. If level A increases, the confidence level decreases, as shown in Eq. (4.2-12).

TABLE 4.2

$P(x \le C)$, %	$C = B\sigma + A$
80	$-0.85\sigma + A$
70	$-0.55\sigma + A$
60	$-0.25\sigma + A$
50	A
40	$0.25\sigma + A$
30	$0.55\sigma + A$
20	$0.85\sigma + A$
16	$1\sigma + A$
10	$1.3\ \sigma + A$
2.28	$2\ \sigma + A$

$$P(x \ge C) = P\left(\frac{x - A}{\sigma} \ge B\right) \tag{4.2-13}$$

Let $C = B\sigma + A$. The different confidence levels are shown in Table 4.2. We can see how to use confidence levels from the following example.

Example 4.4 From the path-loss curve, we read the expected signal level as -100 dBm at 16 km (10 mi). If the standard deviation $\sigma = 8$ dB, what level would the signal equal or exceed for a 20 percent confidence level?

$$P\left(\frac{x - A}{\sigma} \ge B\right) = 20\% \qquad x \ge B\sigma + A \tag{E4.4-1}$$

or from Table 4.2 we obtain

$$x \ge 0.85 \times 8 + (-100) = -93.2 \text{ dBm}$$

The log normal curve with a standard deviation of 8 dB is shown in Fig. 4.6.

4.2.6 Determination of confidence interval

The confidence interval is often confused with confidence level. This usually happens when dealing with a particular run in a particular terrain contour. The signal strength of a run is shown in Fig. 1.6. The local mean is the envelope of the received signal, which also follows a log-normal distribution as shown in Fig. 4.6. The standard deviation of the local mean curve is a reflection of how much variation there is in terrain contour. If we know the standard deviation, then we can estimate how often the local mean (average power of the signal) falls within given limits (confidence interval).

The confidence intervals are defined as

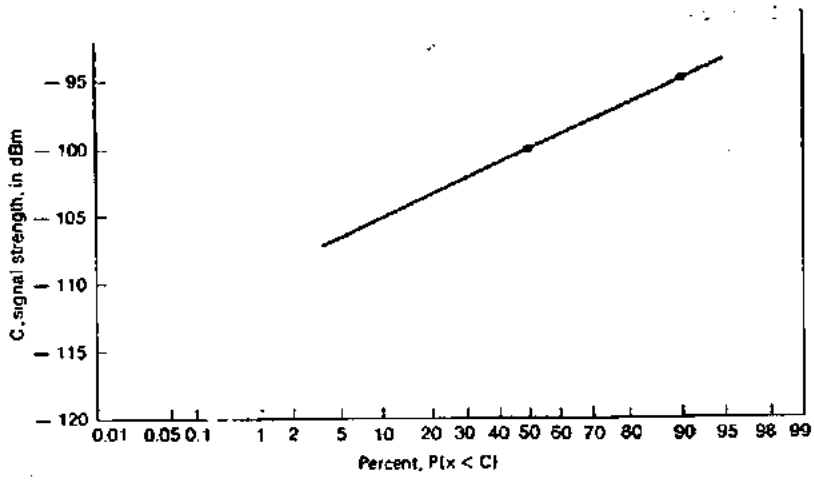

Figure 4.6 A log-normal curve.

$$P(m - \sigma \le x \le m + \sigma) = \int_{m-\sigma}^{m+\sigma} P(z)\,dz$$

$$= \int_{m-\sigma}^{m+\sigma} \frac{1}{\sqrt{2\pi}\sigma} e^{-(x-m)^2/2\sigma^2}\,dx$$

$$= \int_{-1}^{+1} \frac{1}{\sqrt{2\pi}} e^{-y^2}\,dy = 68\% \qquad (4.2\text{-}14)$$

or

$$P(m - 2\sigma \le x \le m + 2\sigma)$$

$$= \int_{m-2\sigma}^{m+2\sigma} \frac{1}{\sqrt{2\pi}\sigma} e^{-(x-m)^2/2\sigma^2}\,dx = 95.45\% \qquad (4.2\text{-}15)$$

where m is the mean of all the data and σ is the standard deviation of all the data.

Equation (4.2-14) indicates that 68 percent of predicted data will fall in the range between $-\sigma$ and $+\sigma$ around this mean value. In other words, we are 68 percent confident that a predicted data point will fall between $m - \sigma$ and $m + \sigma$.

The standard deviation from Fig. 4.6 can be found from Table 4.2 as

$$\sigma = \frac{C - A}{B} \qquad \text{[for a given percentage, } P(x \ge C)\text{]} \qquad (4.2\text{-}16)$$

Example 4.5 Find the standard deviation of a local mean curve as shown in Fig. 4.6. The confidence level for −95 dBm is found to be 10 percent, and the mean is −110 dBm. Then $C = -95$ dBm, $A = -110$ dBm, $B = 1.3$ (from Table 4.2), and

$$\sigma = \frac{-95 - (-110)}{1.3} = 11.54 \text{ dB}$$

Example 4.6 If we do not have Fig. 4.6 in hand but we know the average power and its standard deviation, we can determine the percentage of signal above any level.

Assuming that the average power is −90 dBm and the standard deviation is 9 dB, what would the signal level be if the confidence level is 30 percent?

The level would be (from Table 4.2)

$$0.55 \times 9 + (-90) = -85.05 \text{ dBm}$$

The confidence level and the confidence interval of a signal strength can be calculated from the predicted data applied to a mobile point-to-point model in an area of interest. However, the confidence level and the confidence interval of a signal strength cannot be found from a simple path-loss slope. In other words, it cannot be obtained from an area-to-area model unless the standard deviation of the model from which the curves were generated is known.

F(50,70) is a common notation to indicate that a signal strength is predicted under a confidence level of 50 percent for time to 70 percent for coverage. A detailed description can be found in Ref. 30.

4.2.7 A general formula for mobile radio propagation

Here we are only interested in a general propagation path-loss formula in a general mobile radio environment, which could be a suburban area. The 1-mi intercept level in a suburban area is −61.7 dBm under the standard conditions listed in Table 4.1. Combining these data with the equation shown in Eq. (4.2-10*b*) from the theoretical prediction model, and Eqs. (4.2-10c) and (4.2-11) from the measured data, the received power P_r at the suburban area can be expressed as

$$P_r = (P_t - 40) - 61.7 - 38.4 \log \frac{r_1}{1 \text{ mi}} + 20 \log \frac{h_1}{100 \text{ ft}} + 10 \log \frac{h_2}{10 \text{ ft}} + (G_t - 6) + G_m \quad (4.2\text{-}17)$$

Equation (4.2-17) can be simplified as

$$P_r = P_t - 157.7 - 38.4 \log r_1 + 20 \log h_1 + 10 \log h_2 + G_t + G_m \quad (4.2\text{-}18)$$

where P_t is in decibels above 1 mW, r_1 is in miles, h_1 and h_2 are in feet, and G_t and G_m are in decibels. Equation (4.2-18) is used for suburban areas. We may like to change Eq. (4.2-18) to a general formula

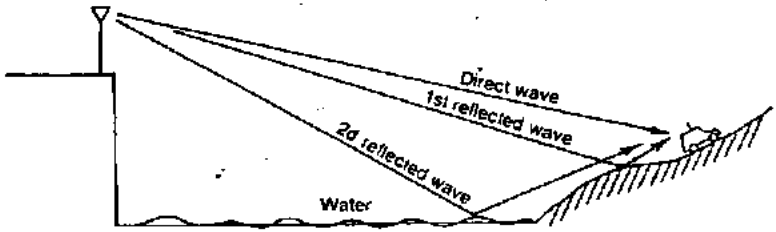

Figure 4.7 A model for propagation over water.

by using P_r at 10 mi as a reference which is -100 dBm, as shown in Fig. 4.3. Also the 40 dB/oct slope used is generous. Then Eq. (4.2-18) changes to

$$P_r = P_t - 156 - 40 \log r_1 + 20 \log h_1 + 10 \log h_2 + G_t + G_m \quad (4.2\text{-}19)$$

where the units of P_t, r_1, h_1, h_2, G_t, and G_m are stated below Eq. (4.2-18). Equation (4.2-19) can be used as a general formula in a mobile radio environment.

The most general formula is expressed as follows

$$P_r = P_t - K - \gamma \log r_1 + 20 \log h_1 + 10 \log h_2 + G_t + G_m \quad (4.2\text{-}20)$$

where $P_r = P_t - K$ at $r_1 = 1$ mile, $h_1 = h_2 = 1'$, and $G_t = G_m = 0$. The value of K and γ will be different and need to be measured in different human-made environment.

4.3 Propagation over Water or Flat Open Area

Propagation over water or flat open area is becoming a big concern because it is very easy to interfere with other cells if we do not make the correct arrangements. Interference resulting from propagation over the water can be controlled if we know the cause.

In general, the permittivities ϵ_r of seawater and fresh water are the same, but the conductivities of seawater and fresh water are different. We may calculate the dielectric constants ϵ_c, where $\epsilon_c = \epsilon_r - j60\sigma\lambda$. The wavelength at 850 MHz is 0.35 m. Then ϵ_c (seawater) $= 80 - j84$ and ϵ_c (fresh water) $= 80 - j0.021$.

However, based upon the reflection coefficients formula[32,33] with a small incident angle, both the reflection coefficients for horizontal polarized waves and vertically polarized waves approach 1. Since the 180° phase change occurs at the ground reflection point, the reflection coefficient is -1. Now we can establish a scenario, as shown in Fig. 4.7. Since the two antennas, one at the cell site and the other at the mobile unit, are well above sea level, two reflection points are gener-

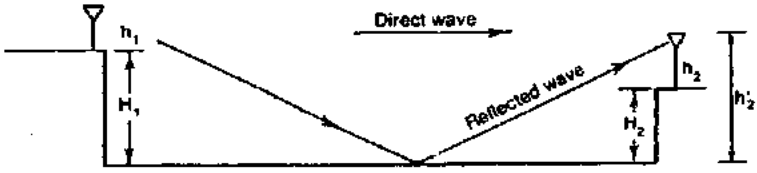

Figure 4.8 Propagation between two fixed stations over water or flat open land.

ated. The one reflected from the ground is close to the mobile unit; the other reflected from the water is away from the mobile unit. We recall that the only reflected wave we considered in the land mobile propagation is the one reflection point which is always very close to the mobile unit. We are now using the formula to find the field strength under the circumstances of a fixed point-to-point transmission and a land-mobile transmission over a water or flat open land condition.

4.3.1 Between fixed stations

The point-to-point transmission between the fixed stations over the water or flat open land can be estimated as follows. The received power P_r can be expressed as (see Fig. 4.8)

$$P_r = P_t \left(\frac{1}{4\pi d/\lambda}\right)^2 \left|1 + a_v e^{-j\phi_v} \exp(j\,\Delta\phi)\right|^2 \tag{4.3-1}$$

where P_t = transmitted power
d = distance between two stations
λ = wavelength
a_v, ϕ_v = amplitude and phase of a complex reflection coefficient, respectively

$\Delta\phi$ is the phase difference caused by the path difference Δd between the direct wave and the reflected wave, or

$$\Delta\phi = \beta\,\Delta d = \frac{2\pi}{\lambda}\Delta d \tag{4.3-2}$$

The first part of Eq. (4.3-1) is the free-space loss formula which shows the 20 dB/dec slope; that is, a 20-dB loss will be seen when propagating from 1 to 10 km.

$$P_0 = \frac{P_t}{(4\pi d/\lambda)^2} \tag{4.3-3}$$

The $a_v e^{-j\phi_v}$ are the complex reflection coefficients and can be found from the formula[32]

$$a_v e^{-j\phi_v} = \frac{\epsilon_c \sin\theta_1 - (\epsilon_c - \cos^2\theta_1)^{1/2}}{\epsilon_c \sin\theta_1 + (\epsilon_c - \cos^2\theta_1)^{1/2}} \tag{4.3-4}$$

When the vertical incidence is small, θ is very small and

$$a_v \approx -1 \qquad \text{and} \qquad \phi_v = 0 \tag{4.3-5}$$

can be found from Eq. (4.3-4). ϵ_c is a dielectric constant that is different for different media. However, when $a_v e^{-j\phi_v}$ is independent of ϵ_c, the reflection coefficient remains -1 regardless of whether the wave is propagated over water, dry land, wet land, ice, and so forth. The wave propagating between fixed stations is illustrated in Fig. 4.8.

Equation (4.3-1) then becomes

$$\begin{aligned} P_r &= \frac{P_t}{(4\pi d/\lambda)^2} |1 - \cos\Delta\phi - j\sin\Delta\phi|^2 \\ &= P_0(2 - 2\cos\Delta\phi) \end{aligned} \tag{4.3-6}$$

since $\Delta\phi$ is a function of Δd and Δd can be obtained from the following calculation. The effective antenna height at antenna 1 is the height above the sea level.

$$h_1' = h_1 + H_1$$

The effective antenna height at antenna 2 is the height above the sea level.

$$h_2' = h_2 + H_2$$

as shown in Fig. 4.8, where h_1 and h_2 are actual heights and H_1 and H_2 are the heights of hills. In general, both antennas at fixed stations are high, so the reflection point of the wave will be found toward the middle of the radio path. The path difference Δd can be obtained from Fig. 4.8 as

$$\Delta d = \sqrt{(h_1' + h_2')^2 + d^2} - \sqrt{(h_1' - h_2')^2 + d^2} \tag{4.3-7}$$

Since $d \gg h_1'$ and h_2', then

$$\Delta d \approx d\left[1 + \frac{(h_1' + h_2')^2}{2d^2} - 1 - \frac{(h_1' - h_2')^2}{2d^2}\right] = \frac{2h_1'h_2'}{d} \tag{4.3-8}$$

Then Eq. (4.3-2) becomes

$$\Delta\phi = \frac{2\pi}{\lambda}\frac{2h_1'h_2'}{d} = \frac{4\pi h_1'h_2'}{\lambda d} \tag{4.3-9}$$

Examining Eq. (4.3-6), we can set up five conditions:

1. $P_r < P_0$. The received power is less than the power received in free space; that is,

$$2 - 2\cos\Delta\phi < 1 \quad \text{or} \quad \Delta\phi < \frac{\pi}{3} \tag{4.3-10}$$

2. $P_r = 0$; that is,

$$2 - 2\cos\Delta\phi = 0 \quad \text{or} \quad \Delta\phi = \frac{\pi}{2}$$

3. $P_r = P_0$; that is,

$$2 - 2\cos\Delta\phi = 1 \quad \text{or} \quad \Delta\phi = \pm 60^\circ = \pm\frac{\pi}{3} \tag{4.3-11}$$

4. $P_r > P_0$; that is,

$$2 - 2\cos\Delta\phi > 1 \quad \text{or} \quad \frac{\pi}{3} < \Delta\phi < \frac{5\pi}{3} \tag{4.3-12}$$

5. $P_r = 4P_0$; that is,

$$2 - 2\cos\Delta\phi = \max \quad \text{or} \quad \Delta\phi = \pi \tag{4.3-13}$$

The value of $\Delta\phi$ can be found from Eq. (4.3-9). Now we can examine the situations resulting from Eq. (4.3-9) in the following examples.

Example 4.7 Let a distance between two fixed stations be 30 km. The effective antenna height at one end h_1 is 150 m above sea level. Find the h_2 at the other end so that the received power always meets the condition $P_r < P_0$ at 850-MHz transmission ($\lambda = 0.35$ m).

solution

$$\frac{4\pi h_1'h_2'}{\lambda d} \le \frac{\pi}{3} \tag{E4.7-1}$$

or

$$h_1' \le \frac{d\lambda}{12h_1'} = \frac{30{,}000 \times 0.35}{12 \times 150} = 6 \text{ m} \qquad \text{(E4.7-2)}$$

Example 4.8 Using the same parameters given in Example 4.7, find the range of h_2 which would keep $P_r > P_0$, and find the maximum received power P_r for $P_r = 4P_0$.

solution

$$a.\ \frac{\pi}{3} \le \frac{4\pi h_1' h_2'}{\lambda d} \le \frac{5\pi}{3} \qquad \text{the range of } h_2 \text{ for } P_r > P_0 \qquad \text{(E4.8-1)}$$

Substituting the values given in Example 4.7, we obtain

$$6 \text{ m} < h_2 < 30 \text{ m} \qquad 42 \text{ m} < h_2 < 66 \text{ m} \qquad \text{(E4.8-2)}$$

$b.$ $\Delta\phi = \pi$ for the maximum received power.

$$h_2 = 18 \text{ m} \qquad h_2 = 54 \text{ m} \qquad h_2 = 6 \text{ m}[3(2n-1)] \qquad \text{(E4.8-3)}$$

where n is any integer.

4.3.2 Land-to-mobile transmission over water

The propagation model would be different for land-to-mobile transmission over water. As depicted in Fig. 4.7, there are always two equal-strength reflected waves, one from the water and one from the proximity of the mobile unit, in addition to the direct wave. The reflected wave, whose reflected point is on the water is counted because there are no surrounding objects near this point. Therefore the reflected energy is strong. The other reflected wave that has a reflection point proximal to the mobile unit also carries strong reflected energy to it.

Therefore, the reflected power of the two reflected waves can reach the mobile unit without noticeable attenuation. The total received power at the mobile unit would be obtained by summing three components.

$$P_r = \frac{P_t}{(4\pi d/\lambda)^2} |1 - e^{j\Delta\phi_1} - e^{j\Delta\phi_2}|^2 \qquad (4.3\text{-}14)$$

where $\Delta\phi_1$ and $\Delta\phi_2$ are the path-length difference between the direct wave and two reflected waves, respectively. Since $\Delta\phi_1$ and $\Delta\phi_2$ are very small usually for the land-to-mobile path, then

$$P_r = \frac{P_t}{(4\pi d/\lambda)^2} |1 - \cos\Delta\phi_1 - \cos\Delta\phi_2 - j(\sin\Delta\phi_1 + \sin\Delta\phi_2)|^2 \qquad (4.3\text{-}15)$$

Follow the same approximation for the land-to-mobile propagation over water.

$$\cos \Delta\phi_1 \approx \cos \Delta\phi_2 \approx 1 \qquad \sin \Delta\phi_1 \approx \Delta\phi_1 \qquad \sin \Delta\phi_2 \approx \Delta\phi_2$$

Then

$$P_r = \frac{P_t}{(4\pi d/\lambda)^2} |- 1 - j(\Delta\phi_2 + \Delta\phi_2)|^2$$

$$= \frac{P_t}{(4\pi d/\lambda)^2} [1 + (\Delta\phi_1 + \Delta\phi_2)^2] \tag{4.3-16}$$

In most practical cases, $\Delta\phi_1 + \Delta\phi_2 < 1$; then $(\Delta\phi_1 + \Delta\phi_2)^2 \ll 1$ and Eq. (4.3-16) reduces to

$$P_r \approx \frac{P_t}{(4\pi d/\lambda)^2} \tag{4.3-17}$$

Equation (4.3-17) is the same as that expressing the power received from the free-space condition. Therefore, we may conclude that the path loss for land-to-mobile propagation over land, 40 dB/dec, is different for land-to-mobile propagation over water. In the case of propagation over water, the free-space path loss, 20 dB/dec, is applied.

4.4 Foliage Loss

Foliage loss is a very complicated topic that has many parameters and variations. The sizes of leaves, branches, and trunks, the density and distribution of leaves, branches, and trunks, and the height of the trees relative to the antenna heights will all be considered. An illustration of this problem is shown in Fig. 4.9. There are three levels: trunks, branches, and leaves. In each level, there is a distribution of sizes of trunks, branches, and leaves and also of the density and spacing between adjacent trunks, branches, and leaves. The texture and thickness of the leaves also count. This unique problem can become very complicated and is beyond the scope of this book. For a system design, the estimate of the signal reception due to foliage loss does not need any degree of accuracy.

Furthermore, some trees, such as maple or oak, lose their leaves in winter, while others, such as pine, never do. For example, in Atlanta, Georgia, there are oak, maple, and pine trees. In summer the foliage is very heavy, but in winter the leaves of the oak and maple trees fall and the pine leaves stay. In addition, when the length of pine needles reaches approximately 6 in., which is the half wavelength at 800 MHz,

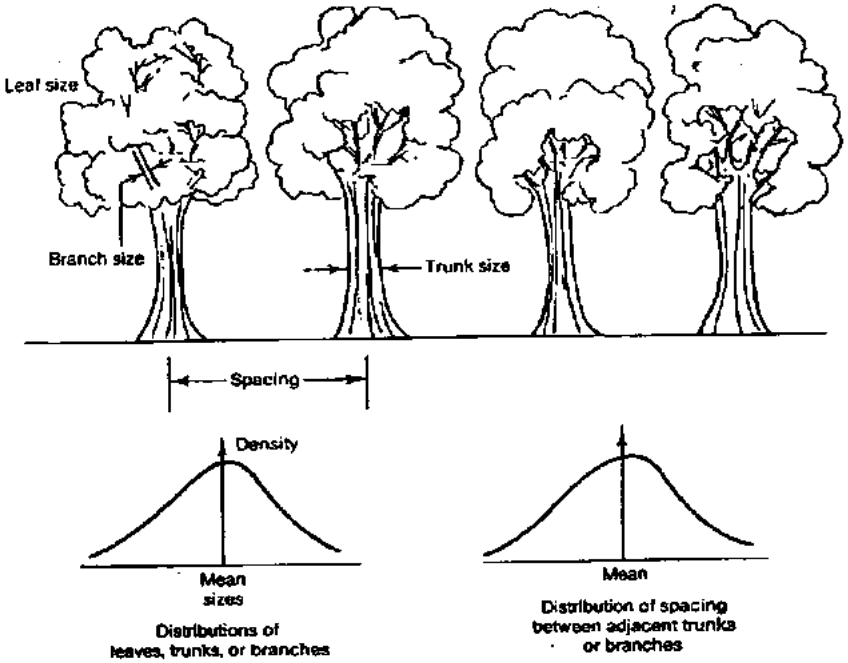

Figure 4.9 A characteristic of foliage environment.

a great deal of energy can be absorbed by the pine trees. In these situations, it is very hard to predict the actual foliage loss.

However, a rough estimate should be sufficient for the purpose of system design. In tropic zones, the sizes of tree leaves are so large and thick that the signal can hardly penetrate. In this case, the signal will propagate from the top of the tree and deflect to the mobile receiver. We will include this calculation also.

Sometime the foliage loss can be treated as a wire-line loss, in decibels per foot or decibels per meter, when the foliage is uniformly heavy and the path lengths are short. When the path length is long and the foliage is nonuniform, then decibels per octaves or decibels per decade is used. Detailed discussion of foliage loss can be found in Refs. 34 to 38. In general, foliage loss occurs with respect to the frequency to the fourth power ($-f^{-4}$). Also, at 800 MHz the foliage loss along the radio path is 40 dB/dec, which is 20 dB more than the free-space loss, with the same amount of additional loss for mobile communications. Therefore, if the situation involves both foliage loss and mobile communications, the total loss would be 60 dB/dec (=20 dB/dec of free-space loss + additional 20 dB due to foliage loss + addi-

tional 20 dB due to mobile communiation). This situation would be the case if the foliage would line up along the radio path. A foliage loss in a suburban area of 58.4 dB/dec is shown in Fig. 4.10.

Example 4.9 In a suburban area two places are covered with trees: 2 to 2.5 mi away from the cell site and 3 to 3.5 mi away from the cell site. The additional loss due to foliage is 3 dB, according to Fig. 4.10.

Example 4.10 In a suburban area, one place is 0.3 to 0.5 mi (a distance of 1056 ft) from the cell site with additional trees. The additional path loss is 5 dB due to the foliage, according to Fig. 4.10.

As demonstrated from the above two examples, close-in foliage at the transmitter site always heavily attenuates signal reception. Therefore, the cell site should be placed away from trees. If the heavy foliage is close in at the mobile unit, the additional foliage loss must be calculated using the diffraction loss formula given in Sec. 4.7.3.

4.5 Propagation in Near-in Distance

4.5.1 Why use a 1-mi intercept?

1. Within a 1-mi radius, the antenna beamwidth, especially of a high-gain omnidirectional antenna, is narrow in the vertical plane. Thus the signal reception at a mobile unit less than 1 mi away will be reduced because of the large elevation angle which causes the mobile unit to be in the shadow region (outside the main beam). The larger the elevation angle, the weaker the reception level due to the antenna's vertical pattern, as shown in Fig. 4.11.
2. There are fewer roads within the 1-mi radius around the cell site. The data are insufficient to create a statistical curve. Also the road orientation, in-line and perpendicular, close to the cell site can cause a big difference in signal reception levels (10–20 dB) on those roads.
3. The near-by surroundings of the cell site can bias the reception level either up or down when the mobile unit is within the 1-mi radius. When the mobile unit is 1-mi away from the cell site, the effect due to the near-by surroundings of the cell site becomes negligible.
4. For land-to-mobile propagation, the antenna height at the cell site strongly affects the mobile reception in the field; therefore, mobile reception 1 mi away has to refer to a given base-station antenna height.

4.5.2 Curves for near-in propagation

We usually worry about propagation at the far distance for coverage purposes. Now we also should investigate the near-in distance prop-

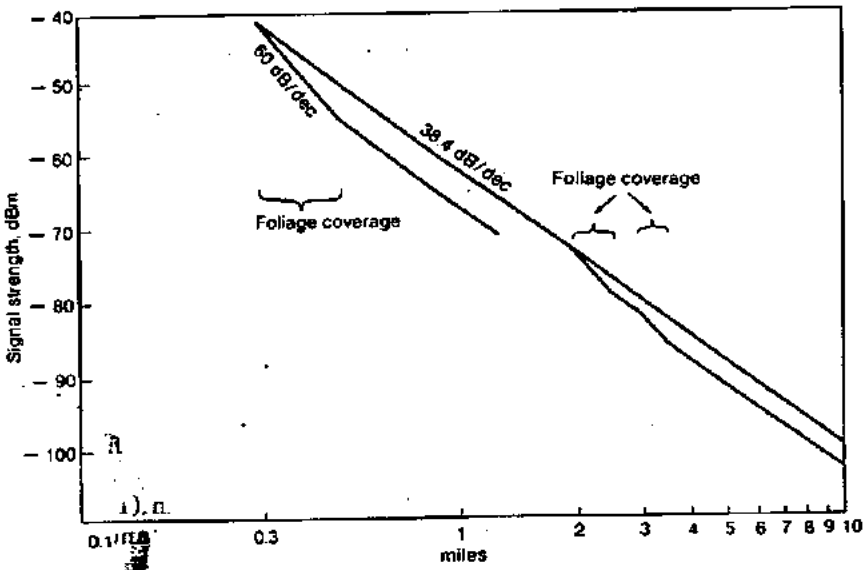

Figure 4.10 Foliage loss calculation in suburban areas.

agation. We may use the suburban area as an example. At the 1-mi intercept the received level is −61.7 dBm based on the reference set of parameters; i.e., the antenna height is 30 m (100 ft). If we increase the antenna height to 60 m (200 ft), a 6-dB gain is obtained. From 60 to 120 m (20 to 400 ft), another 6 dB is obtained. At the 120-m (400-ft) antenna height, the mobile received signal is the same as that received at the free space.

The antenna pattern is not isotropic in the vertical plane. A typical 6-dB omnidirectional antenna vertical beamwidth is shown in Fig.

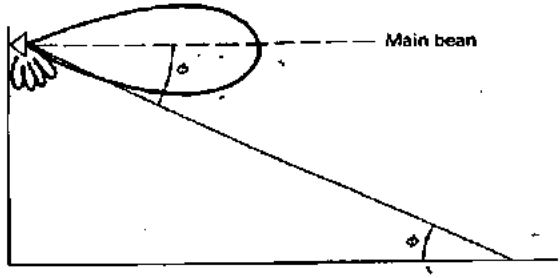

Figure 4.11 Elevation angle of the shadow of the antenna pattern.

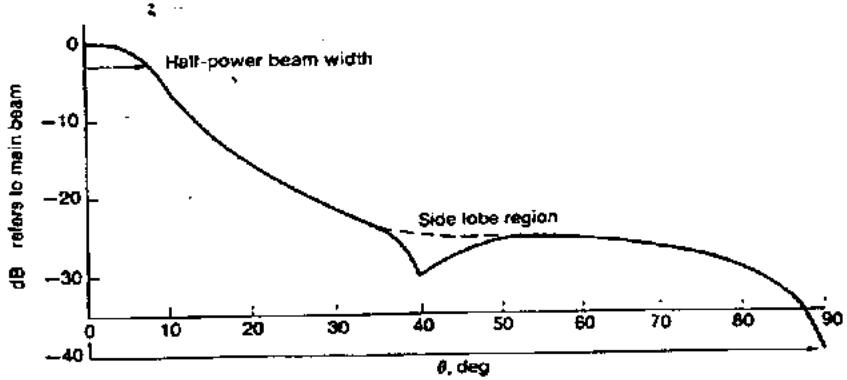

Figure 4.12 A typical 6-dB omnidirectional antenna beamwidth.

4.12. The reduction in signal reception can be found in the figure and is listed in the table below.

At d = 100 m (328 ft) [mobile antenna height = 3 m (10 ft)], the incident angles and elevation angles are 11.77° and 10.72°, respectively.

Antenna height h_1, m (ft)	Incident angle θ, degrees	Elevation angle ϕ, degrees	Attentuation α, dB
90 (300)	30.4	29.6	21
60 (200)	21.61	20.75	16
30 (100)	11.77	10.72	6

Since the incident angle becomes larger, the 40-dB/dec slope is no longer valid. If the antenna beam is aimed at the mobile unit, we will observe 24 dB/dec for an antenna height of 100 ft, 22 dB/dec for an antenna height of 200 ft, and 20 dB/dec for an antenna height of 400 ft or higher. The slope of 20 dB/dec is the free-space loss as shown in Fig. 4.13. The power of 11 dBm received at 0.001 mi is obtained from the free-space formula with an ERP of 46 dBm at the cell site as the standard condition (Table 4.1).

4.5.3 Calculation of near-field propagation

The range d_F of near field can be obtained by letting $\Delta\phi$ in Eq (4.2-7) be π.

$$\Delta\phi = \frac{4\pi h_1 h_2}{\lambda d_F} = \pi \tag{4.5-1}$$

and then

$$d_F = \frac{4h_1 h_2}{\lambda} \tag{4.5-2}$$

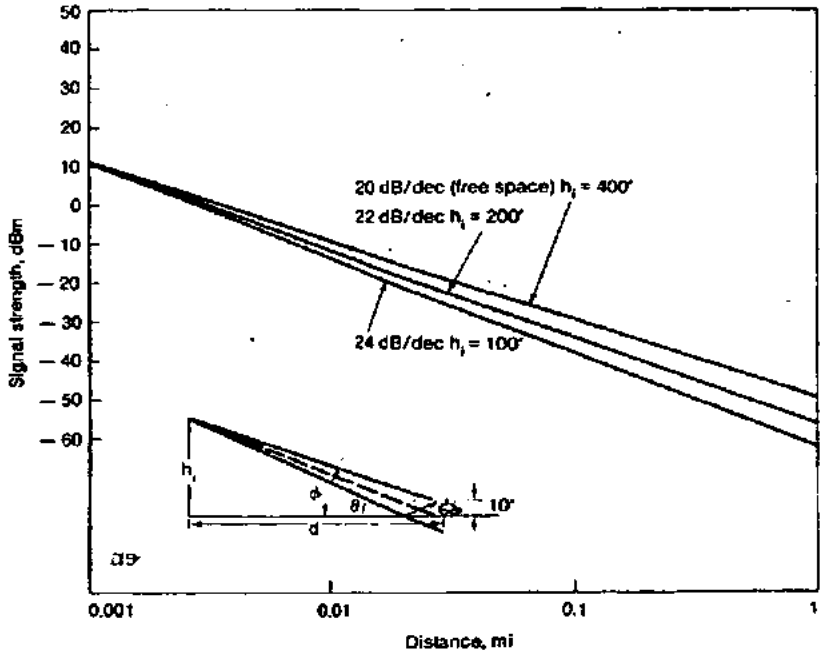

Figure 4.13 Curves for near-in propagation.

The signal received within the nearfield ($d < d_F$) uses the free space loss formula (Eq. (4.3-17)), and the signal received outside the nearfield ($d > d_F$) can use the mobile radio path loss formula (Eq. (4.2-18)), for the best approximation.

4.6 Long-Distance Propagation

The advantage of a high cell site is that it covers the signal in a large area, especially in a noise-limited system where usually different frequencies are repeatedly used in different areas. However, we have to be aware of the long-distance propagation phenomenon. A noise-limited system gradually becomes an interference-limited system as the traffic increases. The interference is due to not only the existence of many cochannels and adjacent channels in the system, but the long-distance propagation also affects the interference.

4.6.1 Within an area of 50-mile radius

For a high site, the low-atmospheric phenomenon would cause the ground wave path to propagate in a non-straight-line fashion. The

phenomenon is usually more pronounced over seawater because the atmospheric situation over the ocean can be varied based on the different altitudes. The wave path can bend either upward or downward. Then we may have the experience that at one spot the signal may be strong at one time but weak at another.

4.6.2 At a distance of 320 km (200 mi)

Tropospheric wave propagation prevails at 800 MHz for long-distance propagation; sometimes the signal can reach 320 km (200 mi) away.

The wave is received 320 km away because of an abrupt change in the effective dielectric constant of the troposphere (10 km above the surface of the earth). The dielectric constant changes with temperature, which decreases with height at a rate of about 6.5°C/km and reaches −50°C at the upper boundary of the troposphere. In tropospheric propagation, the wave may be divided by refraction and reflection.

Tropospheric refraction. This refraction is a gradual bending of the rays due to the changing effective dielectric constant of the atmosphere through which the wave is passing.

Tropospheric reflection. This reflection will occur where there are abrupt changes in the dielectric constant of the atmosphere. The distance of propagation is much greater than the line-of-sight propagation.

Moistness. Actually water content has much more effect than temperature on the dielectric constant of the atmosphere and on the manner in which the radio waves are affected. The water vapor pressure decreases as the height increases.

If the refraction index decreases with height over a portion of the range of height, the rays will be curved downward, and a condition known as *trapping,* or *duct propagation,* can occur. There are surface ducts and elevated ducts. Elevated ducts are due to large air masses and are common in southern California. They can be found at elevations of 300 to 1500 m (1000 to 5000 ft) and may vary in thickness from a few feet to a thousand feet. Surface ducts appear over the sea and are about 1.5 m (5 ft) thick. Over land areas, surface ducts are produced by the cooling air of the earth.

Tropospheric wave propagation does cause interference and can only be reduced by umbrella antenna beam patterns, a directional antenna pattern, or a low-power-low-antenna-mast approach.

4.7 Obtain Path Loss from a Point-to-Point Prediction Model—A General Approach[24,41]

4.7.1 In nonobstructive condition[42]

In this condition, the direct path from the cell site to the mobile unit is not obstructed by the terrain contour. Here, two general terms should be distinguished. The *nonobstructive direct path* is a path unobstructed by the terrain contour. The *line-of-sight path* is a path which is unobstructed by the terrain contour and by man-made structures. In the former case, the cell-site antenna cannot be seen by the mobile user whereas in the latter case, it can be. Therefore, the signal reception is very strong in the line-of-sight case, which is not the case we are worrying about.

In the mobile environment, we do not often have line-of-sight conditions. Therefore we use direct-path conditions which are unobstructed by the terrain contour. Under these conditions, the antenna-height gain will be calculated for every location in which the mobile unit travels, as illustrated in Fig. 4.14. The method for finding the antenna-height gain is as follows.

Finding the antenna-height gain

1. Find the specular reflection point. Take two values from two conditions stated as follows.
   a. Connect the image antenna of the cell-site antenna to the mobile antenna; the intercept point at the ground level is considered as a potential reflection point.
   b. Connect the image antenna of the mobile antenna to the cell-site antenna; the intercept point at the ground level is also considered as a potential reflection point.

   Between two potential reflection points we choose the point which is close to the mobile unit to be the real one because more energy would be reflected to the mobile unit at that point.
2. Extend the reflected ground plane. The reflected ground plane which the reflection point is on can be generated by drawing a tangent line to the point where the ground curvature is, then extending the reflected ground plane to the location of the cell-site antenna.
3. Measure the effective antenna height. The effective antenna height is measured from the point where the reflected ground plan and the cell-site antenna location meet. Between these two cases shown in Fig. 4.14, h_e equals 40 m in Fig. 4.14*a* and 200 m in Fig. 4.14*b*. The actual antenna height h_1 is 100 m.

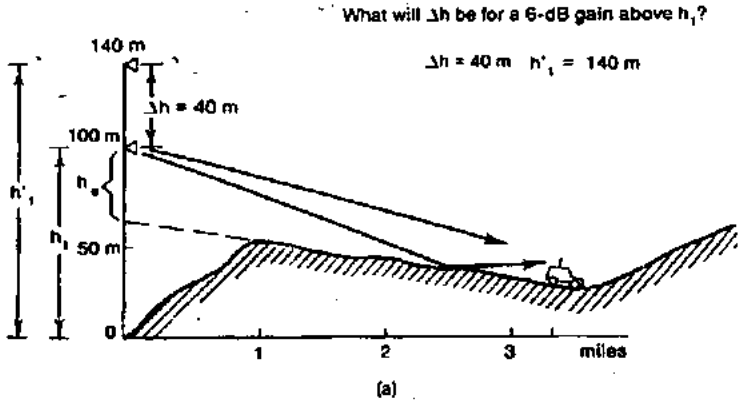

Figure 4.14 Calculation of effective antenna height: (*a*) case 1; (*b*) case 2.

4. Calculate the antenna-height gain ΔG. The formula of ΔG is expressed as [see Eq. (4.2-10*b*)]

$$G = 20 \log \frac{h_e}{h_1} \tag{4.7-1}$$

Then the ΔG from Fig. 4.14*a* is

$$\Delta G = 20 \log \frac{40}{100} = -8 \text{ dB} \qquad \text{(a negative gain in Fig. 4.14}a\text{)}$$

The ΔG from Fig. 4.14*b* is

$$\Delta G = 20 \log \frac{200}{100} = 6 \text{ dB} \qquad \text{(a positive gain in Fig. 4.14}b\text{)}$$

We have to realize that the antenna-height gain ΔG changes as the mobile unit moves along the road. In other words, the effective antenna height at the cell site changes as the mobile unit moves to a new location, although the actual antenna remains unchanged.

Another physical explanation of effective antenna height. Another physical explanation of effective antenna height is shown in Fig. 4.15. In Fig. 4.15*a*, we have to ask which height is the actual antenna height h_1, or is the actual antenna height very important in this situation?

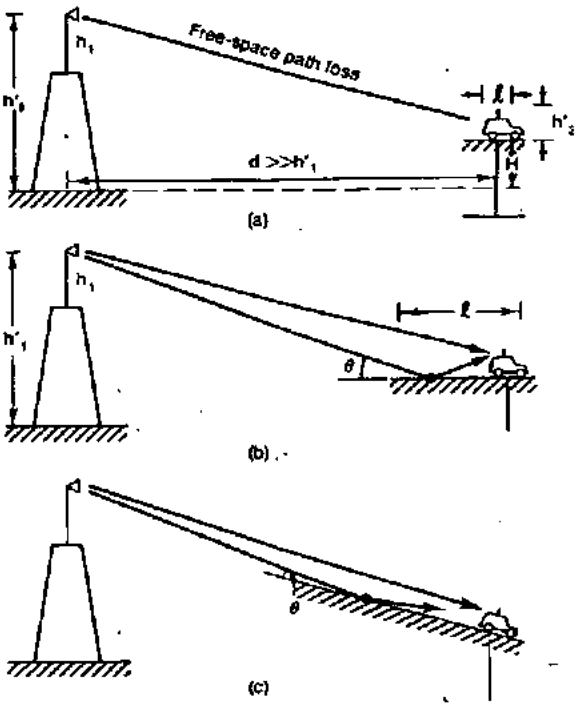

Figure 4.15 Physical explanation of effective antenna heights.

As long as the value of H is much larger than h_2 and the length l of the floor is roughly equal to the length of the vehicle, there is only one direct wave, and the free-space path loss is applied to the situation which provides a strong reception.

In Fig. 4.15*b*, the situation remains the same, except the length l is longer to allow a reflection point to be generated on the floor. Now two waves are created, one direct wave and one reflected wave. The stronger the reflected wave is, the larger the path loss is. The stronger reflected wave occurs at a very small incident angle θ. This means that a small incident angle corresponds to a large reflection coefficient because of the nature of the reflection mechanism, and the wave reflected from the ground is a 180° phase shift. Therefore, no matter what, the amount of reflected energy always becomes negative. The addition of a strong reflected wave to a direct wave tends to weaken the direct wave.

In Fig. 4.15*c*, as the incident angle θ approaches zero, the signal reception becomes very weak. The shadow-loss condition starts when both the direct wave and the reflected wave have been blocked. When the direction of the vehicle-site floor is reversed (i.e., going counterclockwise), the incident angle θ increases and the reflection coefficient decreases. The energy reflected from the floor becomes less, and so the direct wave would reduce the small amount of energy resulting from the negative contribution from the reflected wave. The larger the incident angle of the reflected wave, the weaker the reflected wave, and the signal reception becomes the free-space condition.

When the incident angle of a wave is very small, two conditions shown in Fig. 4.16 can be considered.

1. Sparse human-made structures or trees along the propagation path. When there are few human-made structures along the propagation path, the received power is always higher than when there are many. This is why the power level received in an open area is higher than that received in a suburban area and higher still than that received in an urban area.
2. Dense human-made structures along the propagation path. There are two conditions.
   a. A line-of-sight wave exists between the base station and the mobile unit. When the waves reflected by the surrounding buildings are relatively weak, less fading (rician fading)[40] is observed.
   b. The mobile unit is surrounded by the scatters. If the direct reception is blocked by the surrounding buildings, Rayleigh fading is observed.

   In the above two conditions the average received powers are not the same. However, if the reflected waves from surrounding build-

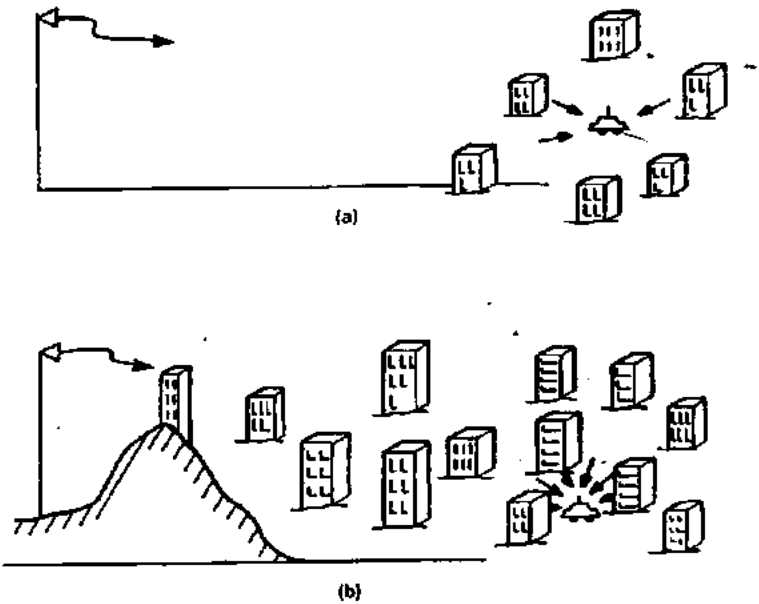

Figure 4.16 Man-made environment. (*a*) Sparse man-made structures. (*b*) Dense man-made structures.

ings are very strong, the average received power from the two different conditions can be very close. It can be seen as an analog to conservation of energy. The total signal received at the mobile unit (or at the cell site) either from a single wave or from many reflected waves tentatively remains a constant. In both conditions, the propagation path loss is 40 dB/dec because both conditions are in a mobile radio environment.

Comments on the contribution of antenna-height gain. If we do not take into account the changes in antenna-height gain due to the terrain contour between the cell site and the mobile unit the path-loss slope will have a standard deviation of 8 dB. If we do take the antenna-height gain into account, values generally have a standard deviation within 2 to 3 dB.

The effects of terrain roughness are illustrated in Fig. 4.17*a* as changing different effective antenna heights, h_e and h_e' at different positions of the mobile unit. Then the effective antenna gain ΔG can be obtained from Eq. (4.7-1) as

$$\Delta G = 20 \log \frac{h_e}{h_e'}$$

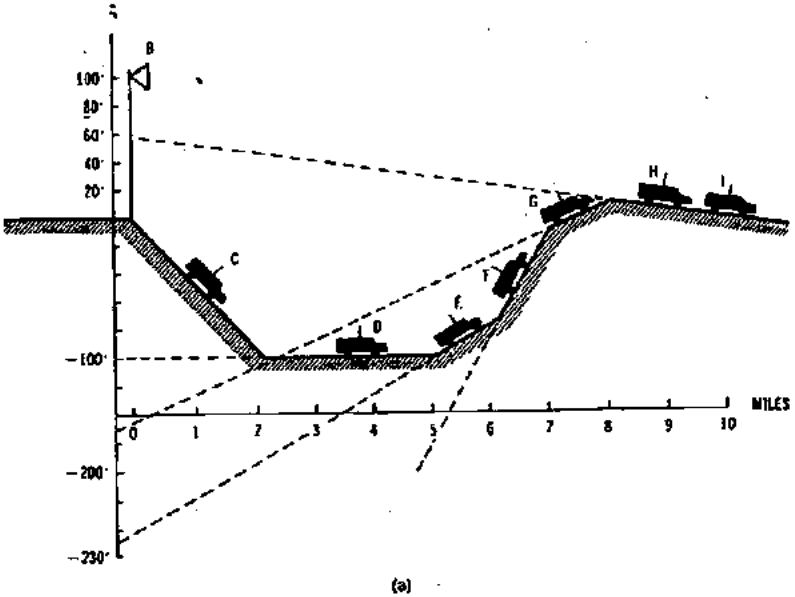

Figure 4.17 Illustration of the terrain effect on the effective antenna gain at each position. (a) Hilly terrain contour. (b) Point-to-point prediction. (*After Lee, Ref. 40, p. 86.*)

Assume that the mobile unit is traveling in a sururban area, say northern New Jersey. The path-loss slope of this suburban area is shown in Fig. 4.3 and then plotted in Fig. 4.17*b*. Then the antenna-height gains or losses are added or subtracted from the slope at their corresponding points. Now we can visualize the difference between an area-to-area prediction (use a path-loss slope) and a point-to-point prediction (after the antenna-height gain correction). The point-to-point

prediction is based on the actual terrain contour along a particular radio path (in this case, the radio path and the mobile path are the same for simplicity), but the area-to-area prediction is not. This is why the area-to-area prediction has a standard deviation of 8 dB but the point-to-point prediction only has a standard deviation of less than 2 to 3 dB (see Sec. 4.8.2).

4.7.2 In obstructive condition

In this condition, the direct path from the cell site to the mobile unit is obstructed by the terrain contour. We would like to treat this condition as follows.

1. *Apply area-to-area prediction.* First, just apply the same steps in the area-to-area prediction as if the obstructive condition did not exist. If the area is in Philadelphia, the Philadelphia path-loss slope applies. All the correction factors would apply to finding the area-to-area prediction for a particular situation.
2. *Obtain the diffraction loss.* The diffraction loss can be found from a single knife-edge or double knife-edge case, as shown in Fig. 4.18.

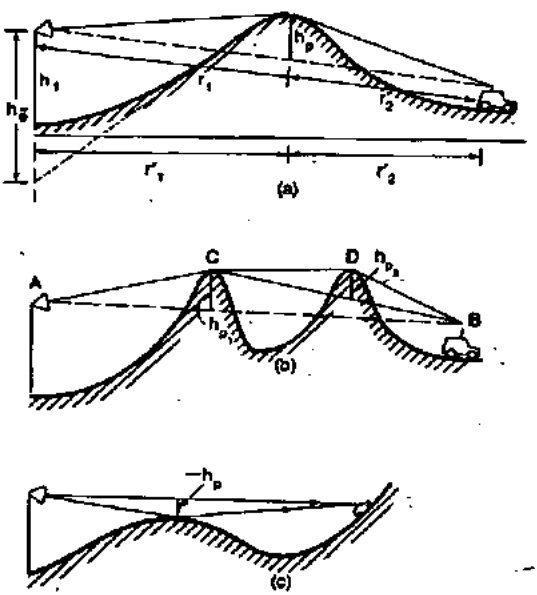

Figure 4.18 Diffraction loss due to obstructive conditions. (*a*) Single knife-edge; (*b*) double knife-edges; (*c*) nonclear path.

a. Find the four parameters for a single knife-edge case. The four parameters, the distances r_1 and r_2 from the knife-edge to the cell site and to the mobile unit, the height of the knife-edge h_p, and the operating wavelength λ, are used to find a new parameter v.

$$v = -h_p \sqrt{\frac{2}{\lambda}\left(\frac{1}{r_1} + \frac{1}{r_2}\right)} \tag{4.7-2}$$

h_p is a positive number as shown in Fig. 4.18*a*, and h_p is a negative number as shown in Fig. 4.18*c*. As soon as the value of v is obtained, the diffraction loss L can be found from the curves shown in Fig. 4.19. The approximate formula below can be used with different values of v to represent the curve and be programmed into a computer.

$$\begin{aligned}
1 \le v &\quad L = 0 \text{ dB} \\
0 \le v < 1 &\quad L = 20 \log (0.5 + 0.62\, v) \\
-1 \le v < 0 &\quad L = 20 \log (0.5e^{0.95v}) \\
-2.4 \le v < -1 &\quad L = 20 \log (0.4 - \sqrt{0.1184 - (0.1\, v + 0.38)^2}) \\
v < -2.4 &\quad L = 20 \log \left(-\frac{0.225}{v}\right)
\end{aligned} \tag{4.7-3}$$

When $h_p = 0$, the direct path is tangential to the knife-edge, and $v = 0$, as derived from Eq. (4.7-2). With $v = 0$, the diffraction loss $l = 6$ dB can be obtained from Fig. 4.19.

b. A double knife-edge case. Two knife edges can be formed by the two triangles *ACB* and *CDB* shown in Fig. 4.18*b*. Each one can be used to calculate v as v_1 and v_2. The corresponding L_1 and L_2 can be found from Fig. 4.19. The total diffraction loss of this double knife-edge model is the sum of the two diffraction losses.

$$L_t = L_1 + L_2$$

4.7.3 Cautions in obtaining defraction loss

We always draw the scales of the y and x axes differently. The same intervals represent 10 m or 10 ft in the y-axis but 1 km or 1 mi in the x-axis. In this way we can depict the elevation change more clearly. Then we have to be aware of the measurement of r_1 and r_2 shown in

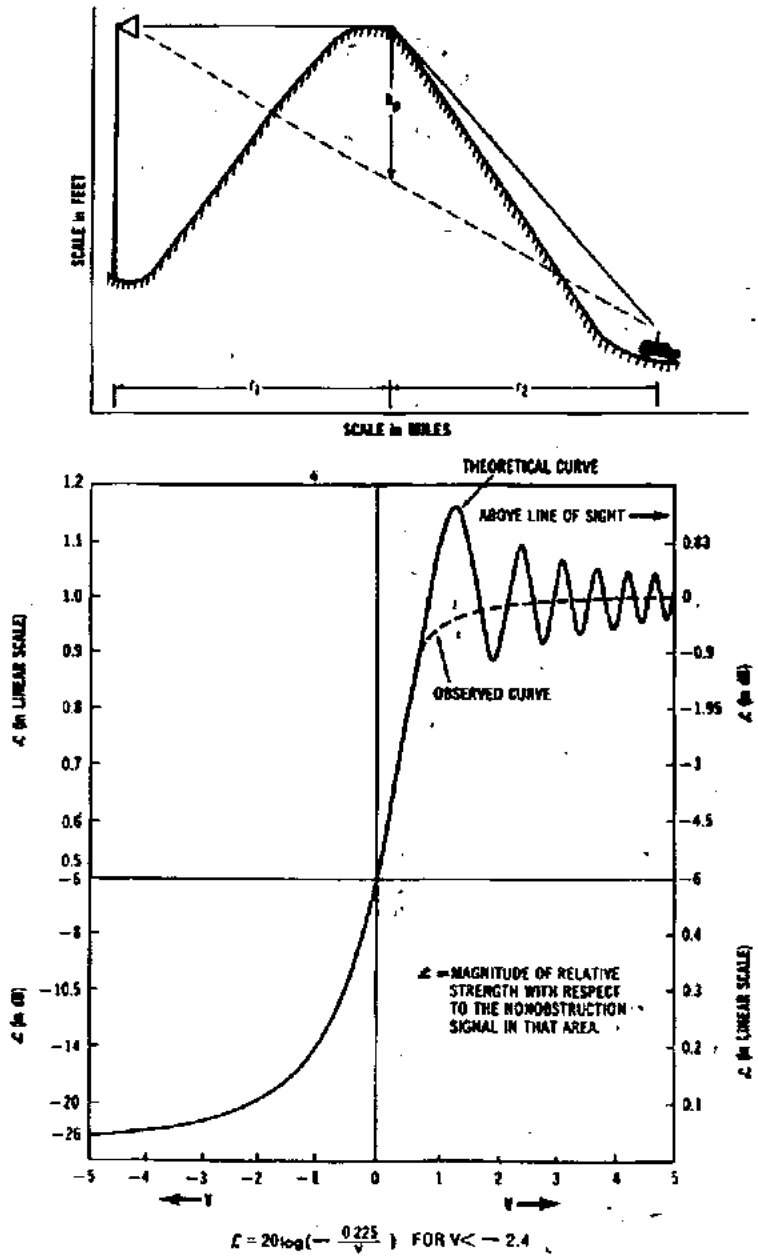

Figure 4.19 Shadow-loss prediction.

Fig. 4.18*a*. The simple way of measuring r_1 and r_2 is based on the horizontal scale as shown in the figure, where $r_1 = r_1'$ and $r_2 = r_2'$. It can be shown that the errors for $r_1 = r_1'$ and $r_2 = r_2'$ are insignificant if the scales used on both the x and y axes are the same.

When the heavy foliage is close in at the mobile unit, the loss due to foliage can be obtained from the diffraction loss. The average foliage configuration resembles the terrain configuration. Therefore the height of knife edge over the foliage configuration can be found. Then the diffraction loss due to the foliage is obtained.

4.8 Form of a Point-to-Point Model

4.8.1 General formula of Lee model

Lee's point-to-point model has been described. The formula of the Lee model can be stated simply in three cases:

1. *Direct-wave case.* The effective antenna height is a major factor which varies with the location of the mobile unit while it travels.
2. *Shadow case.* No effective antenna height exists. The loss is totally due to the knife-edge diffraction loss.
3. *Over-the-water condition.* The free space path-loss is applied.

We form the model as follows:

$$P_r = \begin{cases} \text{nonobstructive path} \\ \quad = \underbrace{P_{r_0} - \gamma \log \frac{r}{r_0}}_{\text{By human-made structure}} + \underbrace{20 \log \frac{h_e'}{h_1} + \alpha}_{\text{By terrain contour}} \qquad (4.8\text{-}1) \\ \text{obstructive path} \\ \quad = P_{r_0} - \gamma \log \frac{r}{r_0} + 20 \log \frac{h_e''}{h_1} + L + \alpha \text{ (where } h_e'' \text{ is shown in Fig. 4.18}a\text{)} \\ \quad = \underbrace{P_{r_0} - \gamma \log \frac{r}{r_0}}_{\text{By human-made structure}} + \underbrace{L + \alpha \text{ (when } h_e'' \approx h_1\text{)}}_{\text{By terrain contour}} \\ \text{land-to-mobile over water} = \text{a free-space formula} \end{cases}$$

(see Sec. 4.3)

Remarks

1. The P_r cannot be higher than that from the free-space path loss.
2. The road's orientation, when it is within 2 mi from the cell site, will affect the received power at the mobile unit. The received power at the mobile unit traveling along an in-line road can be 10 dB higher than that along a perpendicular road.
3. α is the corrected factor (gain or loss) obtained from the condition (see Sec. 4.2.1).
4. The foliage loss (Sec. 4.4) would be added depending on each individual situation. Avoid choosing a cell site in the forest. Be sure that the antenna height at the cell site is higher than the top of the trees.
5. Within one mile (or one kilometer) in a man-made environment, the received signal is affected by the buildings and street orientations. The macrocell prediction formula (Eq. (4.8-1)) can not be applied in such area. A microcell prediction model by Lee is introduced and described in Ref. 45.

4.8.2 The merit of the point-to-point model

The area-to-area model usually only provides an accuracy of prediction with a standard deviation of 8 dB, which means that 68 percent of the actual path-loss data are within the ± 8 dB of the predicted value. The uncertainty range is too large. The point-to-point model reduces the uncertainty range by including the detailed terrain contour information in the path-loss predictions.

The differences between the predicted values and the measured ones for the point-to-point model were determined in many areas. In the following discussion, we compare the differences shown in the Whippany, N.J., area and the Camden-Philadelphia area. First, we plot the points with predicted values at the x-axis and the measured values at the y-axis, shown in Fig. 4.20. The 45° line is the line of prediction without error. The dots are data from the Whippany area, and the crosses are data from the Camden-Philadelphia area. Most of them, except the one at 9 dB, are close to the line of prediction without error. The mean value of all the data is right on the line of prediction without error. The standard deviation of the predicted value of 0.8 dB from the measured one.

In other areas, the differences were slightly larger. However, the standard deviation of the predicted value never exceeds the measured

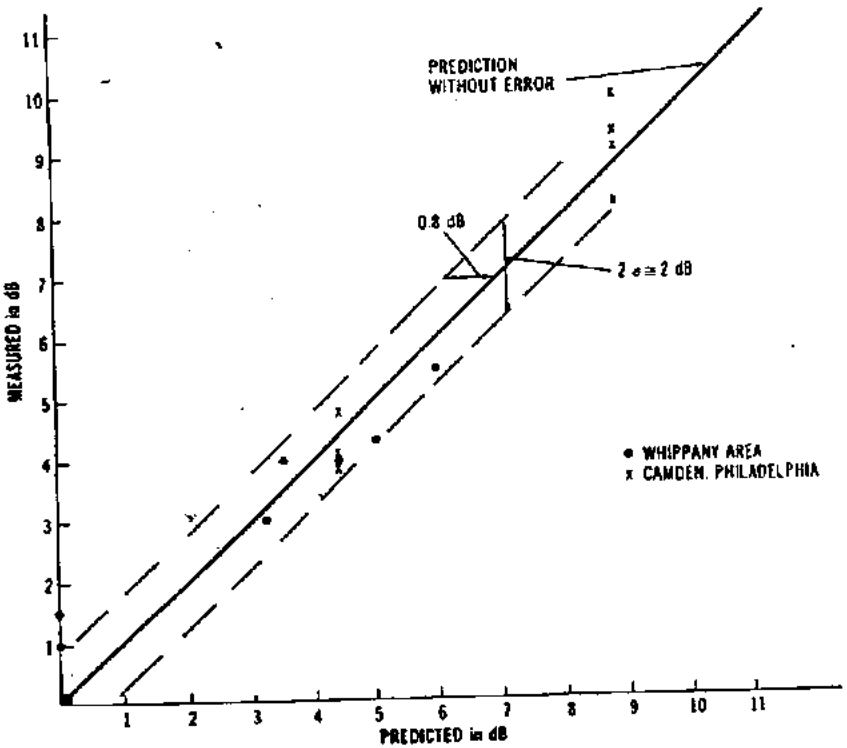

Figure 4.20 Indication of errors in point-to-point predictions under nonobstructive conditions. (*After Lee, Ref. 42.*)

one by more than 3 dB. The standard deviation range is much reduced as compared with the maximum of 8 dB from area-to-area models.

The point-to-point model is very useful for designing a mobile cellular system with a radius for each cell of 10 mi or less. Because the data follow the log-normal distribution, 68 percent of predicted vaues obtained from a point-to-point prediction model are within 2 to 3 dB.

This point-to-point prediction can be used to provide overall coverage of all cell sites and to avoid cochannel interference. Moreover, the occurrence of handoff in the cellular system can be predicted more accurately.

The point-to-point prediction model is a basic tool that is used to generate a signal coverage map, an interference area map, a handoff occurrence map, or an optimum system design configuration, to name a few applications.

4.9 Computer Generation of a Point-to-Point Prediction

The point-to-point prediction described in Sec. 4.8 can easily be used in a computer program. Here we describe the automated prediction in steps.[43]

4.9.1 Terrain elevation data

We may use either a 250,000:1 scale map, called a *quarter-million scale map*, or a 7.5-minute scale map issued by the U.S. Geological Survey. Both maps have the terrain elevation contours. Also, terrain elevation data tapes can be purchased from the DMA (Defense Map Agency). The quarter-million scale map tapes over the whole United States, but the 7.5-minute scale maps are only available for certain areas. Let us discuss the use of these two different scale maps.

1. Use a quarter-million scale map. Each elevation contour increment is 100 ft, which does not provide the fine detail needed for a mobile radio propagation in a hilly area. The quarter-million scale elevation data tapes made by DMA come from the quarter-million scale maps. The elevation data for two adjacent terrain contours is determined by extrapolation. Although the tape gives elevations for every 208 ft (0.01 in on the map), these elevations are not accurate because they are from the quarter-million scale map. However, in most areas, as long as the terrain contour does not change rapidly, the DMA tape can be used as a raw data base. DMA provides two kinds of tapes: a 3-second arc tape and a planar 0.01-in tape. The former has an elevation for every 3-second interval (about 61 to 91.5 m, or 200 to 300 ft, depending on the geographic locations) on the map. The latter has an elevation at intervals of 0.01 in (63.5 m, or 208 ft). Since the arc-second tape provides sample intervals of 3 seconds, a length of 1° has 1200 points. The advantage of using the arc-second tape is the continuity of sample points from one tape to another. However, for the arc-second tape the sample points are not equally far apart on the ground but are in the planar tape. Therefore, if the desired coverage is within one tape's geographic area, the planar tape is used. If the desired area is spread over more than one tape (see Fig. 4.21), the arc-second is used. The structure to a 250,000:1 scale digital elevation format is shown in Fig. 4.22.
2. Use a 7.5-minute map. A 7.5-minute map roughly covers 10×13 km^2, or 6×8 mi^2. The increment of elevation between two contours is 3 or 6 m (10 or 20 ft). The fine resolution of elevation data proves

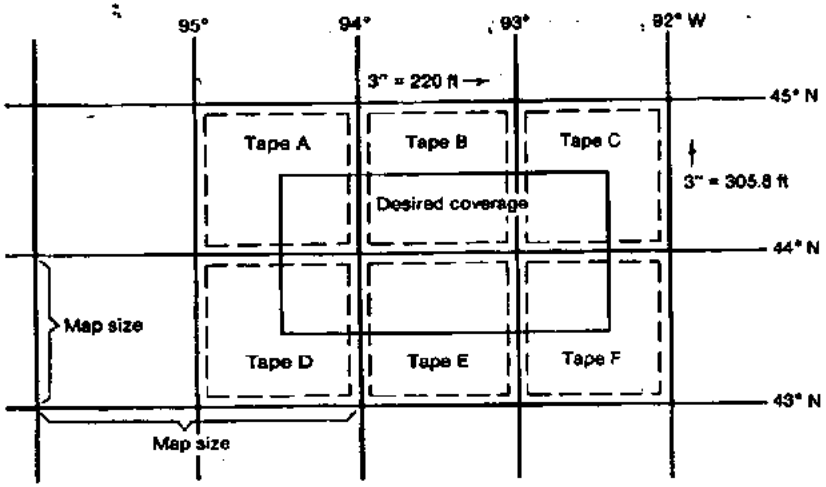

Figure 4.21 A coverage by six tapes.

to be useful for propagation prediction. There are three ways to deal with the 7.5-minute map.

a. Divide a 7.5-minute scale map into either a 30 × 45 grid map, where each grid is 300 × 300 m (1000 × 1000 ft), or into a 15 × 22.5 grid map, where each grid is 600 × 600 m (2000 × 2000 ft). An eyeball estimate of the elevation vaue in each grid is quite adequate.

b. Use DMA tapes in the area if the 7.5-minute tape is available. The 7.5-minute tape can have 150 3-second points. Therefore, a

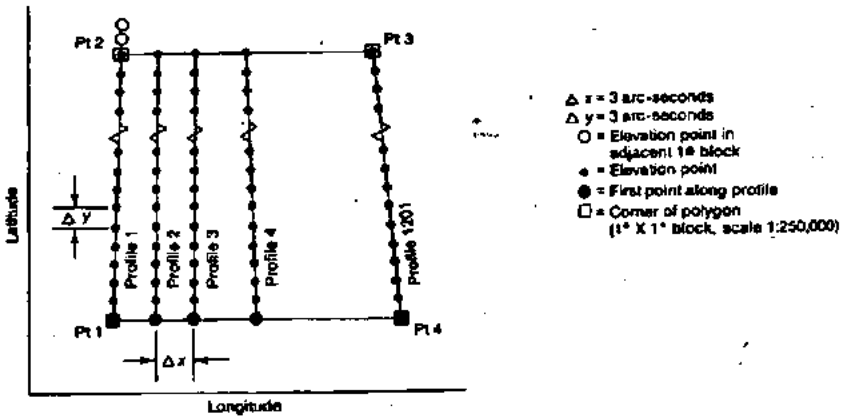

Figure 4.22 Structure of a 250,000:1-scale digital elevation format.

quarter-million scale tape can be replaced by $8 \times 8 = 64$ 7.5 minute maps. The 7.5-minute tapes are used in those areas of the quarter-million map tapes when the terrain contour changes rapidly.

c. The elevation contour line of a 7.5-minute map with the same elevation contour can be digitized in different sample points on the map and stored in a database or on a tape. Then any two points along the terrain elevation contour can be plotted based on the actual contour lines. This is the most accurate method; however, sometimes the accuracy obtained from item *a* is sufficient for predicting the path loss.

4.9.2 Elevation map

We prefer to use the arc-second tape since the continuity of sample points from tape to tape simplifies the calculation. In the area of N40° latitude, the average elevation of a 2000 × 2000 ft (roughly) grid can be found by taking 7 samples in latitude (a length of 2141 ft) and 10 samples in longitude (a length of 2200 ft).

$$\text{Average elevation} = \frac{\sum_{1}^{70} \text{sample elevations}}{70} \quad \text{(in one grid)}$$

Figure 4.23 shows an elevation map whose grids are approximately 2200 × 2200 ft in area. The average elevation of each grid is given along with a (Y, X) tag.

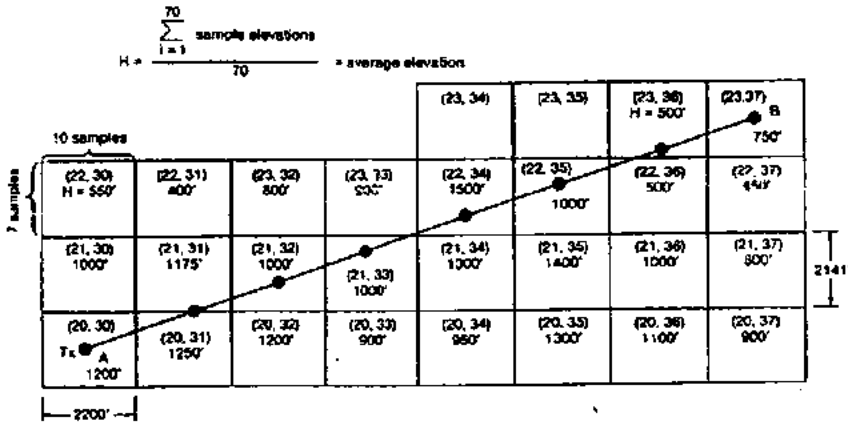

Figure 4.23 Elevation map.

4.9.3 Elevation contour

Assuming that a transmitter is in a grid (20, 30) and the receiver is in a grid (23, 37), then an elevation contour can be plotted with an increment of 2200 ft for every elevation point in its corresponding grid, as shown in Fig. 4.24.

Assume that the antenna height is 100 m (300 ft) at the transmitter and 3 m (10 ft) at the receiver. We can plot a line between two ends and see that shadow-loss condition exists. An example the path loss calculation for this particular path is as follows.

Example 4.11 If the transmitter power is 5 W, the base station antenna gain is 2 dB above dipole, and its height is 300 ft, calculate the path loss from the path shown in Fig. 4.24. The results are given in Table 4.3.

4.10 Cell-Site Antenna Heights and Signal Coverage Cells

4.10.1 Effects of cell-site antenna heights

There are several points which need to be clarified concerning cell-site antenna-height effects.

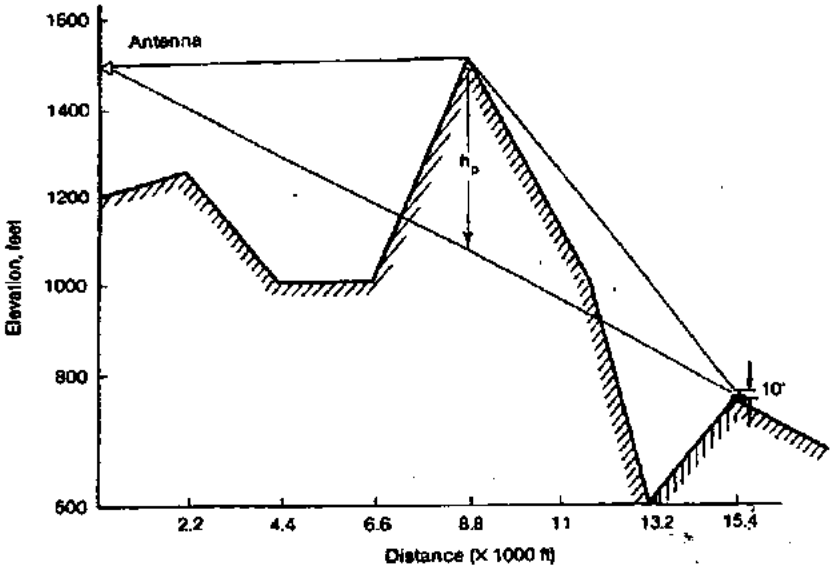

Figure 4.24 Elevation contour.

TABLE 4.3 Work Sheet for Example 4.11

Classification of area: suburban
Distance: 15,400 ft = 2.92 mi
From the curve: (see Fig. 4.3)
P_r = 79.5 dBm

New data:	*Corrections:*
Transmitter power = 5 W	−3 dB
Antenna gain = 2 dB per dipole	−4 dB
Antenna height = 300 ft, 20 log $\frac{300}{100}$ =	+9.5 dB
	+2.5 dB

For flat-terrain case:
New path loss P_r' = −79.5 dBm + 2.5 dB = −77 dBm
For shadow-region case:
r_1 = 8800 ft r_2 = 6600 ft h_p = 450 ft f = 850 MHz
v = −9.63
L = 32.6 $\left[L = 20 \log\left(-\frac{0.225}{v}\right)\right]$
New path loss P_r' = − 77 dB − 33 dB = −110 dBm

Antenna height unchanged. If the power of the cell-site transmitter changes, the whole signal-strength map (obtained from Sec. 4.9) can be linearly updated according to the change in power.

If the transmitted power increases by 3 dB, just add 3 dB to each grid in the signal-strength map. The relative differences in power among the grids remain the same.

Antenna height changed. If the antenna height changes ($\pm\Delta h$), then the whole signal-strength map obtained from the old antenna height cannot be updated with a simple antenna gain formula as

$$\Delta g = 20 \log \frac{h_1'}{h_1} \tag{4.10-1}$$

where h_1 is the old actual antenna height and h_1' is the new actual antenna height. However, we can still use the same terrain contour data along the radio paths (from the cell-site antenna to each grid) to figure out the difference in gain resulting from the different effective antenna heights in each grid.

$$\Delta g' = 20 \log \frac{h_e'}{h_e} = 20 \log \frac{h_e \pm \Delta h}{h_e} \tag{4.10-2}$$

where h_e is the old effective antenna height and h_e' is the new effective antenna height. The additional gain (increase or decrease) will be added to the signal-strength grid based on the old antenna height.

Example 4.12 If the old cell-site antenna height is 30 m (100 ft) and the new one h_1', is 45 m, the mobile unit 8 km (5 mi) away sees the old cell-site effective antenna height (h_e) being 60 m. The new cell-site effective antenna height h'_e seen from the same mobile spot can be derived.

$$h_e' = h_e + (h_1' - h_1) = h_e + (h_e' - h_e) = h_e + \Delta h = 60 + (45 - 30) = 75 \text{ m}$$

Since the difference between two actual antenna heights is the same as the difference between the two corresponding effective antenna heights seen from each grid, the additional gain (or loss) based on the new change of actual antenna height is

$$\Delta g' = 20 \log \frac{h_e'}{h_e} = 20 \log \left(1 + \frac{h_1' - h_1}{h_e}\right) \qquad \text{(E4.12-1)}$$

Location of the antenna changed. If the location of the antenna changes, the point-to-point program has to start all over again. The old point-to-point terrain contour data are no longer useful. The old effective antenna height seen from a distance will be different when the location of the antenna changes, and there is no relation between the old effective antenna height and the new effective antenna height. Therefore, every time the antenna location changes, the new point-to-point prediction calculation starts again.

Visualization of the effective antenna height. The effective antenna height changes when the location of the mobile unit changes. Therefore, we can visualize the effective antenna height as always changing up or down while the mobile unit is moving. This kind of picture should be kept in mind. In addition, the following facts would be helpful.

Case 1: The mobile unit is driven up a positive slope (up to a high spot). The effective antenna height increases if the mobile unit is driving away from the cell-site antenna, and it decreases if the mobile unit is approaching the cell-site antenna. (See Fig. 4.25*a*.)

Case 2: The mobile unit is driven down a hill. The effective antenna height decreases if the mobile unit is driving away from the cell-site antenna, and it increases if the mobile unit is approaching the cell-site antenna. (See Fig. 4.25*a*.)

4.10.2 Visualization of Signal Coverage Cells

A physical cell is usually visualized as a signal-reception region around the cell site. Within the region, there are weak spots called *holes*. This is always true when a cell covers a relative flat terrain.

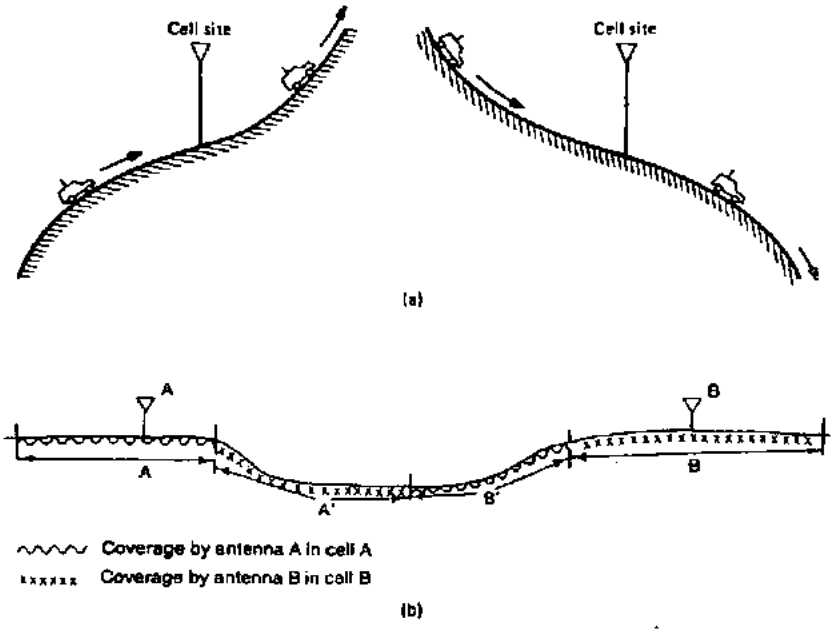

Figure 4.25 Different coverage concept. (*a*) Signal coverage due to effective antenna heights. (*b*) Signal coverage served by two cell sites.

However, a cell can contain a hilly area. Then the coverage patterns of the cell will look like those shown in Fig. 4.25*b*. Here the two cell sites are separated by a river. Because of the shadow loss due to the river bank, cell site A cannot cover area A', but cell site B can. The same situation applies to cell site B in area B'. Now every time the vehicle enters area A', a handoff is requested as if it were in cell B.

Therefore, in most cases, the holes in one cell are covered by the other sites. As long as the processing capacity at the MTSO can handle excessive handoff, this overlapped arrangement for filling the holes is a good approach in a noninterference condition.

4.11 Mobile-to-Mobile Propagation[44]

4.11.1 The transfer function of the propagation channel

In mobile-to-mobile land communication, both the transmitter and the receiver are in motion. The propagation path in this case is usually obstructed by buildings and obstacles between the transmitter and

receiver. The propagation channel acts like a filter with a time-varying transfer function $H(f, t)$, which can be found in this section.

The two mobile units M_1 and M_2 with velocities V_1 and V_2, respectively, are shown in Fig. 4.26. Assume that the transmitted signal from M_1 is

$$s(t) = u(t)e^{j\omega t} \tag{4.11-1}$$

The receiver signal at the mobile unit M_2 from an ith path is

$$s_i = r_i u(t - \tau_i)e^{j[(\omega_0 + \omega_{1i} + \omega_{2i})(t - \tau_i) + \phi_i]} \tag{4.11-2}$$

where $u(t)$ = signal
ω_0 = RF carrier
r_i = Rayleigh-distributed random variable
ϕ_i = uniformly distributed random phase
τ_i = time delay on ith path

and

$$\omega_{1i} = \text{Doppler shift of transmitting mobile unit on } i\text{th path} \tag{4.11-3}$$

$$= \frac{2\pi}{\lambda} V_1 \cos \alpha_{1i}$$

$$\omega_{2i} = \text{Doppler shift of receiving mobile unit on } i\text{th path} \tag{4.11-4}$$

$$= \frac{2\pi}{\lambda} V_2 \cos \alpha_{2i}$$

where α_{1i} and α_{2i} are random angles shown in Fig. 4.26. Now assume that the received signal is the summation of n paths uniformly distributed around the azimuth.

$$s_r = \sum_{i=1}^{n} s_i(t) = \sum_{i=1}^{n} r_i u(t - \tau_i) \times \exp\{j[(\omega_0 + \omega_{1i} + \omega_{2i})(t - \tau_i) + \phi_i]\}$$

$$= \sum_{i=1}^{n} Q(\alpha_{i,t})u(t - \tau_i)e^{j\omega_0(t - \tau_i)} \tag{4.11-5}$$

where
$$Q(\alpha_i, t) = r_i \exp\{j[(\omega_{1i} + \omega_{2i})t + \phi_i']\} \tag{4.11-6}$$

$$\phi_i' = \phi - (\omega_{1i} + \omega_{2i})\tau_i \tag{4.11-7}$$

Equation (4.11-5) can be represented as a statistical model of the channel, as shown in Fig. 4.27.

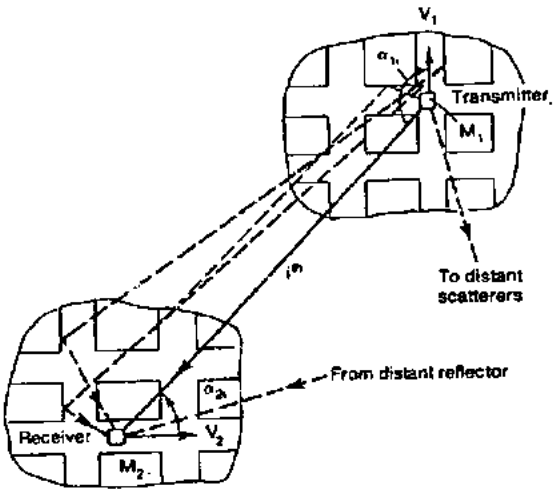

Figure 4.26 Vehicle-to-vehicle transmission.

Let $u(t) = e^{j\omega t}$, then Eq. (4.11-5) becomes

$$e_r(t) = \left[\sum_{i=1}^{n} Q(\alpha_i, t)e^{-j(\omega_0+\omega)\tau_i}\right]e^{j(\omega_0+\omega)t} = H(f, t)e^{j(\omega_0+\omega)t} \quad (4.11\text{-}8)$$

Therefore

$$H(f, t) = \sum_{i=1}^{n} Q(\alpha_i, t)e^{-j(\omega_0+\omega)\tau_i} \quad (4.11\text{-}9)$$

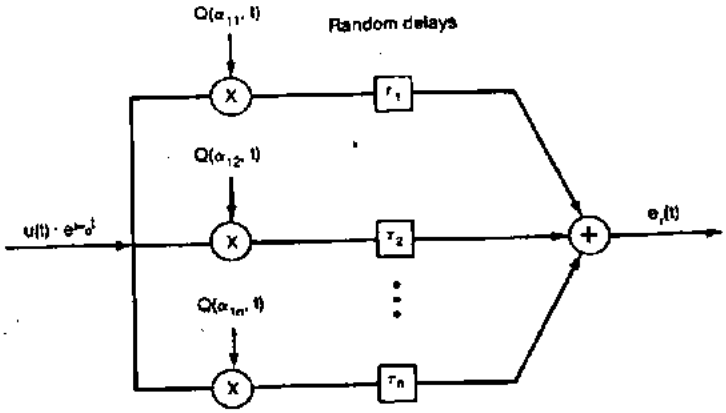

Figure 4.27 Statistical model for mobile-to-mobile channel.

where the signal frequency is $\omega = 2\pi f$. Equation (4.11-9) is expressed in Fig. 4.28.

Let $f = 0$; that is, only a sinusoidal carrier frequency is transmitted. The amplitude of the received signal envelope from Eq. (4.11-8) is

$$r = |H(0, t)| \tag{4.11-10}$$

where r is also a Rayleigh-distributed random variable with its average power of $2\sigma^2$ shown in the probability density function as

$$P(r) = \frac{r}{\sigma^2} e^{-r^2/2\sigma^2} \tag{4.11-11}$$

4.11.2 Spatial time correlation

Let $r_{x_1}(r_1)$ be the received signal envelope at position x_1 at time t_1. Then

$$r_{x_1}(t_1) = \sum_{i=1}^{n} r_i \exp j \left[(\omega_{1i} + \omega_{2i}) + \phi_i + \frac{2\pi}{\lambda} x_1 \cos \alpha_{1i} \right] \tag{4.11-12}$$

The same equation will apply to R_x at position x_2 at time t_2.

The spatial time-correlation function of the envelope is given by

$$R(x_1, x_2, t_1, t_2) = \tfrac{1}{2} \langle r_{x_1}(t_1) r^*_{x_2}(t_2) \rangle \tag{4.11-13}$$

assuming that the random process r is stationary. Then Eq. (4.11-13) can be rewritten as

$$R(\Delta x, \tau) = \sigma^2 J_0(\beta V_1 \tau) J_0(\beta V_2 \tau + \beta \Delta x) \tag{4.11-14}$$

where $\beta = 2\pi/\lambda$
$J_0(\cdot)$ = zero-order Bessel function
$\tau = t_1 - t_2$
$\Delta x = x_1 - x_2$

The normalized time-correlation function is

$$\frac{R(\tau)}{\sigma^2} = J_0(\beta V_1 \tau) J_0(\beta V_2 \tau) \tag{4.11-15}$$

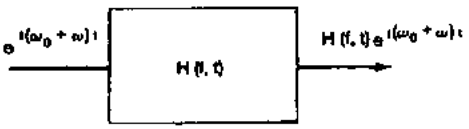

Figure 4.28 A propagation channel model.

Equation (4.11-15) is plotted in Fig. 4.29. The spatial correlation function $R(\Delta x)$ is

$$\frac{R(\Delta x)}{\sigma^2} = J_0(\beta\ \Delta x) \tag{4.11-16}$$

Equation (4.11-16) is the same as for the base-to-mobile channel.

4.11.3 Power spectrum of the complex envelope

The power spectrum $S(f)$ is a Fourier transform of $R(\Delta t)$ from Eq. (4.11-15).

$$S(f) = \int_{-\infty}^{\infty} R(\Delta t)e^{-j2\pi f\Delta t}\, d(\Delta t) \tag{4.11-17}$$

Substituting Eq. (4.11-15) into (4.11-17) yields

$$S(f) = \frac{\sigma^2}{\pi^2 f_1 \sqrt{a}} K\left\{\frac{1+a}{2\sqrt{a}} \sqrt{1 - \left[\frac{f}{(1+a)f_1}\right]^2}\right\} \tag{4.11-18}$$

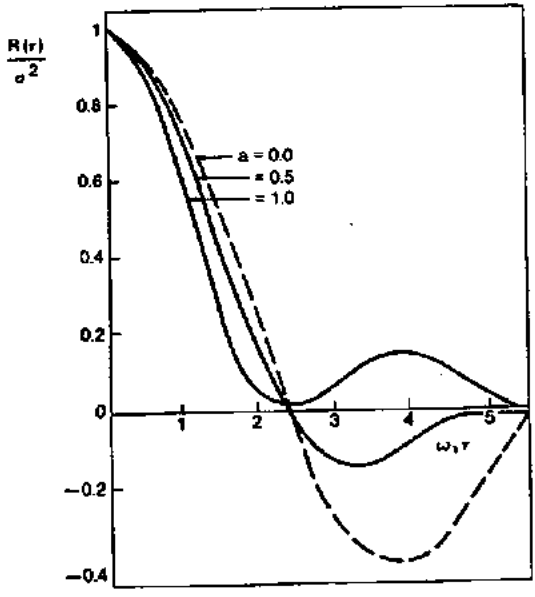

Figure 4.29 Normalized time-correlation function of the complex envelope for different values of $a = V_2/V_1$ versus $\omega_1\ \Delta t$ where $\omega_1 = \beta V_1$. (*After Akki, Ref. 44.*)

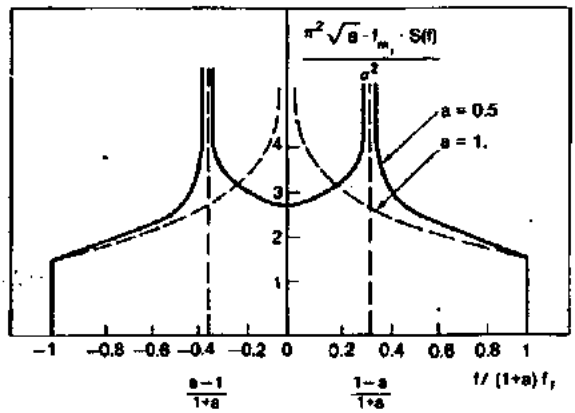

Figure 4.30 Power spectrum of the complex envelope for the case of $a = 0.5$ and $a = 1$ (where $a = V_2/V_1 = f_2/f_1$). (*After Akki, Ref. 44.*)

where $a = f_2/f_1$
$f_1 = V_1/\lambda$
$K(\cdot)$ = complete elliptic integral of the first kind.

Equation (4.11-18) is plotted in Fig. 4.30.

If $V_2 = 0$ and $a = 0$, Eq. (4.11-18) can be reduced to

$$S(f) = \frac{\sigma^2}{\pi\sqrt{f_1^2 - f^2}} \tag{4.11-19}$$

which is the equation for a base-to-mobile channel.

References

1. Y. Okumura et al., "Field Strength and Its Variability in VHF and UHF Land-Mobile Radio Service," *Review of the Electrical Communication Laboratories* Vol. 16, Nos. 9 and 10, 1968, pp. 825–873.
2. M. Hata, "Empirical Formula for Propagation Loss in Land Mobile Radio Services," *IEEE Transactions on Vehicular Technology*, Vol. VT-29, No. 3, 1980, pp. 317–325.
3. A. Akeyama, T. Nagatsu, and Y. Ebine, "Mobile Radio Propagation Characteristics and Radio Zone Design Method in Local Cities," *Review of the Electrical Communication Laboratories* Vol. 30, No. 2, 1982, pp. 308–317.
4. A. G. Longley and P. L. Rice, "Prediction of Tropospheric Radio Transmission Loss Over Irregular Terrain, A Computer Method-1968," ESSA Technical Report ERL 79-ITS 67, NTIS acc. no. 676874, 1968.
5. A. G. Longley, "Radio Propagation in Urban Areas," OT Report 78-144, NTIS, 1978.
6. J. J. Egli, "Radio Propagation Above 40 MC Over Irregular Terrain," *Proceedings of the IRE*, Vol. 45, 1957, pp. 1383–1391.
7. K. Allsebrook and J. D. Parsons, "Mobile Radio Propagation in British Cities at Frequencies in the VHF and UHF Bands," *IEEE Transactions on Vehicular Technology*, Vol. VT-26, No. 4, 1977, pp. 313–323.

7. K. Allsebrook and J. D. Parsons, "Mobile Radio Propagation in British Cities at Frequencies in the VHF and UHF Bands," *IEEE Transactions on Vehicular Technology*, Vol. VT-26, No. 4, 1977, pp. 313–323.
8. K. Bullington, "Radio Propagation for Vehicular Communications," *IEEE Transactions on Vehicular Technology*, Vol. VT-26, No. 4, 1977, pp. 295–308.
9. W. J. Kessler and M. J. Wiggins, "A Simplified Method for Calculating UHF Base-to-Mobile Statistical Coverage Contours over Irregular Terrain," *27th IEEE Vehicular Technology Conference*, 1977, pp. 227–236.
10. W. C. Y. Lee, *Mobile Communications Engineering*, McGraw Hill Book Co., 1982, p. 107.
11. "Bell System Practices Public Land Mobile and UHF Maritime Systems Estimates of Expected Coverage," *Radio Systems General*, July 1963.
12. K. K. Kelly II, "Flat Suburban Area Propagation of 820 MHz," *IEEE Transactions on Vehicular Technology*, Vol. VT-27 November 1978, pp. 198–204.
13. G. D. Ott and A. Plitkins, "Urban Path-Loss Characteristics at 820 MHz," *IEEE Transactions on Vehicular Technology*, Vol. VT-27, November 1978, pp. 189–197.
14. W. R. Young, "Mobile Radio Transmission Compared at 150 to 3700 MC," *Bell System Technical Journal*, Vol. 31, November 1952, pp. 1068–1085.
15. Robert T. Forrest, "Land Mobile Radio, Propagation Measurements for System Design," *IEEE Transactions on Vehicular Technology*, Vol. VT-24, November 1975, pp. 46–53.
16. G. Hagn, "Radio System Performance Model for Predicting Communications Operational Ranges in Irregular Terrain," *29th IEEE Vehicular Technology Conference Record*, 1970, pp. 322–330.
17. Robert Jensen, "900 MHz Mobile Radio Propagation in the Copenhagen Area," *IEEE Transactions on Vehicular Technology, Vol. VT-26, November 1977.*
18. G. L. Turin, "Simulation of Urban Location Systems," *Proceedings of the 21st IEEE Vehicular Technology Conference*, 1970.
19. D. L. Nielson, "Microwave Propagation Measurements for Mobile Digital Radio Applications," *IEEE Transactions on Vehicular Technology*, Vol. VT-27, August 1978, pp. 117–132.
20. V. Graziano, "Propagation Correlations at 900 MHz," *IEEE Transactions on Vehicular Technology*, Vol. VT-27, November 1978, pp. 182–188.
21. D. O. Reudink, "Properties of Mobile Radio Propagation Above 400 MHz," *IEEE Transactions on Vehicular Technology*, Vol. VT-23, November 1974, pp. 143–160.
22. M. F. Ibrahim and J. D. Parsons, "Urban Mobile Propagation at 900 MHz," *IEEE Electrical Letters*, Vol. 18, No. 3, 1982, pp. 113–115.
23. W. C. Y. Lee, *Mobile Communications Engineering*, McGraw-Hill Book Co., 1982, Chap. 4.
24. W. C. Y. Lee, *Mobile Communications Design Fundamentals*, John Wiley & Sons, 1993, pp. 72–94.
25. N. H. Shepherd, "Radio Wave Loss Deviation and Shadow Loss at 900 MHz," *IEEE Transactions on Vehicular Technology*, Vol. VT-26, November 1977, pp. 309–313.
26. B. Bodson, G. F. McClure, and S. R. McConoughey, *Land-Mobile Communications Engineering*, IEEE Press, 1984.
27. H. F. Schmid, "A Prediction Model for Multipath Propagation of Pulse Signals at VHF and UHF over Irregular Terrain," *IEEE Transactions on Antennas and Propagation*, Vol. AP-18, March 1970, pp. 253–258.
28. H. Suzuki, "A Statistical Model for Urban Radio Propagation," *IEEE Transactions on Communications*, Vol. Com-25, July 1977.
29. W. C. Y. Lee, *Mobile Communications Engineering*, McGraw-Hill Book Co., 1982, chap. 4.
30. W. C. Y. Lee, *Mobile Communications Engineering*, McGraw-Hill Book Co., 1982, pp. 137–139.
31. J. S. Bendat and A. G. Piersol, *Random Data, Analysis and Measurement Procedures*, Wiley/Interscience, 1971.
32. E. C. Jordan, *Electromagnetic Waves and Radiation Systems*, Prentice-Hall, 1950, p. 141.

33. W. C. Y. Lee, *Mobile Communications Engineering*, McGraw-Hill Book Co., 1982, p. 92.
34. S. Swarup and R. K. Tewari, "Propagation Characteristics of VHF/UHF Signals in Tropical Moist Deciduous Forest," *Journal of the Institution of Electronics and Telecommunication Engineers*, Vol. 21, No. 3, 1975, pp. 123–125.
35. S. Swarup and R. K. Tewari, "Depolarization of Radio Waves in a Jungle Environment," *IEEE Transactions on Antennas and Propagation*, Vol. AP-27, No. 1, January 1979, pp. 113–116.
36. W. R. Vincent and G. H. Hagn, "Comments on the Performance of VHF Vehicular Radio Sets in Tropical Forests," *IEEE Transactions on Vehicular Technology*, Vol. VT-18, No. 2, August 1969, pp. 61–65.
37. T. Tamir, "On Radio-Wave Propagation in Forest Environments," *IEEE Transactions on Antenna and Propagation, Vol. AP-15, November 1967, pp. 806–817.*
38. T. Tamir, "On Radio-Wave Propagation Along Mixed Paths in Forest Environments," *IEEE Transactions on Antennas and Propagation*, Vol. AP-25, July 1971, pp. 471–477.
39. E. C. Jordan (ed.), *Reference Data for Engineers*, 7th ed., Howard W. Sams & Co., 1985, chap. 33.
40. W. C. Y. Lee, *Mobile Communications Design Fundamentals*, John Wiley & Sons, 1993, pp. 30–31.
41. W. C. Y. Lee, "A New Propagation Path-Loss Prediction Model for Military Mobile Access," 1985 IEEE Military Communications Conference, Boston, Conference Record, Vol. 2, pp. 19–21.
42. W. C. Y. Lee, "Studies of Base Station Antenna Height Effect on Mobile Radio," *IEEE Transactions on Vehicular Technology*, Vol. VT-29, May 1980, pp. 252–260.
43. George Washington University, Continuing Engineering Education Program, course 1086, "Mobile Cellular Telecommunications Systems." A lecture note prepared by W. C. Y. Lee.
44. A. S. Akki, F. Haber, "A Statistical Model of Mobile-to-Mobile Land Communication Channels," *IEEE Transactions on Vehicular Technology*, Vol. VT-35, February 1986, p. 2.
45. W. C. Y. Lee, "Mobile Communications Design Fundamentals," John Wiley & Sons, 1993, pp. 88–94.

Chapter

5

Cell-Site Antennas and Mobile Antennas

5.1 Equivalent Circuits of Antennas

The operating conditions of an actual antenna (Fig. 5.1*a*) can be expressed in an equivalent circuit for both receiving (Fig. 5.1*b*) and transmitting (Fig. 5.1c). In Fig. 5.1, Z_a is the antenna impedance, Z_L is the load impedance, and Z_T is the impedance at the transmitter terminal.

5.1.1 From the transmitting end (obtaining free-space path-loss formula)

Power P_t originates at a transmitting antenna and radiates out into space. (Equivalent circuit of a transmitting antenna is shown in Fig. 5.1*b*.) Assume that an isotropic source P_t is used and that the power in the spherical space will be measured as the power per unit area. This power density, called the *Poynting vector* ρ or the outward flow of electromagnetic energy through a given surface area, is expressed as

$$\rho = \frac{P_t}{4\pi r^2} \quad \text{W/m}^2 \tag{5.1-1}$$

A receiving antenna at a distance r from the transmitting antenna with an aperture A will receive power

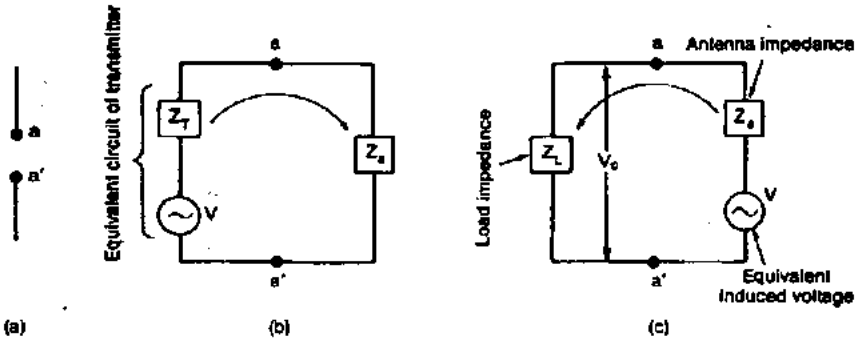

Figure 5.1 An actual antenna and its equivalent circuit. (*a*) An actual antenna; (*b*) equivalent circuit of a transmitting antenna; (*c*) equivalent circuit of a receiving antenna.

$$P_r = \rho A = \frac{P_t A}{4\pi r^2} \quad \text{W} \tag{5.1-2}$$

Figure 5.2 is a schematic representation of received power in space.

From Eq. (5.1-2) we can derive the free-space path-loss formula because we know the relationship between the aperture A and the gain G.

$$G = \frac{4\pi A}{\lambda^2} \tag{5.1-3}$$

For a short dipole, $G = 1$. Then

$$A = \frac{\lambda^2}{4\pi} \tag{5.1-4}$$

Substitution of Eq. (5.1-4) into Eq. (5.1-2) yields the free-space formula

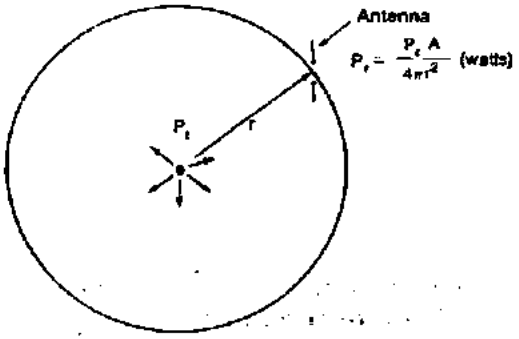

Figure 5.2 Received power in space.

$$P_r = P_t \frac{1}{(4\pi r/\lambda)^2} \tag{5.1-5}$$

5.1.2 At the receiving end dBμV ↔ dBm (decibels above 1 μV ↔ decibels above 1 mW)

We can obtain the received power from Fig. 5.1c

$$P_r = \frac{V^2 Z_L}{(Z_L + Z_a)^2} \tag{5.1-6}$$

where V is the induced voltage in volts. For a maximum power delivery $Z_L = Z_a^*$, where the notation * indicates complex conjugate. Then we obtain $Z_L + Z_a = 2R_L$, where R_L is the real-load resistance. Equation (5.1-6) becomes

$$P_r = \frac{V^2}{4R_L} \tag{5.1-7}$$

Assume that a dipole or a monopole is used as a receiving antenna. The induced voltage V can be related to field strength E as[1]

$$V = \frac{E\lambda}{\pi} \tag{5.1-8}$$

where E is expressed in volts or microvolts per meter. Substitution of Eq. (5.1-7) into Eq. (5.1-8) yields

$$P_r = \frac{E^2\lambda^2}{4\pi^2 R_L} \tag{5.1-9}$$

If we set $R_L = 50\ \Omega$, P_r in decibels above 1 mW, and E in decibels (microvolts per meter), Eq. (5.1-9) becomes

$$P_r(\text{dBm}) = E\ (\text{dB}\mu\text{V}) - 113\ \text{dBm} + 10 \log \left(\frac{\lambda}{\pi}\right)^2 \tag{5.1-10}$$

The notation "dBμV" in Eq. (5.1-10) is a simplification of decibels above 1 μV/m, and has been accepted by the Institute of Radio Engineers. We can find the equivalent aperture A of Eq. (5.1-2) because the Poynting vector ρ can be expressed as

$$\rho = \frac{E^2}{Z_0} \tag{5.1-11}$$

where Z_0 is the instrinsic impedance of the space (= 120 π). By sub-

stituting Eq. (5.1-11) into Eq. (5.1-2) and comparing it with Eq. (5.1-9) we obtain the equivalent aperture A.

$$A = \frac{\lambda^2 Z_0}{4\pi^2 R_L} \tag{5.1-12}$$

Equation (5.1-12) is the same as that given in Eq. 3.11 in Ref. 2.

5.1.3 Practical use of field-strength–received-power conversions

There is always confusion between the following two conversions.

Measuring field strength and converting it to received power. From Eq. (5.1-10), converting field strength in decibels above 1 μV/m to power received in decibels above 1 mW at 850 MHz by a dipole with a 50-Ω load is −132 dB.

$$P_r \quad \text{dBm} = E \quad \text{dB } (\mu\text{V/m}) - 132 \text{ dB} \tag{5.1-13}$$

at 850 MHz

$$39 \text{ dB } (\mu\text{V/m}) = -93 \text{ dBm} \tag{5.1-14}$$

The notation "39-dBμV contour" is commonly used to mean 39 dB (μV/m) in cellular system design. Equation (5.1-13) is valid only at a given frequency (850 MHz), for a given antenna (monopole or dipole antenna), and for a given antenna load (50 Ω). Otherwise the field strength and the power have to be adjusted accordingly.

Measuring the voltage V_0 at the load terminal (Fig. 5.1c) and converting to received power. Given $P_r = (V_0^2/R_L)$, where $R_L = 50$ Ω, we can obtain a relationship

$$0 \text{ dB}\mu\text{V} \; (=) \; -107 \text{ dBm} \tag{5.1-15}$$

For example, if a voltage meter at V_0 is 7 dBμV, then the received power is −100 dBm. Equation (5.1-15) expresses a voltage-to-power ratio which varies with the load impedance but is independent of the frequency and the type of antenna.

5.1.4 Effective radiated power

There is a standard way of specifying the power radiated within a given geographic area. The radiated power that can be transmitted should be converted to the amount of power radiated from an omni-

directional antenna (particularly a dipole antenna). If a high-gain antenna is used, the transmitted power should be reduced. Therefore, if the specification states that the effective radiated power (ERP) or the transmitted power multiplied by the antenna gain is 100 W (50 dBm) and if a 10-dB high-gain antenna is used, the actual transmitted power should be 10 W (40 dBm).

There is also a term called *effective isotropic radiated power* (EIRP). EIRP is referenced to an isotropic point source. The difference between ERP and EIRP is 2 dB.

$$\text{ERP} = \text{EIRP} - 2 \text{ dB}$$

5.2 The Gain-and-Pattern Relationship

5.2.1 The gain of an antenna or an antenna array

$$G = \frac{4\pi(\text{maximum radiation intensity})}{\text{total power radiated}}$$

$$= \frac{E_{\max}^2(\theta_m, \phi_m)}{\overline{E}^2(\theta, \phi)} \tag{5.2-1}$$

where E = electric field
$E_{\max}$ = maximum of E
$\overline{E}^2$ = average value of E^2 which is related to the radiation intensity
θ, ϕ = angles shown in Fig. 5.3

We can obtain the antenna pattern E from either a measurement or an analytic form. Then the gain G from the pattern E can be calculated.

5.2.2 The pattern and gain of an antenna array

Frequently, it is necessary to calculate the gain of an antenna array. The general field pattern can be expressed as[3]

$$E(\theta, \phi) = \frac{\sin\left[N\pi(d\cos\phi \cdot \sin\theta + \psi)\right]}{N\sin\left[\pi(d\cos\phi \cdot \sin\theta + \psi)\right]} \times \begin{pmatrix}\text{individual antenna}\\ \text{element pattern}\end{pmatrix} \tag{5.2-2}$$

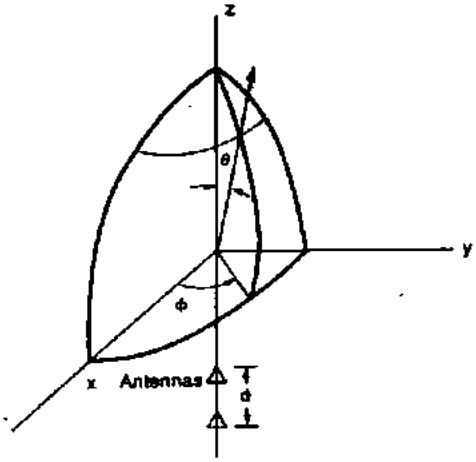

Figure 5.3 A coordinate of antenna arrays.

where N = number of elements in an array
d = spacing between adjacent elements in wavelength
ψ = phase difference between two adjacent elements
ϕ, θ = radiation angles are shown in Fig. 5.3
$\theta = 90°$ = direction perpendicular to the array axis

The gain of the array can be obtained by substituting Eq. (5.2-2) into Eq. (5.2-1). Two cases are listed below.

1. *A broadside-array case* ($\psi = 0$). The individual elements are in parallel and lie in the y-z plane. In this case the gain related to a single element of any type of antenna is shown below.

	Gain G, dB	
N	$d = 0.5\lambda$	$d = 0.9\lambda$
2	4	4.6
3	5.5	6
4	7	8
6	9	10.4
8	10	12
12	12	14
16	13.2	15.4

2. *A collinear-array case* ($\psi = 0$). The individual elements are collinear in the z axis. In this case, the gain related to a single dipole element is as shown in the following table.

	Gain G, dB	
N	$d = 0.5\lambda$	$d = 0.9\lambda$
2	2.2	3.7
3	3.8	5.7
4	4.9	8.1
6	6.5	9.0
8	8.8	9.4
12	9.4	12.2
16	10.7	13.4

5.2.3 The relationship between gain and beamwidth

A general formula. Assume that the gain G and the directivity D are nearly the same. Then[4]

$$G \approx D = \frac{32{,}400}{\phi^\circ\theta^\circ} \qquad \text{for small } \phi \text{ and } \theta \tag{5.2-3}$$

where ϕ° and θ° are the 3-dB beamwidths in two planes. Elliott[4] points out that when ϕ and θ are small (<40°) the figure in Eq. (5.2-3) reported by Kraus[5] (41,253) is based on the incorrect assumption that the cross section formed by θ and ϕ is rectangular. It is, in fact, elliptical, so its area is $\pi/4$ that of Kraus' figure, or 32,400. However, for large (>40°) ϕ° and θ°, the Kraus equation

$$G \approx D = \frac{41{,}253}{\phi^\circ\theta^\circ} \qquad \text{for large } \phi^\circ \text{ and } \theta^\circ \tag{5.2-4}$$

has been shown to be valid. For a high-gain or high-directivity antenna, the gain G resulting from decreased efficiency through the system has only 50 to 70 percent of the directivity D.

For a linear element or collinear array. If a linear element is used, the approximate gain also can be obtained from a vertical 3-dB beamwidth. Assume that the array or the linear element has a doughnut pattern. The relationship between the 3-dB beamwidth θ_0 and the gain G for a linear element or a collinear array can be derived in decibels, above an isotropic source which is a unity gain from Eq. (5.2-3) provided the angle θ_0 is small (<40°).[6]

$$G \approx D = \frac{101.5^\circ}{\theta_0} \qquad \text{or} \qquad D = 10 \log \left(\frac{101.5}{\theta_0}\right) \qquad \text{for small } \theta_0 \tag{5.2-5}$$

Assume that the gain G and the directivity D are the same. The gain G always refers to an isotropic source which is 2 dB lower than the gain of a dipole. Equation (5.2-5), which is valid for small θ_0, may have an error of $\pm 1°$ as compared with the measured pattern. For large θ_0, the relationship between G and θ_0 can be found from Eq. (5.2-4) as

$$G \approx D = \frac{114.6°}{\theta_0} \tag{5.2-6}$$

Example 5.1 For gain of 9 dB with respect to a dipole antenna or 11 dB with respect to a short dipole, 3-dB beamwidth is

$$\theta_0 = \frac{101.5°}{10^{1.1}} = \frac{101.5°}{12.59} = 8°$$

For a gain of 6 dB with respect to a dipole antenna, the 3-dB beamwidth is

$$\theta_0 = \frac{101.5°}{6.32} = 16°$$

In reality, because of the inefficiency of power delivery, the gain would decrease by 1 dB as a result of a mismatch measured from a (voltage standing-wave ratio) (VSWR)

$$G = 10 \log \frac{101.5}{\theta_0} - 1 \quad \text{dB} \tag{5.2-7}$$

Equation (5.2-7) would be used for an antenna operating within its marginal frequency range.

5.3 Sum-and-Difference Patterns—Engineering Antenna Pattern

After obtaining a predicted field-strength contour (see Sec. 4.8), we can engineer an antenna pattern to conform to uniform coverage. For different antennas pointing in different directions and with different spacings, we can use any of a number of methods. If we know the antenna pattern and the geographic configuration of the antennas, a computer program can help us to find the coverage. Several synthesis methods can be used to generate a desired antenna configuration.

5.3.1 General formula

Many applications of linear arrays are based on sum-and-difference patterns. The mainbeam of the pattern is always known as the sum

pattern pointing at an angle θ_0. The difference pattern produces twin mainbeams straddling θ_0. When $2N$ elements are in an array, equispaced by a separation d, the general pattern for both sum and difference is

$$A(\theta) = \sum_{n=1}^{N} I_n \exp\left[j\frac{2n-1}{2}\beta d(\cos\theta - \cos\theta_0)\right] + I_{-n}\exp\left[-j\frac{2n-1}{2}\beta d(\cos\theta - \cos\theta_0)\right] \quad (5.3\text{-}1)$$

where β = wavenumber = $2\pi/\lambda$
I_n = normalized current distributions
N = total number of elements

For a sum pattern, all the current amplitudes are the same.

$$I_n = I_{-n} \quad (5.3\text{-}2)$$

For a difference pattern, the current amplitudes of one side (half of the total elements) are positive and the current amplitudes of the other side (half of the total elements) are negative.

$$I_n = -I_{-n} \quad (5.3\text{-}3)$$

Most pattern synthesis problems can be solved by determining the current distribution I_n. A few solutions follow.

5.3.2 Synthesis of sum patterns

Dolph-Chebyshev synthesis of sum patterns. This method can be used to reduce the level of sidelobes; however, one disadvantage of further reduction of sidelobe level is broadening of the mainbeam. The techniques are discussed in Ref. 7.

Taylor synthesis. A continuous line-source distribution or a distribution for discrete arrays can give a desired pattern which contains a single mainbeam of a prescribed beamwidth and pointing direction with a family of sidelobes at a common specified level. The Taylor synthesis is derived from the following equation, where an antenna pattern $F(\theta)$ is determined from an aperture current distribution $g(l)$

$$F(\theta) = \int_{-a}^{a} g(l)e^{j\beta l\cos\theta}\,dl \quad (5.3\text{-}4)$$

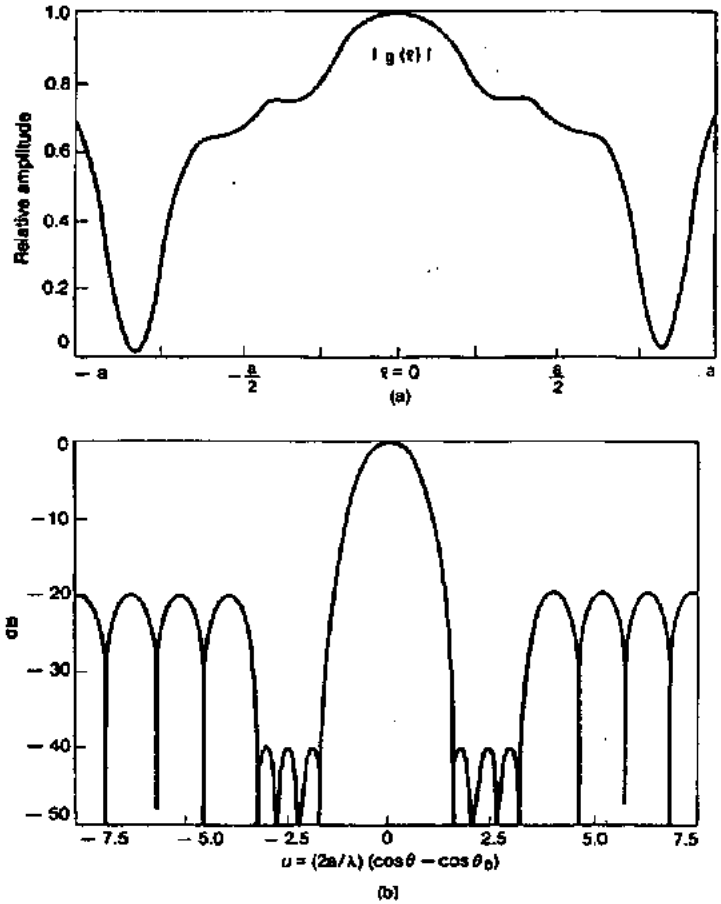

Figure 5.4 A symmetrical sum pattern (*reprinted from Elliot, Ref. 8*). (*a*) The aperture distribution for the two-antenna arrangement shown in Fig. 5.11*b* (© *1976 IEEE; reprinted from IEEE AP Transactions, 1976, pp. 76–83*). (*b*) The evolution of a symmetrical sum pattern with reduced inner sidelobes (© *1976 IEEE; reprinted from IEEE AP Transactions, 1976, pp. 76–83*).

Symmetrical pattern.[8] For production of a symmetrical pattern at the mainbeam, the current-amplitude distribution $|g(l)|$ is the only factor to consider. The phase of the current distribution can remain constant. A typical pattern (Fig. 5.4*a*) would be generated from a current-amplitude distribution (Fig. 5.4*b*).

Asymmetrical pattern. For production of an asymmetrical pattern, both current amplitude $|g(l)|$ and phase $\arg g(l)$ should be considered.

5.3.3 Synthesis of difference patterns (Bayliss synthesis)[9]

To find a continuous line source that will produce a symmetrical difference pattern, with twin mainbeam patterns and specified sidelobes, we can set

$$D(\theta) = \int_{-a}^{a} g(l)e^{j\beta l \cos\theta}\, dl \tag{5.3-5}$$

For a desired difference pattern such as that shown in Fig. 5.5*a*, the current-amplitude distributions $|g(l)|$ should be designed as shown in Fig. 5.5*b* and the phase $\arg g(l)$ as shown in Fig. 5.5*c*.

5.3.4 Null-free patterns

In mobile communications applications, field-strength patterns without nulls are preferred for the antennas in a vertical plane. The typical vertical pattern of most antennas is shown in Fig. 5.6*a*. The field pattern can be represented as

$$F(u) = \sum_{n=0}^{N} K_n \frac{\sin \pi u}{\pi u} \tag{5.3-6}$$

where $u = (2a/\lambda)(\cos\theta - \cos\theta_n)$. The concept is to add all $(\sin \pi u)/(\pi u)$ patterns at different pointing angles as shown in Fig. 5.6*a*. K_n is the maximum signal level. The resulting pattern does not contain nulls. The null-free pattern can be applied in the field as shown in Fig. 5.6*b*.

5.3.5 Practical applications

In designing a collinear array for the high-gain omnidirectional antenna, it is possible to control the current distribution by a microprocessor. This synthesis technique awaits further investigation by antenna research-and-development (R&D) specialists.

5.4 Antennas at Cell Site

5.4.1 For coverage use—omnidirectional antennas

High-gain antennas. There are standard 6-dB and 9-dB gain omnidirectional antennas. The antenna patterns for 6-dB gain and 9-dB gain are shown in Fig. 5.7.

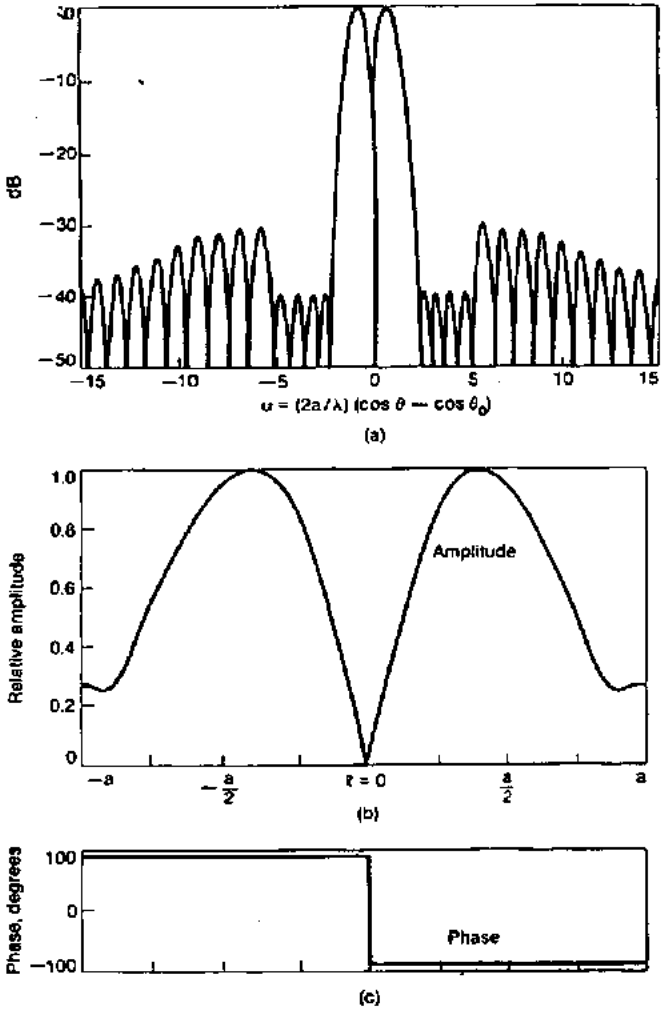

Figure 5.5 A symmetrical difference pattern (*reprinted from Elliot, Ref. 9*). (a) A modified Bayliss difference pattern; inner sidelobes symmetrically depressed. (© *IEEE; reprinted from IEEE AP Transactions, 1976, pp. 310–316*). (*b*, c) Aperture distribution for the pattern. (© *IEEE; reprinted from IEEE AP Transactions, 1976, pp. 310–316*).

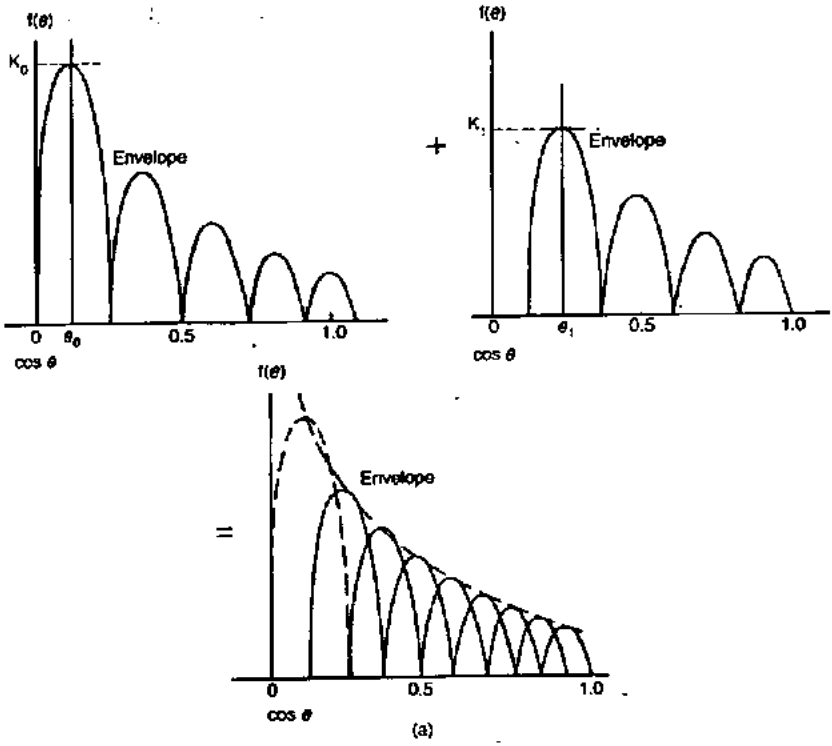

Figure 5.6 Null-free patterns. (*a*) Formation of a null-free pattern; (*b*) application of a null-free pattern (*reprinted from Elliott, Ref. 4, p. 192*).

Start-up system configuration. In a start-up system, an omnicell, in which all the transmitting antennas are omnidirectional, is used. Each transmitting antenna can transmit signals from 16 radio transmitters simultaneously using a 16-channel combiner. Each cell normally can have three transmitting antennas which serve 45 voice radio transmitters* simultaneously. Each sending signal is amplified by its own channel amplifier in each radio transmitter, then 16 channels (radio signals) pass through a 16-channel combiner and transmit signals by means of a transmitting antenna (see Fig. 5.8*a*).

Two receiving antennas commonly can receive all 45 voice radio signals simultaneously. Then in each channel, two identical signals re-

* The combiner is designed for combining 16 voice channels. However, the cellular system divides its 312 voice channels into 21 sets; each set consists of only about 15 voice channels. Therefore the dummy loads have to be put on some empty ports of a 16-channel combiner.

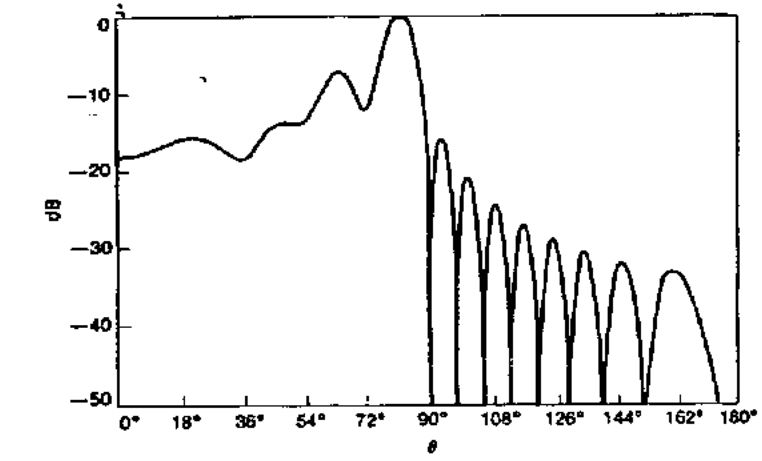

Null-Filled Cosecant Squared Pattern

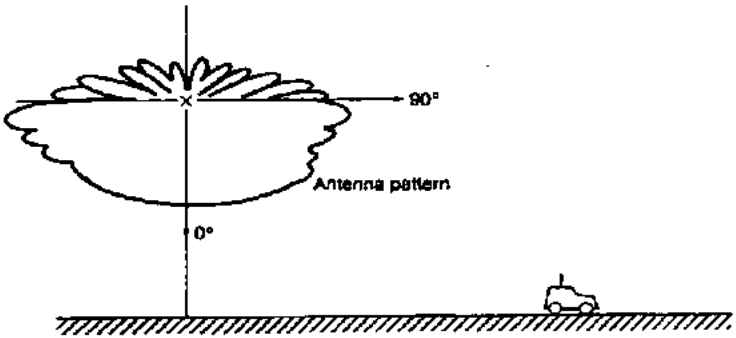

(b)

Figure 5.6 (*Continued*)

ceived by two receiving antennas pass through a diversity receiver of that channel. The receiving antenna configuration on the antenna mast is shown in Fig. 5.8. The separation of antennas for a diversity receiver is discussed in Sec. 5.5.

Abnormal antenna configuration. Usually, the call traffic in each cell increases as the number of customers increases. Some cells require a greater number of radios to handle the increasing traffic. An omnicell site can be equipped with up to 90 voice radios. In such cases six transmitting antennas should be used as shown in Fig. 5.8*b*. In the meantime, the number of receiving antennas is still two. In order to reduce the number of transmitting antennas, a hybrid ring combiner

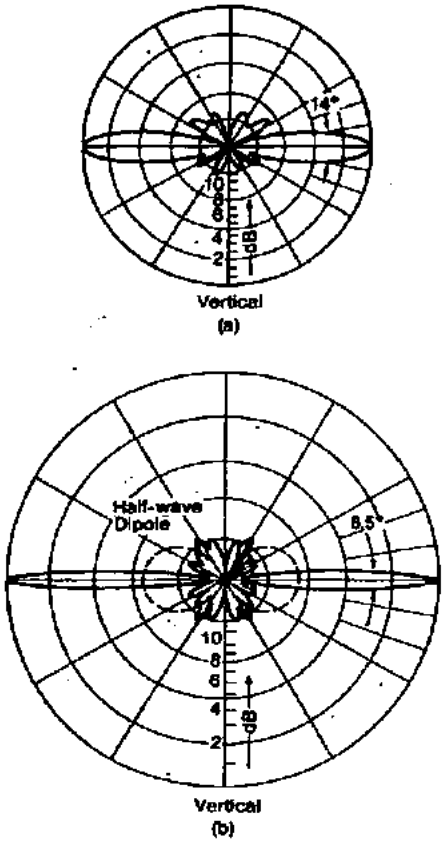

Figure 5.7 High-gain omnidirectional antennas (*reprinted from Kathrein Mobile Communications Catalog*). Gain with reference to dipole: (*a*) 6 dB; (*b*) 9 dB.

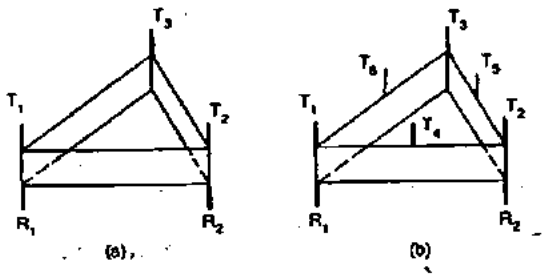

Figure 5.8 Cell-site antennas for omnicells: (*a*) for 45 channels; (*b*) for 90 channels.

which can combine two 16-channel signals is found.[10] This means that only three transmitting antennas are needed to transmit 90 radio signals. However, the ring combiner has a limitation of handling power up to 600 W with a loss of 3 dB.

5.4.2 For interference reduction use—directional antennas

When the frequency reuse scheme must be used, cochannel interference will occur. The cochannel interference reduction factor $q = D/R = 4.6$ is based on the assumption that the terrain is flat. Because actual terrain is seldom flat, we must either increase q or use directional antennas.

Directional antennas. A 120°-corner reflector or 120°-plane reflector can be used in a 120°-sector cell. A 60°-corner reflector can be used in a 60°-sector cell. A typical pattern for a directional antenna of 120° beamwidth is shown in Fig. 5.9.

Normal antenna (mature system) configuration

1. $K = 7$ cell pattern (120° sectors). In a $K = 7$ cell pattern for frequency reuse, if 333 channels are used, each cell would have about 45 radios. Each 120° sector would have one transmitting antenna and two receiving antennas and would serve 16 radios. The two receiving antennas are used for diversity (see Fig. 5.10*a*).
2. $K = 4$ cell pattern (60° sectors). We do not use $K = 4$ in an omnicell system because the cochannel reuse distance is not adequate. Therefore, in a $K = 4$ cell pattern, 60° sectors are used.[11] There are 24 sectors. In this $K = 4$ cell-pattern system, two approaches are used.
   a. Transmitting-receiving 60° sectors. Each sector has a transmitting antenna carrying its own set of frequency radios and hands off frequencies to other neighboring sectors or other cells. This is a full $K = 4$ cell-pattern system. If 333 channels are used, with 13 radios per sector, there will be one transmitting antenna and one receiving antenna in each sector. At the receiving end, two of six receiving antennas are selected for an angle diversity for each radio channel (see Fig. 5.10*b*).
   b. Receiving 60° sectors. Only 60°-sector receiving antennas are used to locate mobile units and hand off to a proper neighboring cell with a high degree of accuracy. All the transmitting antennas are omnidirectional within each cell. At the receiving end, the angle diversity for each radio channel is also used in this case.

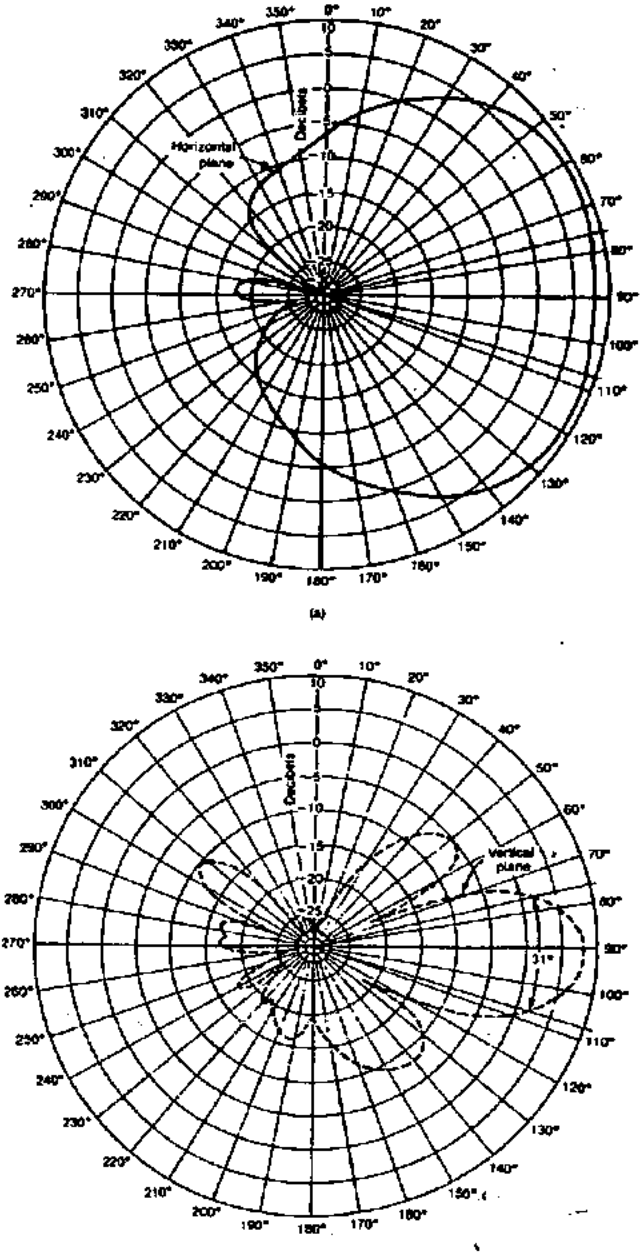

Figure 5.9 A typical 8-dB directional antenna pattern. (*Reprinted from Bell System Technical Journal, Vol. 58, January 1979, pp. 224–225.*) (*a*) Azimuthal pattern of 8-dB directional antenna. (*b*) Vertical pattern of 8-dB directional antenna.

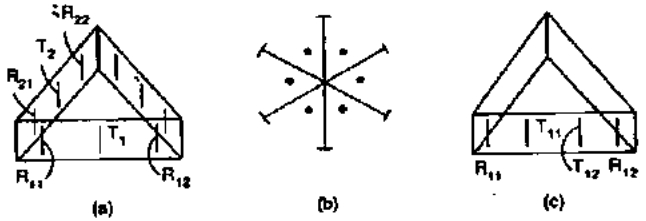

Figure 5.10 Directional antenna arrangement: (*a*) 120° sector (45 radios); (*b*) 60° sector; (*c*) 120° sector (90 radios).

Abnormal antenna configuration. If the call traffic is gradually increasing, there is an economic advantage in using the existing cell systems rather than the new splitting cell system (splitting into smaller cells). In the former, each site is capable of adding more radios. In a $K = 7$ cell pattern with 120° sectors, two transmitting antennas at each sector are used (Fig. 5.10c). Each antenna serves 16 radios if a 16-channel combiner is used. One observation from Fig. 5.10c should be mentioned here. The two transmitting antennas in each sector are placed relatively closer to the receiving antennas than in the single transmitting antenna case. This may cause some degree of desensitization in the receivers. The current technology can combine 32 channels[10] in a combiner; therefore, only one transmitting antenna is needed in each sector. However, this one transmitting antenna must be capable of withstanding a high degree of transmitted power. If each channel transmits 100 W, the total power that the antenna terminal could withstand is 3.2 kW.

The 32-channel combiner has a power limitation which would be specified by different manufacturers. Two receiving antennas in each 120° sector remain the same for space diversity use.

5.4.3 Location antennas

In each cell site a location receiver connects to the respective location antenna. This antenna can be either omnidirectional or shared-directional. The location receiver can tune a channel to one of 333 channels either upon demand or periodically. This operation is discussed in Chaps. 8 and 9.

5.4.4 Setup-channel antennas

The setup-channel antenna is used to page a called mobile unit or to access a call from a mobile unit. It transmits only data. The setup-channel antenna can be an omnidirectional antenna or consist of sev-

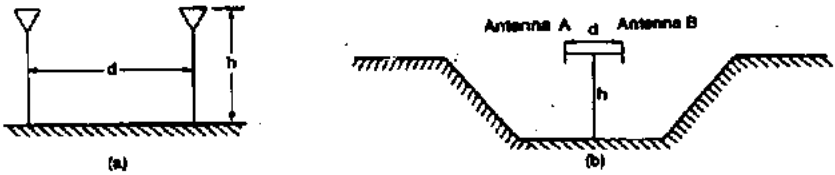

Figure 5.11 Diversity antenna spacing at the cell site: (*a*) $\eta = h/d$; (*b*) proper arrangement with two antennas.

eral directional antennas at one cell site. In general, in both omnicell and sector-cell systems, one omnidirectional antenna is used for transmitting signals and another for receiving signals in each cell site. Setup–channel operational procedures are discussed in Chap. 8.

5.4.5 Space-diversity antennas used at cell site

Two-branch space-diversity antennas are used at the cell site to receive the same signal with different fading envelopes, one at each antenna. The degree of correlation between two fading envelopes is determined by the degree of separation between two receiving antennas. When the two fading envelopes are combined, the degree of fading is reduced; this improvement is discussed in Ref. 12. Here the antenna setup is shown in Fig. 5.11*a*. Equation (5.4-1) is presented as an example for the designer to use.

$$\eta = \frac{h}{D} = 11 \tag{5.4-1}$$

where h is the antenna height and D is the antenna separation. From Eq. (5.4-1), the separation $d \geq 8\lambda$ is needed for an antenna height of 100 ft (30 m) and the separation $d \geq 14\lambda$ is needed for an antenna height of 150 ft (50 m). In any omnicell system, the two space-diversity antennas should be aligned with the terrain, which should have a U shape[13] as shown in Fig. 5.11*b*.

Space-diversity antennas can separate only horizontally, not vertically; thus, there is no advantage in using a vertical separation in the design.[13] The use of space-diversity antennas at the base station is discussed in detail in Ref. 13.

5.4.6 Umbrella-pattern antennas

In certain situations, umbrella-pattern antennas should be used for the cell-site antennas.

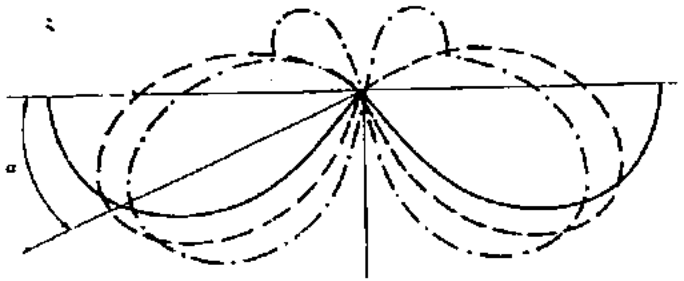

Figure 5.12 Vertical-plane patterns of quarter-wavelength stub antenna on infinite ground plane (solid) and on finite ground planes several wavelengths in diameter (dashed line) and about one wavelength in diameter (dotted line) (*after Kraus, Ref. 14*).

Normal umbrella-pattern antenna.[14] For controlling the energy in a confined area, the umbrella-pattern antenna can be developed by using a monopole with a top disk (top-loading) as shown in Fig. 5.12. The size of the disk determines the tilting angle of the pattern. The smaller the disk, the larger the tilting angle of the umbrella pattern.

Broadband umbrella-pattern antenna. The parameters of a *discone antenna* (a bioconical antenna in which one of the cones is extended to 180° to form a disk) are shown in Fig. 5.13*a*. The diameter of the disk, the length of the cone, and the opening of the cone can be adjusted to create an umbrella-pattern antenna as described in Ref. 15.

High-gain broadband umbrella-pattern antenna. A high-gain antenna can be constructed by vertically stacking a number of umbrella-pattern antennas as shown in Fig. 5.13*b*

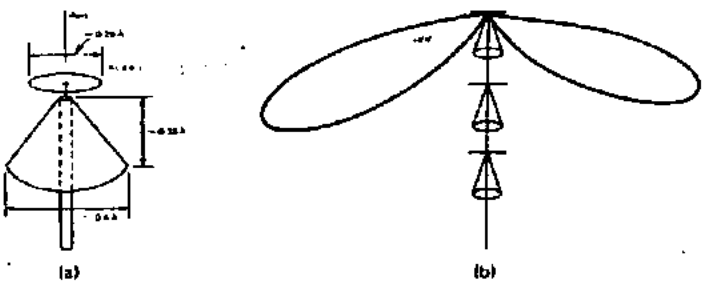

Figure 5.13 Discone antennas. (*a*) Single antenna. (*b*) An array of antennas.

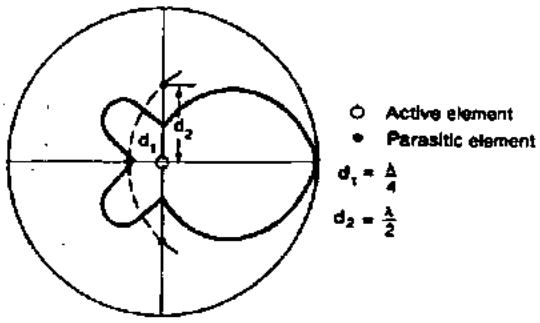

Figure 5.14 Application of parasitic elements (*after Jasik, Ref. 16*).

$$E_0 = \frac{\sin\left[(Nd/2\lambda)\cos\phi\right]}{\sin\left[(d/2\lambda)\cos\phi\right]} \cdot \text{(individual umbrella pattern)}$$

where ϕ = direction of wave travel
N = number of elements
d = spacing between two adjacent elements

5.4.7 Interference reduction antenna[15]

A design for an antenna configuration that reduces interference in two critical directions (areas) is shown in Fig. 5.14. The parasitic (insulation) element is about 1.05 times longer than the active element. The separation d and the various values of parasitic element reactance X_{22} were shown by Brown for this application.[17]

5.5 Unique Situations of Cell-Site Antennas

5.5.1 Antenna pattern in free space and in mobile environments

The antenna pattern we normally use is the one measured from an antenna range (open, nonurban area) or an antenna darkroom. However, when the antenna is placed in a surburban or urban environment and the mobile antenna is lower than the heights of the surroundings, the cell-site antenna pattern as a mobile unit received in a circle equidistant around the cell site is quite different from the free-space antenna pattern. Consider the following facts in the mobile radio environment.

1. The strongest reception still coincides with the strongest signal strength of the directional antenna.

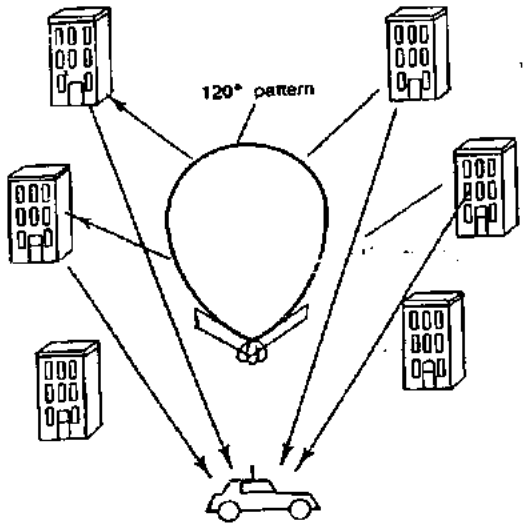

Figure 5.15 Front-to-back ratio of a directional antenna in a mobile radio environment.

2. The pattern is distorted in an urban or suburban environment.

3. For a 120° directional antenna, the backlobe (or front-to-back ratio) is about 10 dB less than the frontlobe, regardless of whether a weak sidelobe pattern or no sidelobe pattern is designed in a free-space condition. This condition exists because the strong signal radiates in front, bouncing back from the surroundings so that the energy can be received from the back of the antenna. The energy-reflection mechanism is illustrated in Fig. 5.15.

4. A design specification of the front-to-back ratio of a directional antenna (from the manufacturer's catalog) is different from the actual front-to-back ratio in the mobile radio environment. Therefore the environment and the antenna beamwidth determine how the antenna will be used in a mobile radio environment. For example, if a 60° directional antenna is used in a mobile radio environment, the actual front-to-back ratio can vary depending on the given environment. If the close-in man-made structures in front of the antenna are highly reflectable to the signal, then the front-to-back ratio of a low-master directional antenna can be as low as 6 dB in some circumstances. In this case, the directional antenna beamwidth pattern has no correlation between it measured in the free space and it measured in the mobile radio environment. If all the buildings are far away from the

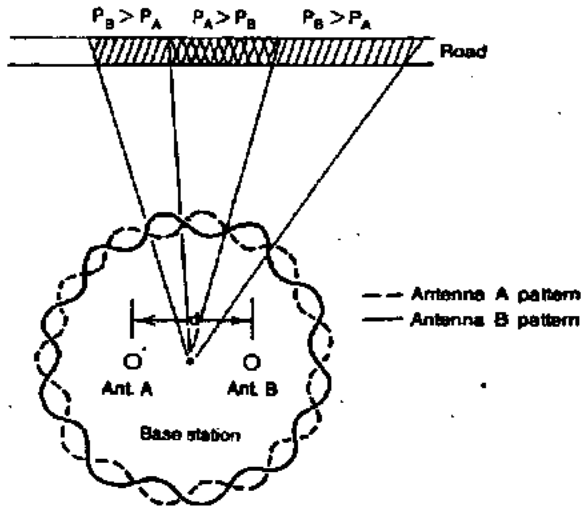

Figure 5.16 Antenna pattern ripple effect.

directional antenna, then the front-to-back ratio measured in the field will be close to the specified antenna pattern, usually 20 dB.

5.5.2 Minimum separation of cell-site receiving antennas

Separation between two transmitting antennas should be minimized to avoid the intermodulation discussed in Chap. 7. The minimum separation between a transmitting antenna and a receiving antenna necessary to avoid receiver desensitization is also described in Chap. 7. Here we are describing a minimum separation between two receiving antennas to reduce the antenna pattern ripple effects.

The two receiving antennas are used for a space-diversity receiver. Because of the near-field disturbance due to the close spacing, ripples will form in the antenna patterns (Fig. 5.16). The difference in power reception between two antennas at different angles of arrival is shown in Fig. 5.16. If the antennas are located closer, the difference in power between two antennas at a given pointing angle increases. Although the power difference is confined to a small sector, it affects a large section of the street as shown in Fig. 5.16. If the power difference is excessive, use of a space diversity will have no effect reducing fading. At 850 MHz, the separation of eight wavelengths between two receiving antennas creates a power difference of ± 2 dB, which is tolerable for the advantageous use of a diversity scheme.[18]

5.5.3 Regular check of the cell-site antennas

Air-pressurized cable is often used in cell-site antennas to prevent moisture from entering the cable and causing excessive attenuation. One method of checking the cell-site antennas is to measure the power delivered to the antenna terminal; however, few systems have this capability. The other method is to measure the VSWR at the bottom of the tower. In this case the loss of reflected power due to the cable under normal conditions should be considered. For a high tower, the VSWR reading may not be accurate.

If each cable connector has 1-dB loss due to energy leakage and two midsection 1-dB loss connectors are used in the transmitted system as shown in Fig. 5.17, the reflected power P_b indicated in the VSWR would be 4 dB less than the real reflected power.

5.5.4 Choosing an antenna site

In antenna site selection we have relied on the point-to-point prediction method (discussed in Chap. 4), which is applicable primarily for coverage patterns under conditions of light call traffic in the system. Reduction of interference is an important factor in antenna site selection.

When a site is chosen on the map, there is a 50 percent chance that the site location cannot be acquired. A written rule states that[24] an antenna location can be found within a quarter of the size of cell $R/4$. If the site is an 8-mi cell, the antenna can be located within a 2-mi radius. This hypothesis is based on the simulation result that the change in site within a 2-mi radius would not affect the coverage pattern at a distance 8 mi away. If the site is a 2-mi cell, the antenna can be located within a 0.5-mi radius.

The quarter-radius rule can be applied only on relatively flat terrain, not in a hilly area. To determine whether this rule can be applied in a general area, one can use the point-to-point prediction method to plot the coverage at different site locations and compare the differences. Usually when the point-to-point prediction method (tool) can be used to design a system, the quarter-radius rule becomes useless.

5.6 Mobile Antennas

The requirement of a mobile (motor-vehicle–mounted) antenna is an omnidirectional antenna which can be located as high as possible from the point of reception. However, the physical limitation of antenna height on the vehicle restricts this requirement. Generally the an-

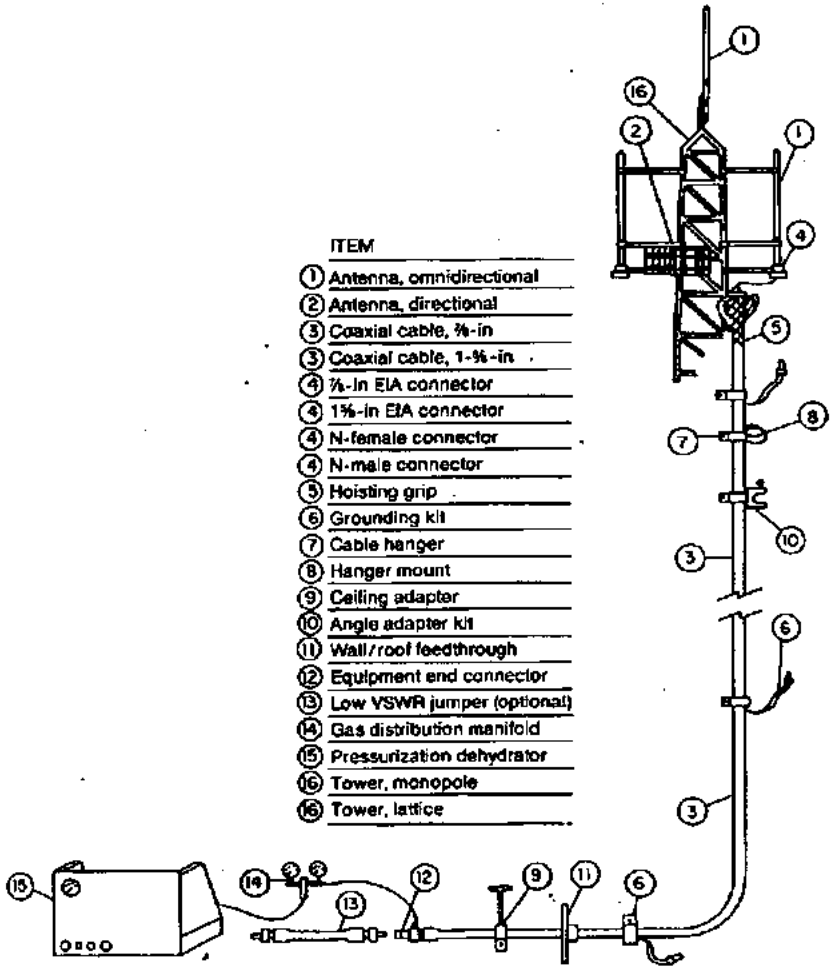

Figure 5.17 Antenna system at cell site.

tenna should at least clear the top of the vehicle. Patterns for two types of mobile antenna are shown in Fig. 5.18.

5.6.1 Roof-mounted antenna

The antenna pattern of a roof-mounted antenna is more or less uniformly distributed around the mobile unit when measured at an antenna range in free space as shown in Fig. 5.19. The 3-dB high-gain

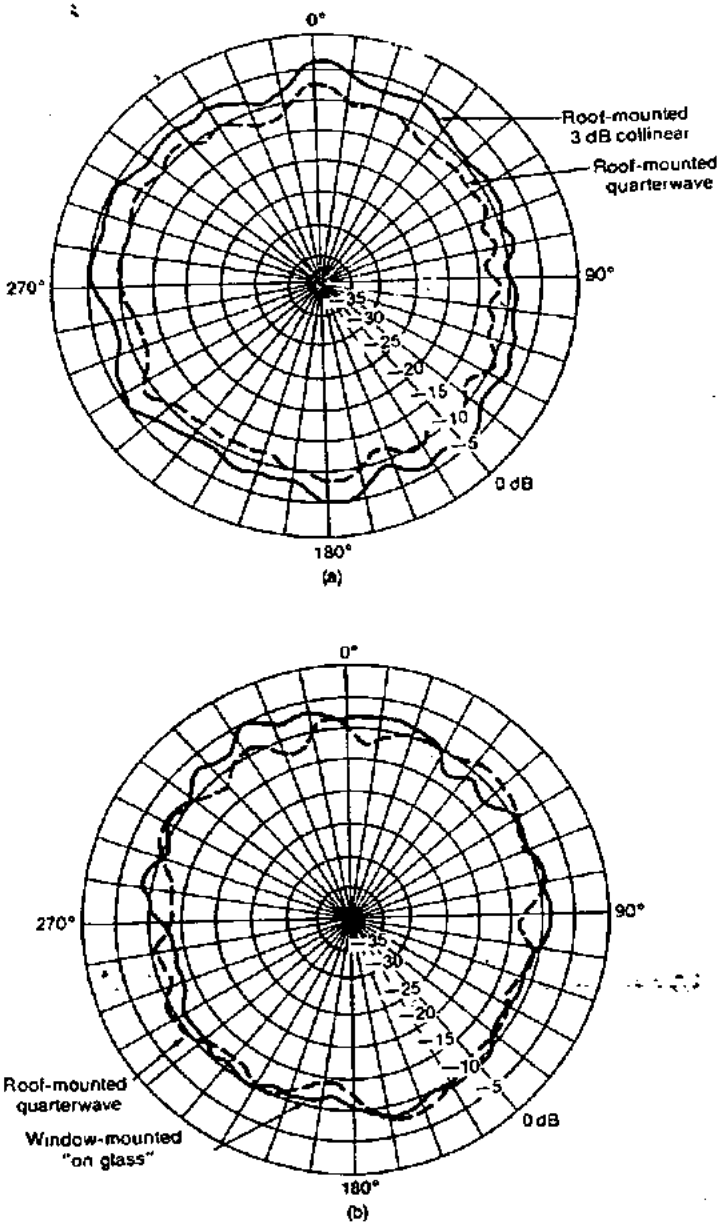

Figure 5.18 Mobile antenna patterns (*from Antenna Specialist Co., Ref. 10*). (*a*) Roof-mounted 3-dB-gain collinear antenna versus roof-mounted quarter-wave antenna. (*b*) Window-mounted "on-glass" gain antenna versus roof-mounted quarter-wave antenna.

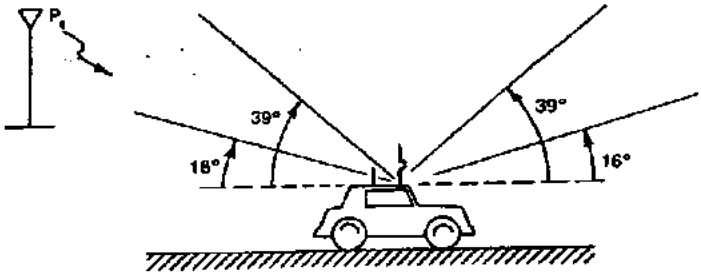

Figure 5.19 Vertical angle of signal arrival.

antenna shows a 3-dB gain over the quarter-wave antenna. However, the gain of the antenna used at the mobile unit must be limited to 3 dB because the cell-site antenna is rarely as high as the broadcasting antenna and out-of-sight conditions often prevail. The mobile antenna with a gain of more than 3 dB can receive only a limited portion of the total multipath signal in the elevation as measured under the out-of-sight condition.[19] This point is discussed in detail in Sec. 5.6.3.

5.6.2 Glass-mounted antennas[10,20]

There are many kinds of glass-mounted antennas. Energy is coupled through the glass; therefore, there is no need to drill a hole. However, some energy is dissipated on passage through the glass. The antenna gain range is 1 to 3 dB depending on the operating frequency.

The position of the glass-mounted antenna is always lower than that of the roof-mounted antenna; generally there is a 3-dB difference between these two types of antenna. Also, glass-mounted antennas cannot be installed on the shaded glass found in some motor vehicles because this type of glass has a high metal content.

5.6.3 Mobile high-gain antennas

A high-gain antenna used on a mobile unit has been studied.[19] This type of high-gain antenna should be distinguished from the directional antenna. In the directional antenna, the antenna beam pattern is suppressed horizontally; in the high-gain antenna, the pattern is suppressed vertically. To apply either a directional antenna or a high-gain antenna for reception in a radio environment, we must know the origin of the signal. If we point the directional antenna opposite to the transmitter site, we would in theory receive nothing.

In a mobile radio environment, the scattered signals arrive at the mobile unit from every direction with equal probability. That is why an omnidirectional antenna must be used. The scattered signals also

arrive from different elevation angles. Lee and Brandt[19] used two types of antenna, one $\lambda/4$ whip antenna with an elevation coverage of 39° and one 4-dB-gain antenna (4-dB gain with respect to the gain of a dipole) with an elevation coverage of 16°, and measured the angle of signal arrival in the suburban Keyport-Matawan area of New Jersey. There are two types of test: a line-of-sight condition and an out-of-sight condition. In Lee and Brandt's study the transmitter was located at an elevation of approximately 100 m (300 ft) above sea level. The measured areas were about 12 m (40 ft) above sea level and the path length about 3 mi. The received signal from the 4-dB-gain antenna was 4 dB stronger than that from the whip antenna under line-of-sight conditions. This is what we would expect. However, the received signal from the 4-dB-gain antenna was only about 2 dB stronger than that from the whip antenna under out-of-sight conditions. This is surprising.

The reason for the latter observation is that the scattered signals arriving under out-of-sight conditions are spread over a wide elevation angle. A large portion of the signals outside the elevation angle of 16° cannot be received by the high-gain antenna. We may calculate the portion being received by the high-gain antenna from the measured beamwidth [the beamwidth can be roughly obtained from Eq. (5.2-6)]. For instance, suppose that a 4:1 gain (6 dBi) is expected from the high-gain antenna, but only 2.5:1 is received. Therefore, 63 percent of the signal* is received by the 4-dB-gain antenna (i.e., 6 dBi) and 37 percent is felt in the region between 16 and 39°. Consider the data in the following table.

	Gain, dBi	Linear ratio	$\theta_e/2$, degrees
Whip antenna (2 dB above isotropic)	2	1.58:1	39
High-gain antenna	6	4:1	16
Low-gain antenna	4	2.5:1	24

Therefore, a 2- to 3-dB-gain antenna (4 to 5 dBi) should be adequate for general use. An antenna gain higher than 2 to 3 dB does not serve the purpose of enhancing reception level. Moreover, measurements reveal that the elevation angle for scattered signals received in urban areas is greater than that in suburban areas.

5.6.4 Horizontally oriented space-diversity antennas

A two-branch space-diversity receiver mounted on a motor vehicle has the advantage of reducing fading and thus can operate at a lower

* For a Rayleigh fading signal, 63 percent will be below its power level.

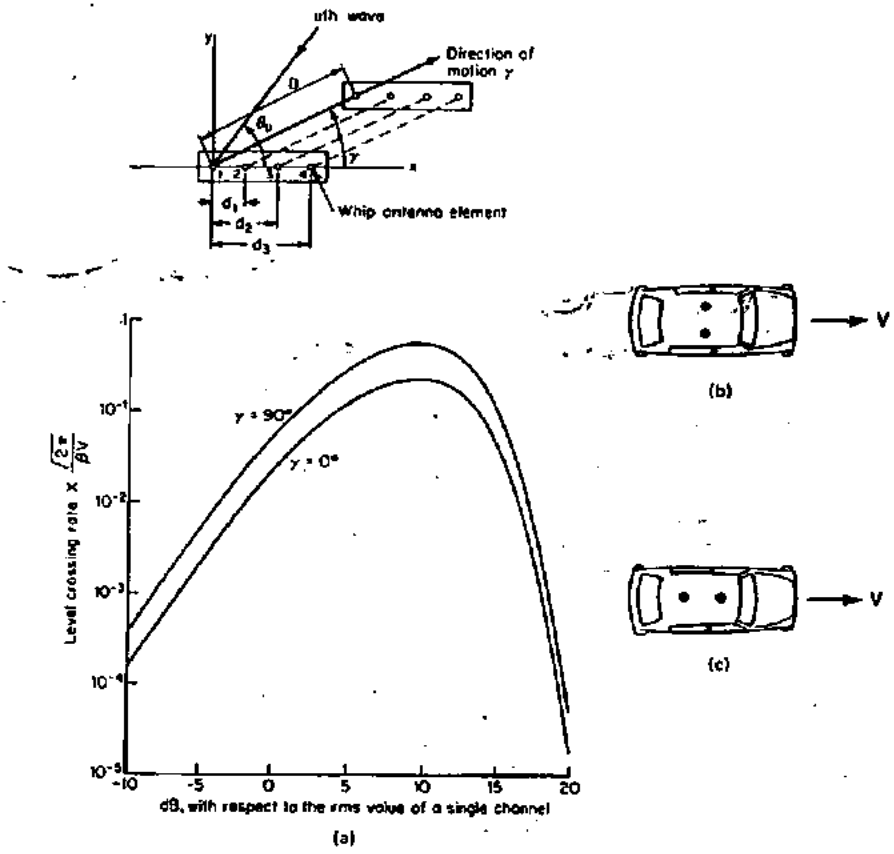

Figure 5.20 Horizontally spaced antennas. (*a*) Maximum difference in lcr of a four-branch equal-gain signal between $\alpha = 0$ and $\alpha = 90°$ with antenna spacing of 0.15λ. (*b*) Not recommended. (*c*) Recommended.

reception level. The advantage of using a space-diversity receiver to reduce interference is discussed in Chap. 7. The discussion here concerns a space-diversity scheme in which two vehicle-mounted antennas separated horizontally by 0.5λ wavelength[21] (15 cm or 6 in) can achieve the advantage of diversity.

We must consider the following factor. The two antennas can be mounted either in line with or perpendicular to the motion of the vehicle. Theoretical analyses and measured data indicate that the in-line arrangement of the two antennas produces fewer level crossings, that is, less fading, than the perpendicular arrangement does. The level crossing rates of two signals received from different horizontally oriented space-diversity antennas are shown in Fig. 5.20.

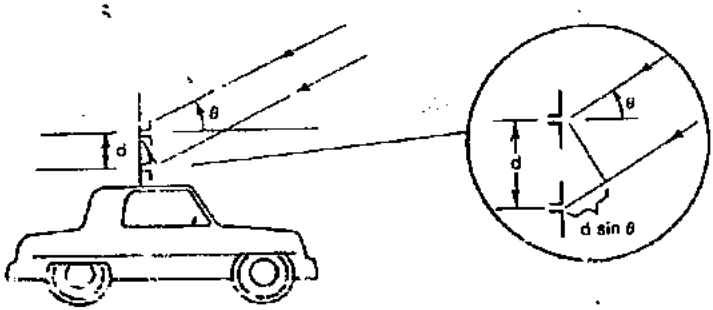

Figure 5.21 Vertical separation between two mobile antennas.

5.6.5 Vertically oriented space-diversity antennas[22]

The vertical separation between two space-diversity antennas can be determined from the correlation between their received signals. The positions of two antennas X_1 and X_2 are shown in Fig. 5.21. The theoretical derivation of correlation is[23]

$$\rho\left(\frac{d}{\lambda}, \theta\right) = \frac{\sin[(\pi d/\lambda)\sin\theta]}{(\pi d/\lambda)\sin\theta} \tag{5.6-1}$$

Equation (5.6-1) is plotted in Fig. 5.22. A set of measured data was obtained by using two antennas vertically separated by 1.5λ wavelengths. The mean values of three groups of measured data are also shown in Fig. 5.22. In one group, in New York City, low correlation coefficients were observed. In two other groups, both in New Jersey, the average correlation coefficient for perpendicular streets was 0.35 and for radial streets, 0.225. The following table summarizes the correlation coefficients in different areas and different street orientations.

Area	Correlation coefficient	
	Average	Standard deviation
New York City	0.1	0.06
Suburban New Jersey		
Radial streets	0.226	0.127
Perpendicular streets	0.35	0.182

From Fig. 5.22 we can also see that the signal arrives at an elevation angle of 29° in the suburban radial streets and 33° in the suburban perpendicular streets. In New York City the angle of arrival approaches 40°.

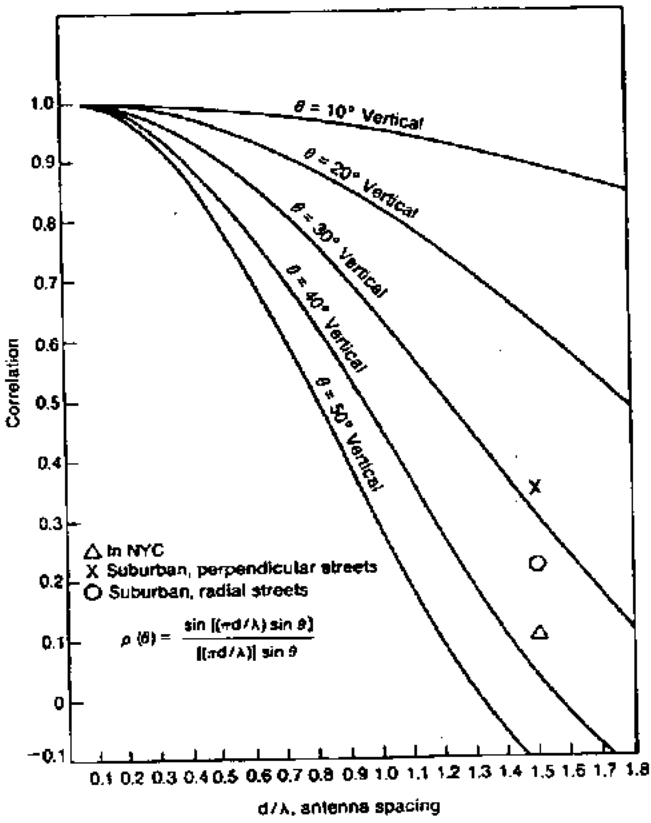

Figure 5.22 Two vertically spaced antennas mounted on a mobile unit.

References

1. E. C. Jordan (ed.), *Reference Data for Engineers: Radio, Electronics, Computer, and Communications*, 7th ed., Howard W. Sams & Co., 1985, pp. 32–34.
2. J. D. Kraus, *Antennas*, McGraw-Hill Book Co., 1950, p. 44.
3. J. D. Kraus, *Antennas*, McGraw-Hill Book Co., 1950, p. 78.
4. R. S. Elliott, *Antenna Theory and Design*, Prentice-Hall, Inc., 1981, p. 206.
5. J. D. Kraus, *Antennas*, McGraw-Hill Book Co., 1950, p. 25.
6. R. S. Elliott, *Antenna Theory and Design*, Prentice-Hall, Inc., 1981, p. 157.
7. C. L. Dolph, "A Current Distribution for Broadside Arrays Which Optimizes the Relationship between Beamwidth and Side-Lobe Level," *Proceedings of the IRE*, Vol. 34, No. 6, June 1946, pp. 335–348.
8. R. S. Elliott, "Design of Live-Source Antennas for Sum Patterns with Sidelobes of Individually Arbitrary Heights," *IEEE Transactions on Antennas and Propagation*, Vol. AP-24, 1976, pp. 76–83.

9. R. S. Elliott, "Design of Line-Source Antennas from Difference Patterns with Side Lobes of Individually Arbitrary Heights," *IEEE Transactions on Antennas and Propagation*, Vol. AP-24, 1976, pp. 310–316.
10. Antenna Specialist Co. catalog product branches, Antenna Specialist Co., Cleveland, Ohio.
11. American Radio Telephone Service (ARTS) development license application to the Federal Communications Commission, Feb. 14, 1977. In the application, a proposed system from Motorola was described.
12. W. C. Y. Lee, "Mobile Radio Signal Correlation versus Antenna Height and Space," *IEEE Transactions on Vehicular Technology*, Vol. VT-25, August 1977, pp. 290–292.
13. W. C. Y. Lee, *Mobile Communications Design Fundamentals*, Howard W. Sams & Co., 1986, p. 202.
14. J. D. Kraus, *Antennas*, McGraw-Hill Book Co., 1950, p. 421.
15. A. G. Kandoian, "Three New Antenna Types and Their Applications," *Proceedings of the IRE*, Vol. 34, February 1946, pp. 70W–75W.
16. H. Jasik (ed.), *Antenna Engineering Handbook*, McGraw-Hill Book Co., 1961, pp. 5–7.
17. G. H. Brown, "Directional Antennas," *Proceedings of the IRE*, Vol. 25, January 1937, pp. 75–145.
18. W. C. Y. Lee, *Mobile Communications Engineering*, McGraw-Hill Book Co., 1982, p. 152.
19. W. C. Y. Lee and R. H. Brandt, "The Elevation Angle of Mobile Radio Signal Arrival," *IEEE Transactions on Communications*, Vol. Com-21, November 1973, pp. 1194–1197.
20. Mobile Mark, Inc., Mobile Mark Model OW-900.
21. W. C. Y. Lee, *Mobile Communications Design Fundamentals*, Howard W. Sams & Co., 1986, p. 222.
22. J. S. Bitler, "Correlation Measurements of Signals Received on Vertically Spaced Antennas," Microwave Radio Symposium, Boulder, Colorado, 1972.
23. M. J. Gans, private communications.
24. V. H. MacDonald, "The Cellular Concept," *Bell System Technical Journal*, Vol. 58, January 1979, p. 27.

Chapter

6

Cochannel Interference Reduction

6.1 Cochannel Interference

The frequency-reuse method is useful for increasing the efficiency of spectrum usage but results in cochannel interference because the same frequency channel is used repeatedly in different cochannel cells. Application of the cochannel interference reduction factor $q = D/R = 4.6$ for a seven-cell reuse pattern ($K = 7$) is described in Sec. 2.4.[1]

In most mobile radio environments, use of a seven-cell reuse pattern is not sufficient to avoid cochannel interference. Increasing $K > 7$ would reduce the number of channels per cell, and that would also reduce spectrum efficiency. Therefore, it might be advisable to retain the same number of radios as the seven-cell system but to sector the cell radially, as if slicing a pie. This technique would reduce cochannel interference and use channel sharing and channel borrowing schemes to increase spectrum efficiency.

6.2 Exploring Cochannel Interference Areas in a System

Problems in mobile telephone coverage (service), particularly holes (weak signal strength*) which result in call drops during the customer's conversation, have been partially solved by applying the propagation (wave motion) studies discussed in Chap. 4 for the case where no cochannel interference exists.

* Signal strength is measured in dBm, and field strength is measured in dB(μV/m). The conversion between these units can be found in Sec. 5.1.3.

When customer demand increases, the channels, which are limited in number, have to be repeatedly reused in different areas, which provides many cochannel cells, which increases the system's capacity. But cochannel interference may be the result. In this situation, the received voice quality is affected by both the grade of coverage and the amount of cochannel interference. For detection of serious channel interference areas in a cellular system, two tests are suggested.

Test 1—find the cochannel interference area from a mobile receiver. Cochannel interference which occurs in one channel will occur equally in all the other channels in a given area. We can then measure cochannel interference by selecting any one channel (as one channel represents all the channels) and transmitting on that channel at all cochannel sites at night while the mobile receiver is traveling in one of the cochannel cells.

While performing this test we watch for any change detected by a field-strength recorder in the mobile unit and compare the data with the condition of no cochannel sites being transmitted. This test must be repeated as the mobile unit travels in every cochannel cell. To facilitate this test, we can install a channel scanning receiver in one car.

One channel (f_1) records the signal level (no-cochannel condition), another channel (f_2) records the interference level (six-cochannel condition is the maximum), while the third channel receives f_3, which is not in use. Therefore, the noise level is recorded only in f_3 (see Fig. 6.1).

We can obtain, in decibels, the carrier-to-interference ratio C/I by subtracting the result obtained from f_2 from the result obtained from f_1 (carrier minus interference $C - I$) and the carrier-to-noise ratio C/N by subtracting the result obtained from f_3 from the result obtained from f_2 (carrier minus noise $C - N$). Four conditions should be used to compare the results.

1. If the carrier-to-interference ratio C/I is greater than 18 dB throughout most of the cell, the system is properly designed.
2. If C/I is less than 18 dB and C/N is greater than 18 dB in some areas, there is cochannel interference.
3. If both C/N and C/I are less than 18 dB and $C/N \approx C/I$ in a given area, there is a coverage problem.
4. If both C/N and C/I are less than 18 dB and $C/N > C/I$ in a given area, there is a coverage problem *and* cochannel interference.

Test 2—find the cochannel interference area which affects a cell site. The reciprocity theorem can be applied for the coverage problem but not for cochannel interference. Therefore, we cannot assume that the first

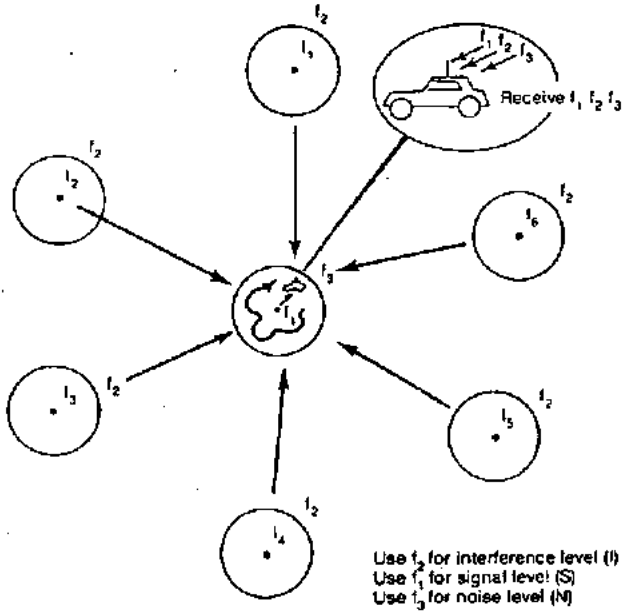

Figure 6.1 Test 1: cochannel interference at the mobile unit.

test result will apply to the second test condition. We must perform the second test as well.

Because it is difficult to use seven cars simultaneously, with each car traveling in each cochannel cell for this test, an alternative approach may be to record the signal strength at every cochannel cell site while a mobile unit is traveling either in its own cell or in one of the cochannel cells shown in Fig. 6.2.

First we find the areas in an interfering cell in which the top 10 percent level of the signal transmitted from the mobile unit in those areas is received at the desired site (Jth cell in Fig. 6.1). This top 10 percent level can be distributed in different areas in a cell. The average value of the top 10 percent level signal strength is used as the interference level from that particular interfering cell. The mobile unit also travels in different interfering cells. Up to six interference levels are obtained from a mobile unit running in six interfering cells. We then calculate the average of the bottom 10 percent level of the signal strength which is transmitted from a mobile unit in the desired cell (Jth cell) and received at the desired cell site as a carrier reception level.

Then we can reestablish the carrier-to-interference ratio received at a desired cell, say, the Jth cell site as follows.

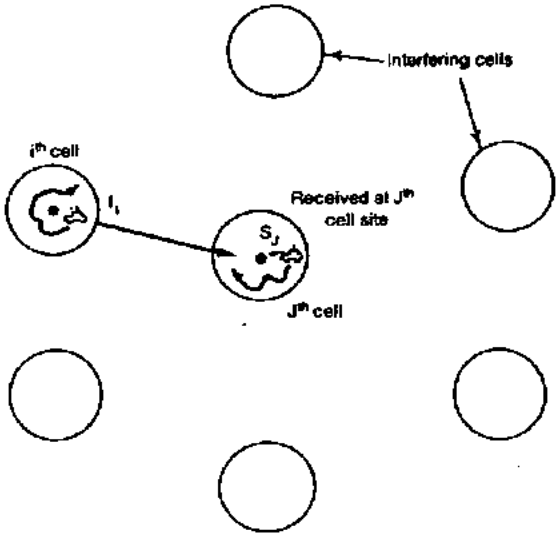

Figure 6.2 Test 2: cochannel interference at the cell site.

$$\frac{C_J}{I} = \frac{C_J}{\sum_{\substack{i=1 \\ i \neq J}}^{6} I_i}$$

The number of cochannel cells in the system can be less than six. We must be aware that all C_J and I_i were read in decibels. Therefore, a translation from decibels to linear is needed before summing all the interfering sources. The test can be carried out repeatedly for any given cell. We then compare

$$\frac{C_J}{I} \quad \text{and} \quad \frac{C_J}{N_J}$$

and determine the cochannel interference condition, which will be the same as that in test 1. N_J is the noise level in the Jth cell assuming no interference exists.

6.3 Real-Time Cochannel Interference Measurement at Mobile Radio Transceivers

When the carriers are angularly modulated by the voice signal and the RF frequency difference between them is much higher than the

fading frequency measurement of the signal carrier-to-interference ratio C/I reveals that the signal is

$$e_1 = S(t)\sin(\omega t + \phi_1) \tag{6.3-1}$$

and the interference is

$$e_2 = I(t)\sin(\omega t + \phi_2) \tag{6.3-2}$$

The received signal is

$$e(t) = e_1(t) + e_2(t) = R\sin(\omega t + \psi) \tag{6.3-3}$$

where

$$R = \sqrt{[S(t)\cos\phi_1 + I(t)\cos\phi_2]^2 + [S(t)\sin\phi_1 + I(t)\sin\phi_2]^2} \tag{6.3-4}$$

and

$$\psi = \tan^{-1}\frac{S(t)\sin\phi_1 + I(t)\sin\phi_2}{S(t)\cos\phi_1 + I(t)\cos\phi_2} \tag{6.3-5}$$

The envelope R can be simplified in Eq. (6.3-4), and R^2 becomes

$$R^2 = [S^2(t) + I^2(t) + 2S(t)I(t)\cos(\phi_1 - \phi_2)] \tag{6.3-6}$$

Following Kozono and Sakamoto's[2] analysis of Eq. (6.3-6) the term $S^2(t) + I^2(t)$ fluctuates close to the fading frequency V/λ and the term $2S(t)I(t)\cos(\phi_1 - \phi_2)$ fluctuates to a frequency close to $d/dt(\phi_1 - \phi_2)$, which is much higher than the fading frequency. Then the two parts of the squared envelope can be separated as

$$X = S^2(t) + I^2(t) \tag{6.3-7}$$

$$Y = 2S(t)I(t)\cos(\phi_1 - \phi_2) \tag{6.3-8}$$

Assume that the random variables $S(t)$, $I(t)$, ϕ_1, and ϕ_2 are independent; then the average processes on X and Y are

$$\overline{X} = \overline{S^2(t)} + \overline{I^2(t)} \tag{6.3-9}$$

$$\overline{Y^2} = 4\overline{S^2(t)}\,\overline{I^2(t)}(\tfrac{1}{2}) = 2\overline{S^2(t)}\,\overline{I^2(t)} \tag{6.3-10}$$

The signal-to-interference ratio Γ becomes

$$\Gamma = \frac{\overline{S^2(t)}}{\overline{I^2(t)}} = k + \sqrt{k^2 - 1} \tag{6.3-11}$$

where
$$k = \frac{\overline{X}^2}{\overline{Y}^2} - 1 \tag{6.3-12}$$

Since X and Y can be separated in Eq. (6.3-6), the preceding computation of Γ in Eq. (6.3-11) could have been accomplished by means of an envelope detector, and analog-to-digital converter, and a microcomputer. The sampling delay time Δt should be small enough to satisfy

$$S(t) \approx S(t + \Delta t), \qquad I(t) \approx I(t + \Delta t) \tag{6.3-13}$$

and
$$\overline{\cos [\phi_1(t) - \phi_2(t)] \cos [\phi_1(t + \Delta t) - \phi_2(t + \Delta t)]} \approx 0 \tag{6.3-14}$$

Determining the delay time Δt to meet the requirement of Eq. (6.3-13) for this calculation is difficult and is a drawback to this measurement technique. Therefore, real-time cochannel interference measurement is difficult to achieve in practice.

6.4 Design of an Omnidirectional Antenna System in the Worst Case

In Sec. 2.4 we proved that the value of $q = 4.6$ is valid for a normal interference case in a $K = 7$ cell pattern.[3] In this section we would like to prove that a $K = 7$ cell pattern does not provide a sufficient frequency-reuse distance separation even when an ideal condition of flat terrain is assumed. The worst case is at the location where the mobile unit would receive the weakest signal from its own cell site but strong interferences from all interfering cell sites.

In the worst case the mobile unit is at the cell boundary R, as shown in Fig. 6.3. The distances from all six cochannel interfering sites are also shown in the figure: two distances of $D - R$, two distances of D, and two distances of $D + R$.

Following the mobile radio propagation rule of 40 dB/dec shown in Chap. 4, we obtain

$$C \propto R^{-4} \qquad I \propto D^{-4}$$

Then the carrier-to-interference ratio is

$$\frac{C}{I} = \frac{R^{-4}}{2(D - R)^{-4} + 2(D)^{-4} + 2(D + R)^{-4}}$$

$$= \frac{1}{2(q - 1)^{-4} + 2(q)^{-4} + 2(q + 1)^{-4}} \tag{6.4-1a}$$

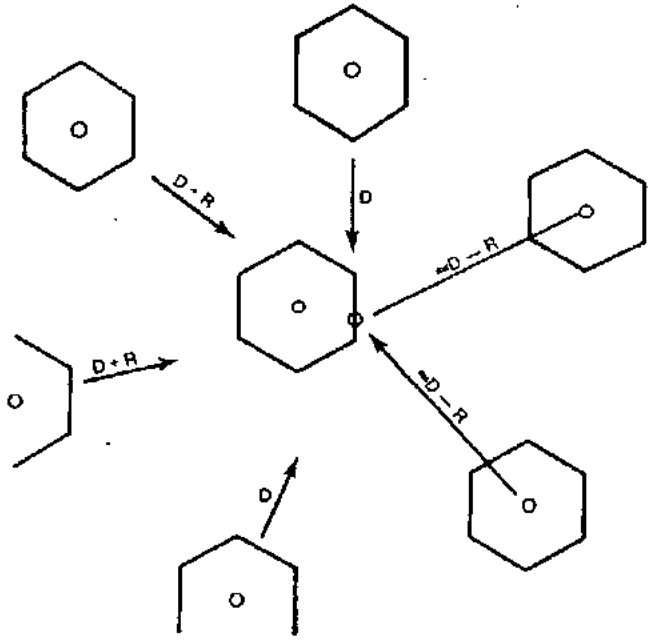

Figure 6.3 Cochannel interference (a worst case).

where $q = 4.6$ is derived from the normal case shown in Eq. (2.4-7). Substituting $q = 4.6$ into Eq. (6.4-1*a*), we obtain $C/I = 54$ or 17 dB, which is lower than 18 dB. To be conservative, we may use the shortest distance $D - R$ for all six interferers as a worst case; then Eq. (6.4-1*a*) is replaced by

$$\frac{C}{I} = \frac{R^{-4}}{6(D-R)^{-4}} = \frac{1}{6(q-1)^{-4}} = 28 = 14.47 \text{ dB} \qquad (6.4\text{-}1b)$$

In reality, because of the imperfect site locations and the rolling nature of the terrain configuration, the C/I received is always worse than 17 dB and could be 14 dB and lower. Such an instance can easily occur in a heavy traffic situation; therefore, the system must be designed around the C/I of the worst case. In that case, a cochannel interference reduction factor of $q = 4.6$ is insufficient.

Therefore, in an omnidirectional-cell system, $K = 9$ or $K = 12$ would be a correct choice. Then the values of q are

$$q = \begin{cases} \dfrac{D}{R} = \sqrt{3K} & \\ 5.2 & K = 9 \\ 6 & K = 12 \end{cases} \tag{6.4-2}$$

Substituting these values in Eq. (6.4-1), we obtain

$$\frac{C}{I} = 84.5\ (=)\ 19.25\ \text{dB} \qquad K = 9 \tag{6.4-3}$$

$$\frac{C}{I} = 179.33\ (=)\ 22.54\ \text{dB} \qquad K = 12 \tag{6.4-4}$$

The $K = 9$ and $K = 12$ cell patterns, shown in Fig. 6.4, are used when the traffic is light. Each cell covers an adequate area with adequate numbers of channels to handle the traffic.

6.5 Design of a Directional Antenna System

When the call traffic begins to increase, we need to use the frequency spectrum efficiently and avoid increasing the number of cells K in a seven-cell frequency-reuse pattern. When K increases, the number of frequency channels assigned in a cell must become smaller (assuming a total allocated channel divided by K) and the efficiency of applying the frequency-reuse scheme decreases.

Instead of increasing the number K in a set of cells, let us keep $K = 7$ and introduce a directional-antenna arrangement. The cochannel interference can be reduced by using directional antennas. This means that each cell is divided into three or six sectors and uses three or six directional antennas at a base station. Each sector is assigned a set of frequencies (channels). The interference between two cochannel cells decreases as shown Fig. 6.5.

6.5.1 Directional antennas in $K = 7$ cell patterns

Three-sector case. The three-sector case is shown in Fig. 6.5. To illustrate the worst-case situation, two cochannel cells are shown in Fig. 6.6*a*. The mobile unit at position E will experience greater interference in the lower shaded cell sector than in the upper shaded cell-sector site. This is because the mobile receiver receives the weakest signal from its own cell but fairly strong interference from the interfering

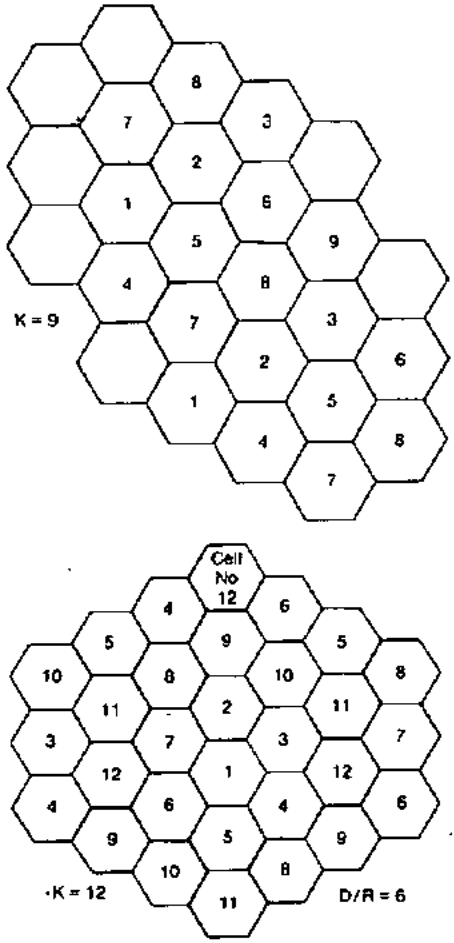

Figure 6.4 Interference with frequency-reuse patterns $K = 9$ and $K = 12$.

cell. In a three-sector case, the interference is effective in only one direction because the front-to-back ratio of a cell-site directional antenna is at least 10 dB or more in a mobile radio environment. The worst-case cochannel interference in the directional-antenna sectors in which interference occurs may be calculated. Because of the use of directional antennas, the number of principal interferers is reduced from six to two (Fig. 6.5). The worst case of C/I occurs when the mobile unit is at position E, at which point the distance between the

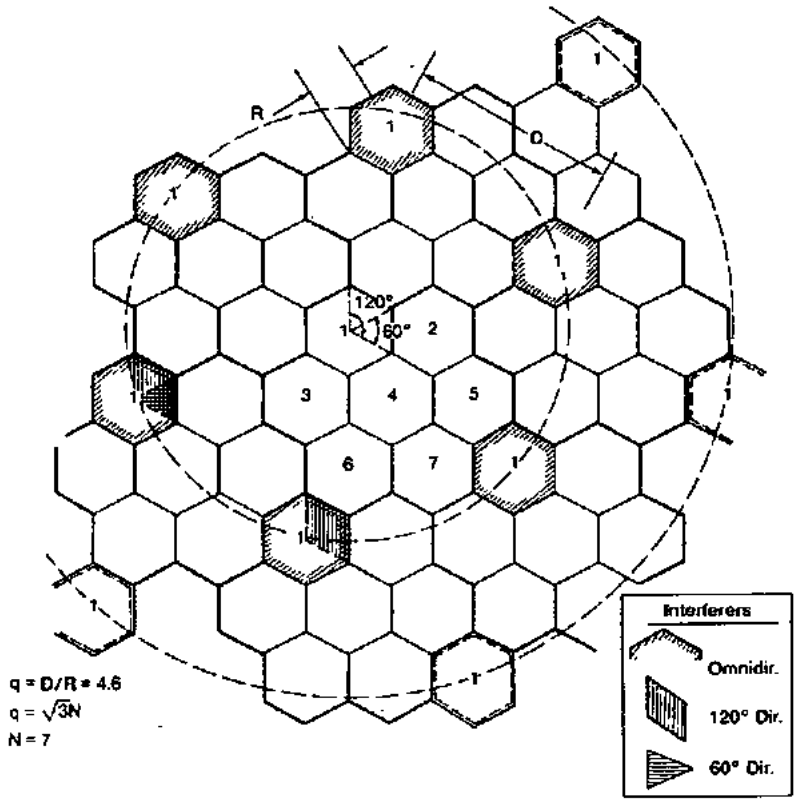

Figure 6.5 Interfering cells shown in a seven-cell system (two-tiers).

mobile unit and the two interfering antennas is roughly $D + (R/2)$; however, C/I can be calculated more precisely as follows.* The value of C/I can be obtained by the following expression (assuming that the worst case is at position E at which the distances from two interferers are $D + 0.7$ and D).

$$\frac{C}{I}\,(\text{worst case}) = \frac{R^{-4}}{(D + 0.7R)^{-4} + D^{-4}}$$

$$= \frac{1}{(q + 0.7)^{-4} + q^{-4}} \qquad (6.5\text{-}1)$$

* The difference in results between using a closed form and an approximate calculation is small.

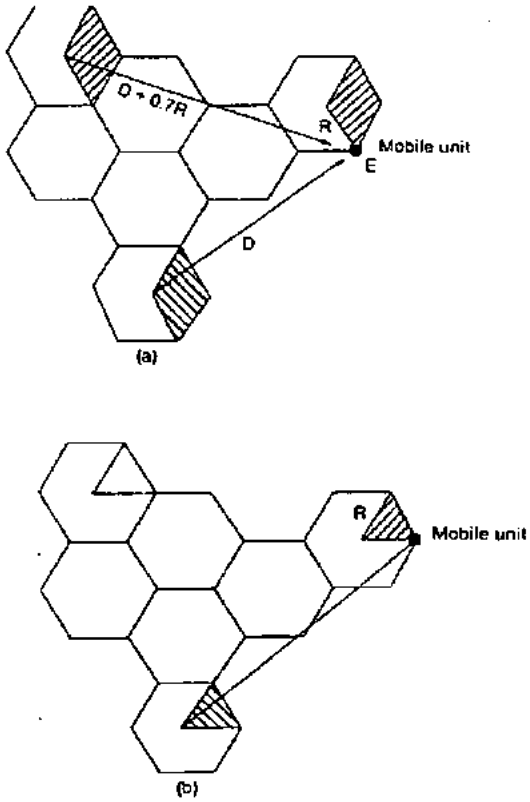

Figure 6.6 Determination of carrier-to-interference ratio C/I in a directional antenna system. (*a*) Worst case in a 120° directional antenna system ($N = 7$); (*b*) worst case in a 60° directional antenna system ($N = 7$).

Let $q = 4.6$; then Eq. (6.5-1) becomes

$$\frac{C}{I}\text{ (worst case)} = 285\ (=)\ 24.5\text{ dB} \qquad (6.5\text{-}2)$$

The C/I received by a mobile unit from the 120° directional antenna sector system expressed in Eq. (6.5-2) greatly exceeds 18 dB in a worst case. Equation (6.5-2) shows that using directional antenna sectors can improve the signal-to-interference ratio, that is, reduce the cochannel interference. However, in reality, the C/I could be 6 dB weaker than in Eq. (6.5-2) in a heavy traffic area as a result of irregular terrain contour and imperfect site locations. The remaining 18.5 dB is still adequate.

Six-sector case. We may also divide a cell into six sectors by using six 60°-beam directional antennas as shown in Fig. 6.6*b*. In this case, only one instance of interference can occur in each sector as shown in Fig. 6 5. Therefore, the carrier-to-interference ratio in this case is

$$\frac{C}{I} = \frac{R^{-4}}{(D + 0.7R)^{-4}} = (q + 0.7)^4 \tag{6.5-3}$$

For $q = 4.6$, Eq. (6.5-3) becomes

$$\frac{C}{I} = 794\ (=)\ 29\ \text{dB} \tag{6.5-4}$$

which shows a further reduction of cochannel interference. If we use the same argument as we did for Eq. (6.5-2) and subtract 6 dB from the result of Eq. (6.5-4), the remaining 23 dB is still more than adequate. When heavy traffic occurs, the 60°-sector configuration can be used to reduce cochannel interference. However, fewer channels are generally allowed in a 60° sector and the trunking efficiency decreases. In certain cases, more available channels could be assigned in a 60° sector.

6.5.2 Directional antenna in $K = 4$ cell pattern

Three-sector case. To obtain the carrier-to-interference ratio, we use the same procedure as in the $K = 7$ cell-pattern system. The 120° directional antennas used in the sectors reduced the interferers to two as in $K = 7$ systems, as shown in Fig. 6.7. We can apply Eq. (6.5-1) here. For $K = 4$, the value of $q = \sqrt{3K} = 3.46$; therefore, Eq. (6.5-1) becomes

$$\frac{C}{I}\ (\text{worst case}) = \frac{1}{(q + 0.7)^{-4} + q^{-4}} = 97 = 20\ \text{dB} \tag{6.5-5}$$

If, using the same reasoning used with Eq. (6.5-4), 6 dB is subtracted from the result of Eq. (6.5-5), the remaining 14 dB is unacceptable.

Six-sector case. There is only one interferer at a distance of $D + R$ shown in Fig. 6.7. With $q = 3.46$, we can obtain

$$\frac{C}{I}\ (\text{worst case}) = \frac{R^{-4}}{(D + R)^{-4}} = \frac{1}{(q + 1)^{-4}} = 355 = 26\ \text{dB} \tag{6.5-6}$$

If 6 dB is subtracted from the result of Eq. (6.5-6), the remaining 21

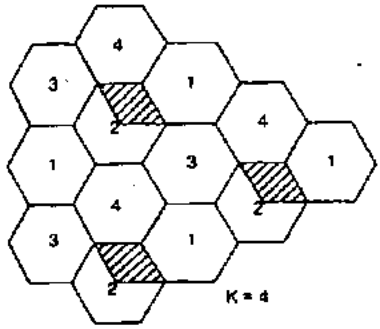

Figure 6.7 Interference with frequency-reuse pattern $K = 4$.

dB is adequate. Under heavy traffic conditions, there is still a great deal of concern over using a $K = 4$ cell pattern in a 60° sector. An explanation of this point is given in the next section.

6.5.3 Comparing $K = 7$ and $K = 4$ systems

A $K = 7$ cell-pattern system is a logical way to begin an omnicell system. The cochannel reuse distance is more or less adequate, according to the designed criterion. When the traffic increases, a three-sector system should be implemented, that is, with three 120° directional antennas in place. In certain hot spots, 60° sectors can be used locally to increase the channel utilization.

If a given area is covered by both $K = 7$ and $K = 4$ cell patterns and both patterns have a six-sector configuration, then the $K = 7$ system has a total of 42 sectors, but the $K = 4$ system has a total of only 26 sectors and, of course, the system of $K = 7$ and six sectors has less cochannel interference.

One advantage of 60° sectors with $K = 4$ is that they require fewer cell sites than 120° sectors with $K = 7$. Two disadvantages of 60° sectors are that (1) they require more antennas to be mounted on the antenna mast and (2) they often require more frequent handoffs because of the increased chance that the mobile units will travel across the six sectors of the cell. Furthermore, assigning the proper frequency channel to the mobile unit in each sector is more difficult unless the antenna height at the cell site is increased so that the mobile unit can be located more precisely. In reality the terrain is not flat, and coverage is never uniformly distributed; in addition, the directional antenna front-to-back power ratio in the field is very difficult to predict (see Sec. 5.4.2). In small cells, interference could become uncontrol-

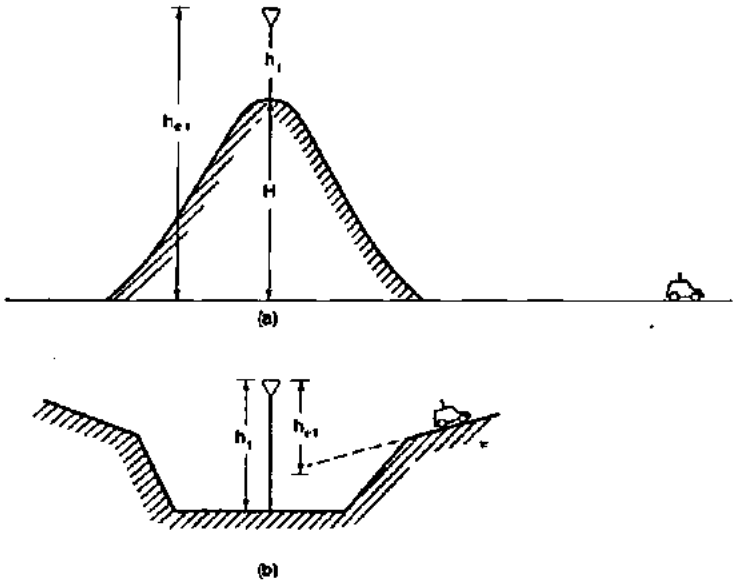

Figure 6.8 Lowering the antenna height (*a*) on a high hill and (*b*) in a valley.

lable; thus the use of a $K = 4$ pattern with 60° sectors in small cells needs to be considered only for special implementations such as portable cellular systems (Sec. 13.5) or narrowbeam applications (Sec. 10.6). For small cells, a better alternative scheme is to use a $K = 7$ pattern with 120° sectors plus the underlay-overlay configuration described in Sec. 11.4.

6.6 Lowering the Antenna Height

Lowering the antenna height does not always reduce the cochannel interference. In some circumstances, such as on fairly flat ground or in a valley situation, lowering the antenna height will be very effective for reducing the cochannel and adjacent-channel interference. However, there are three cases where lowering the antenna height may or may not effectively help reduce the interference.

On a high hill or a high spot. The effective antenna height, rather than the actual height, is always considered in the system design. Therefore, the effective antenna height varies according to the location of the mobile unit, as described in Chap. 4. When the antenna site is on a hill, as shown in Fig. 6.8*a*, the effective antenna height is $h_t + H$.

If we reduce the actual antenna height to $0.5h_1$, the effective antenna height becomes $0.5h_1 + H$. The reduction in gain resulting from the height reduction is

$$G = \text{gain reduction} = 20 \log_{10} \frac{0.5h_1 + H}{h_1 + H}$$

$$= 20 \log_{10} \left(1 - \frac{0.5h_1}{h_1 + H}\right) \qquad (6.6\text{-}1)$$

If $h_1 \ll H$, then Eq. (6.6-1) becomes

$$G \approx 20 \log_{10} 1 = 0 \text{ dB}$$

This simply proves that lowering antenna height on the hill does not reduce the received power at either the cell site or the mobile unit.

In a valley. The effective antenna height as seen from the mobile unit shown in Fig. 6.8*b* is h_{e1}, which is less than the actual antenna height h_1. If $h_{e1} = \frac{2}{3}h_1$ and the antenna is lowered to $\frac{1}{2}h_1$, then the new effective antenna height, determined from Chap. 4, is

$$h_{e1} = \tfrac{1}{2}h_1 - (h_1 - \tfrac{2}{3}h_1) = \tfrac{1}{6}h_1$$

Then the antenna gain is reduced by

$$G = 20 \log \frac{\frac{1}{6}h_1}{\frac{2}{3}h_1} = -12 \text{ dB}$$

This simply proves that the lowered antenna height in a valley is very effective in reducing the radiated power in a distant high elevation area. However, in the area adjacent to the cell-site antenna, the effective antenna height is the same as the actual antenna height. The power reduction caused by decreasing antenna height by half is only

$$20 \log \frac{\frac{1}{2}h_1}{h_1} = -6 \text{ dB}$$

In a forested area. In a forested area, the antenna should clear the tops of any trees in the vicinity, especially when they are very close to the antenna. In this case decreasing the height of the antenna would not be the proper procedure for reducing cochannel interference because excessive attenuation of the desired signal would occur in the vicinity of the antenna and in its cell boundary if the antenna were below the treetop level. This phenomenon is described in Sec. 4.4.

6.7 Reduction of Cochannel Interference by Means of a Notch in the Tilted Antenna Pattern

6.7.1 Introduction

Reduction of cochannel interference in a cellular mobile system is always a challenging problem. A number of methods can be considered, such as (1) increasing the separation between two cochannel cells, (2) using directional antennas at the base station, or (3) lowering the antenna heights at the base station. Method 1 is not advisable because as the number of frequency-reuse cells increases, the system efficiency, which is directly proportional to the number of channels per cell, decreases. Method 3 is not recommended because such an arrangement also weakens the reception level at the mobile unit. However, method 2 is a good approach, especially when the number of frequency-reuse cells is fixed. The use of directional antennas in each cell can serve two purposes: (1) further reduction of cochannel interference if the interference cannot be eliminated by a fixed separation of cochannel cells and (2) increasing the channel capacity when the traffic increases. In this chapter we try to further reduce the cochannel interference by intelligently setting up the directional antenna.

6.7.2 Theoretical analysis

Under normal circumstances radiation from a cochannel serving site can easily interfere with another cochannel cell as shown in Fig. 6.8. Installation of a 120° directional antenna can reduce the interference in the system by eliminating the radiation to the rest of its 240° sector. However, cochannel interference can exist even when a directional antenna is used, as the serving site can interfere with the cochannel cell that is directly ahead. Let us assume that a seven-cell cellular system ($K = 7$) is used. The cochannel interference reduction factor q becomes

$$q = \sqrt{3N} = 4.6 \tag{6.7-1}$$

and the cochannel cell separation D can be found if the cell radius is known.

$$D = qR = 4.6R \tag{6.7-2}$$

With a separation of $4.6R$, the area of interference at the interference-receiving cell is illuminated by the central 19° sector of the entire (120°) transmitting antenna pattern at the serving cell (see Fig. 6.9). If three identical directional antennas are implemented in every cell,

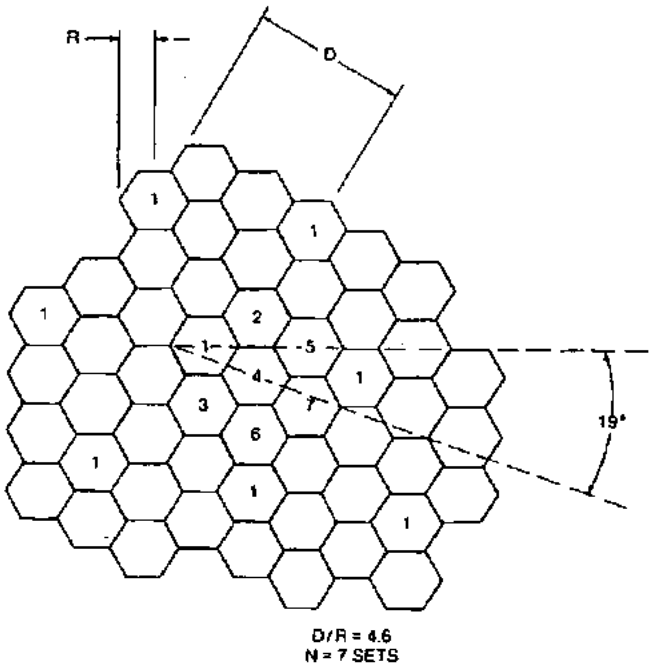

Figure 6.9 A seven-cell cellular configuration.

with each antenna covering a 120° sector, then every sector receives interference in the central 19° sector of the entire 120° angle at the interfering cell. Therefore, attempts should be made to reduce the signal strength of the interference in this 19° sector.

There are two ways to tilt down the antenna patterns; electronically and mechanically. The electronic downtilting is to change the phases among the elements of a colinear array antenna. The mechanical downtilting is to downtilt the antenna physically.

To achieve a significant gain of C/I in the interference-receiving cell, we should consider using a notch in the center of the antenna pattern at the interfering cell. An antenna pattern with a notch in the center can be obtained in a number of ways. One relatively simple way is to tilt the high-gain directional antenna mechanical downward.[4] A discussion of this method follows.

6.7.3 The effect of mechanically downtilting antenna on the coverage pattern

Because the shape of the antenna pattern at the base station relates directly to the reception level of signal strength at the mobile unit,

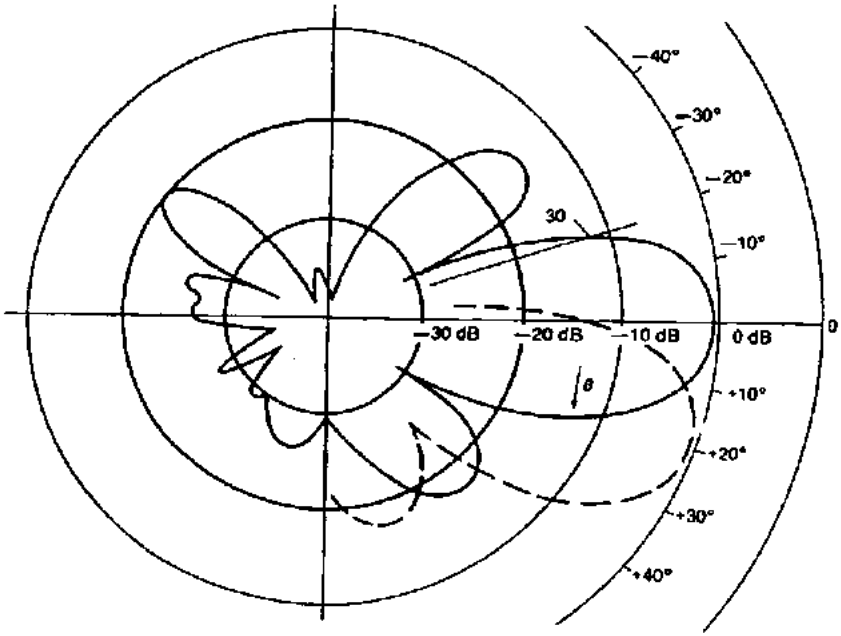

Figure 6.10 Vertical antenna pattern of a 120° directional antenna.

the following antenna pattern effect must be analyzed.

When a high-gain directional antenna (the pattern in the horizontal x-y plane is shown in Fig. 6.10 and in the vertical x-z plane, in Fig. 6.11) is physically (mechanically) tilted at an angle θ in the x-y plane shown in Fig. 6.11, how does the pattern in the x-y plane change? The antenna pattern obtained in the x-y plane after tilting the antenna is shown in Fig. 6.11. When the center beam is tilted downward by an angle θ, the off-center beam is tilted downward by only an angle ψ as shown in Fig. 6.12. The pattern in the x-y plane can be plotted by varying the angle ϕ. From the diagram in Fig. 6.12, we can obtain a derivation which provides the relationship among the angles ψ, θ, and ϕ as

$$\sin\frac{\theta}{2} = \frac{d}{l} \tag{6.7-3}$$

$$\frac{\overline{DB}}{\sin\phi} = \frac{l}{\sin(135° - \phi)} \tag{6.7-4}$$

$$\overline{CD} = l\,\frac{\sin 45°}{\sin(135 - \phi)} \tag{6.7-5}$$

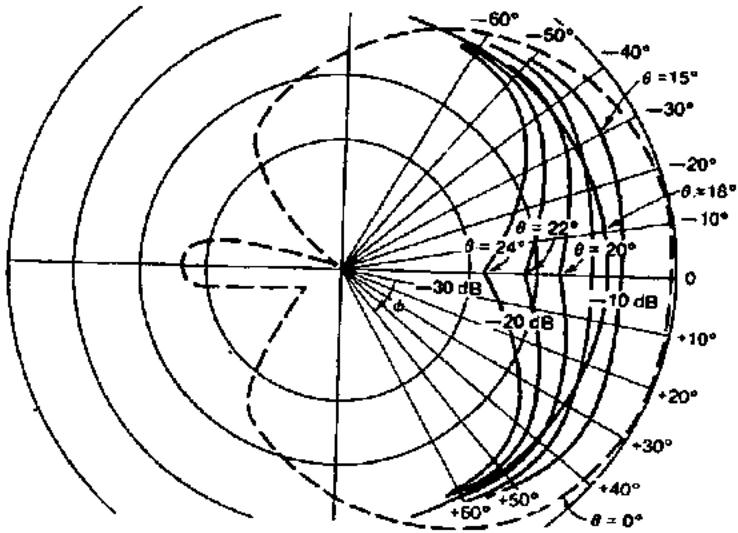

Figure 6.11 Notch appearing in tilted antenna pattern. (*Reprinted after Lee, Ref. 4.*)

$$\frac{\overline{AD}}{\overline{DF}} = \frac{\overline{AB}}{2d} = \frac{\sqrt{2}l}{2d} \tag{6.7-6}$$

$$\overline{AD} = \overline{AB} - \overline{DB} \tag{6.7-7}$$

$$\cos\psi = \frac{2\overline{CD} - \overline{DF}}{2\overline{CD}} = 1 - \frac{\overline{DF}}{2\overline{CD}} \tag{6.7-8}$$

Substituting Eqs. (6.7-3) to (6.7-7) into Eq. (6.7-8), we obtain

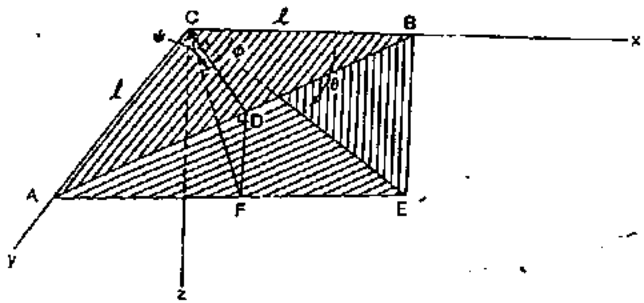

Figure 6.12 Coordinate of the tilting antenna pattern.

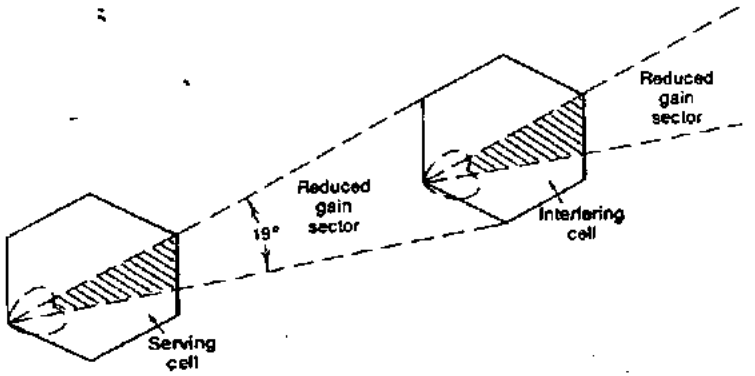

Figure 6.13 Reduced-gain sector of two cochannel cells.

$$\cos \psi = 1 - \cos^2 \phi \, (1 - \cos \theta) \tag{6.7-9}$$

or

$$\psi = \cos^{-1} [1 - \cos^2 \phi \, (1 - \cos \theta)] \tag{6.7-10}$$

If the physically tilted angle is $\theta = 18°$, then the off-center beam ψ is tilted downward.

$$\phi = \begin{cases} 0° \\ 45° \\ 90° \end{cases} \qquad \psi = \begin{cases} 18° = \theta \\ 12.7° \\ 0° \end{cases}$$

This list tells us that the physically tilted angle ϕ and the angle ψ are not linearly related, and that when $\phi = 90°$, then $\psi = 0°$. When the angle θ increases beyond 18°, the notch effect of the pattern in the x-y plane becomes evident, as indicated in Fig. 6.11.

6.7.4 Suggested method for reducing interference

Suppose that we would like to take advantage of this notch effect. From Fig. 6.13, we notice that the interfering site could cause interference at those cells within a 19° sector in front of the cell.

In an ideal situation such as that shown in Fig. 6.13, the antenna pattern of the serving cell must be rotated clockwise by 10° such that the notch can be aimed properly at the interfering cell. The antenna tilting angle θ may be between 22 to 24° in order to increase the carrier-to-interference ratio C/I by an additional 7 to 8 dB in the interfering cell as shown in Fig. 6.11. Now we can reduce cochannel interference by an additional 7 to 8 dB because of the notch in the

mechanically tilted-antenna pattern. Although signal coverage is rather weak in a small shaded area in the serving cell, as shown in Fig. 6.13, the use of sufficient transmitting power should correct this situation.

6.7.5 Cautions in tilting antennas

When a base-station antenna is tilted down mechanically or electronically by 10°, the strength of the received signal in the horizontal direction, as shown in Fig. 6.10, is decreased by 4 dB. But the strength of the received signal 1° below the horizontal is decreased by 3.5 dB—only 0.5 dB stronger than in the 0° case. This is a very important observation. For example, the elevation angle at the boundary of a 2-mi serving cell with a 100-ft antenna mast is about 0.5°. This means that the serving cell and the interfering cell are separated by only 0.5° at most. Then by tilting the antenna down by 10°, the interference by the interfering cell is reduced by an additional 0.25 dB. This is an insignificant improvement, yet the total power received is 4 dB less than in the no-tilt case. If the tilt is increased to 20°, the received power drops by 16 dB and the reduction in interference due to tilting the antenna is only 1 dB at the interfering cell (see Fig. 6.10). The justification for implementing the tilting antenna is that the new carrier-to-interference ratio ($\alpha C/\beta I$) after tilting is significantly higher than C/I before tilting, where α and β are those constants which can be expressed if the following expression holds.

$$\frac{\alpha C}{\beta I} \text{ (linear scale)} \Rightarrow \frac{C}{I} + (\alpha - \beta) \text{ (dB scale)}$$

In the above example, at a 10° tilt, $\alpha = 3.75$ dB and $\beta = 4$ dB, and the improved new carrier-to-interference ratio is $(C/I) + 0.25$ dB, which is an insignificant improvement. Therefore, the antenna vertical pattern and the antenna height play a major role in justifying antenna tilting. Some calculations are shown in Sec. 6.8.2. Sometimes, tilting the antenna upward may increase signal coverage if interference is not a problem.

6.8 Umbrella-Pattern Effect

The umbrella pattern can be achieved by use of a staggered discone antenna as discussed in Sec. 5.4.6. The umbrella pattern can be ap-

plied to reduce cochannel interference just as the downward tilted directional antenna pattern is. The umbrella pattern can be used for an omnidirectional pattern, but not for a directional antenna pattern. The tilted directional antenna pattern can create a notch after tilting 20° or more in front of the beam, but the umbrella pattern cannot.

Of most concern for future cellular systems is the long-distance interference due to tropospheric propagation as mentioned in Sec. 4.6. In the future, one system may experience long-distance interference resulting from other systems located approximately 320 km (200 mi) away. Cochannel interference, especially cross talk, could be a severe problem. Therefore, the umbrella pattern might be recommended for every cell site where interference prevails.

6.8.1 Elevation angle of long-distance propagation

The elevation of the tropospheric layer is 16 km (10 mi)[5] and the propagation distance is about 320 km (200 mi); thus, the angle of the wave propagating through the tropospheric layers is (see Fig. 6.14) roughly

$$\theta = \tan^{-1} \frac{10 \text{ mi}}{100 \text{ mi}} = 5.7°$$

It indicates that no strong power should be transmitted upward by 5° or more in order to avoid long-distance propagation.

6.8.2 Benefit of the umbrella pattern

The umbrella pattern, in which energy is confined to the immediate area of the antenna, is effective in reducing both cochannel and long-distance interference. Also, in hilly terrain areas there are many holes (weak signal spots). With a normal antenna pattern, we cannot raise the antenna high enough to cover these holes and decrease cochannel interference at the same time. However, the advantage of the umbrella pattern is that we can increase the antenna height and still decrease cochannel interference.

The frequency-reuse distance can be shortened by use of the umbrella pattern. To demonstrate this fact, we first calculate the two angles, one from the cell-site antenna to the cell boundary and the other from the cell-site antenna to the cochannel cell (the two angles are shown in Fig. 6.14).

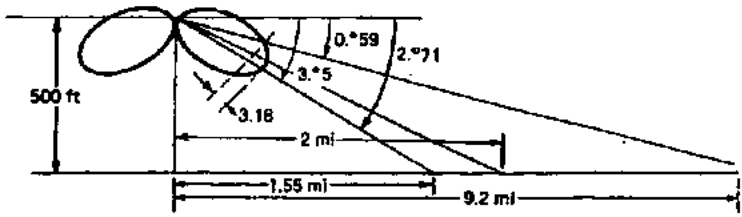

Figure 6.14 Coverage with the tilted-beam pattern.

Antenna height, ft	Desired maximum beam angle at boundary of a 2-mi cell, degrees	Angle toward cochannel cell at a distance of 4.6R (9.2 mi), degrees
100	0.54	0.12
300	1.63	0.35
500	2.71	0.59

Suppose that we are using an umbrella-pattern antenna with 11-dB gain,* and that the half-power beamwidth is above 5°. A tower of 500 ft is also used to cover a 2-mi cell. Then an approximate 3-dB difference due to the antenna pattern shown in Fig. 6.14 is obtained between the area at the maximum beam angle and the area at the angle reaching the cochannel cell.

$$\frac{R^{-4}}{6D^{-4}} = 18 \text{ dB} - 3 \text{ dB} = 15 \text{ dB}$$

$$q^4 = 6 \times 31.6 = 189.74$$

$$q = 3.7$$

where beam strengths in two regions are different by 3 dB. This demonstrates that the required frequency-reuse distance can be reduced. In other words, more protection against cochannel interference is possible with the use of an umbrella pattern than with an omnidirectional beam pattern.

6.9 Use of Parasitic Elements

Interference at the cell site can sometimes be reduced by using parasitic elements, creating a desired pattern in a certain direction. In

* Normally antenna gain is measured with respect to a dipole.

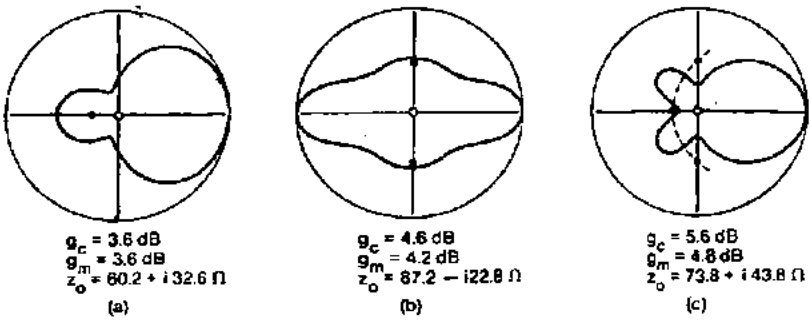

Figure 6.15 Parasitic elements with effective interference reduction. (*a*) One-quarter wavelength spacing; (*b*) one-half wavelength spacing; (c) combination of *a* and *b*. (*Reprint after Jasik, Ref. 6.*)

such instances, the currents appearing in several parasitic antennas are caused by radiation from a nearby drive antenna. A driven antenna and a single parasite can be combined in several ways.

1. *Normal spacing.*[6] We may first generate two separate patterns as shown in Fig. 6.15*a* and *b*. A single parasite spaced approximately one-quarter wavelength from the driven element is shown in Fig. 6.15*a*. Because the current flowing in the parasite is much weaker than that in the driven antenna, the front-to-back ratio is usually high. The two parasites spaced one-half wavelength from the driven element are shown in Fig. 6.15*b*. A combination of Fig. 6.15*a* and *b* forming a pattern very similar to that of a parabola dish is shown in Fig. 6.15c. This is an effective arrangement for cell-site directional antennas with a non-wind-resistant structure: a four-element structure that has only one active element.
2. *Relatively close spacing.*[7] In relatively close spacing two elements are placed as close as 0.04λ. Three cases can be described here.
   a. The lengths of two elements are identical. Two elements, one active and one parasitic, are separated by only 0.04λ. At this close spacing, the current flowing in the parasite is very strong. The two elements form a null along the *y* axis in the horizontal plane and along the *z* axis in the vertical plane. There is a directive gain of 3 dB relative to a single element. The horizontal pattern and the vertical pattern of the closely spaced arrangement are shown in Fig. 6.16*a*.
   b. The length of the parasite is 5 percent longer than that of the active one. In this case, the parasite acts as a reflector. The pat-

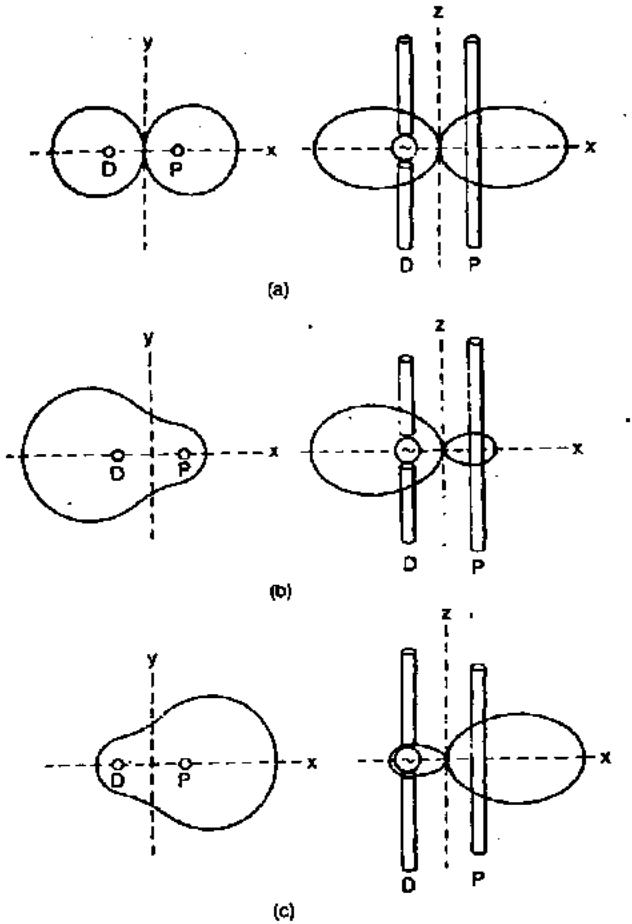

Figure 6.16 A close-in parasitic element with effective interference reduction (D = length of dipole; P = length of parasite). (*a*) $D = P$; (*b*) $D < P$; (*c*) $D > P$. (*Reprint after Jasik, Ref. 6.*)

terns are shown in Fig. 6.16*b* in both the horizontal and vertical planes. A directive gain of 6 dB is obtained.

c. *The length of the parasite is shorter than that of the active one.* In this case, the parasite acts as a director. The patterns are shown in Fig. 6.16c in the vertical and horizontal planes. A gain of 8 dB is obtained.

The pattern shown in Fig. 6.16*a* can be used for eliminating the interference to or from a given direction as shown by the

null in the y axis. Two elements can be set up such that the y axis is aligned with the direction of interference.

Besides, we should emphasize that a directive antenna can be structured by a single parasite with a single active element (Fig. 6.16*b* and *c*). Therefore, a corner reflector or a ground reflector is not needed.

6.10 Power Control

6.10.1 Who controls the power level

The power level can be controlled only by the mobile transmitting switching office (MTSO), not by the mobile units, and there can be only limited power control by the cell sites as a result of system limitations.

The reasons are as follows. The mobile transmitted power level assignment must be controlled by the MTSO or the cell site, not the mobile unit. Or, alternatively, the mobile unit can lower the power level but cannot arbitrarily increase it. This is because the MTSO is capable of monitoring the performance of the whole system and can increase or decrease the transmitted power level of those mobile units to render optimum performance. The MTSO will not optimize performance for any particular mobile unit unless a special arrangement is made.

6.10.2 Function of the MTSO

The MTSO controls the transmitted power levels at both the cell sites and the mobile units. The advantages of having the MSTO control the power levels are described in this section.

1. Control of the mobile transmitted power level. When the mobile unit is approaching the cell site, the mobile unit power level should be reduced for the following reasons.
   a. Reducing the chance of generating intermodulation products from a saturated receiving amplifier. This point is discussed in Chap. 7.
   b. Lowering the power level is equivalent to reducing the chance of interfering with other cochannel cell sites.
   c. Reducing the near-end–far-end interference ratio (see Sec. 7.3.1).

   Reducing the power level if possible is always the best strategy.
2. Control of the cell-site transmitted power level. When the signal received from the mobile unit at the cell site is very strong, the

MTSO should reduce the transmitted power level of that particular radio at the cell site and, at the same time, lower the transmitted power level at the mobile unit. The advantages are as follows.

a. For a particular radio channel, the cell size decreases significantly, the cochannel reuse distance increases, and the cochannel interference reduces further. In other words, cell size and cochannel interference are inversely proportional to cochannel reuse distance.

b. The adjacent channel interference in the system is also reduced.

However, in most cellular systems, it is not possible to reduce only one or a few channel power levels at the cell site because of the design limitation of the combiner. The channel isolation in the combiner is 18 dB. If the transmitted power level of one channel is lower, the channels having high transmitted power levels will interfere with this low-power channel. (The channel combiner is described in Chap. 7.) The manufacturer should design an unequal-power combiner for the system operator so that the power level of each channel can be controlled at the cell site.

3. The power transmitted from a small cell is always reduced, and so is that from a mobile unit. The MTSO can facilitate adjustment of the transmitted power of the mobile units as soon as they enter the cell boundary.

6.11 Diversity Receiver

The diversity scheme applied at the receiving end of the antenna is an effective technique for reducing interference because any measures taken at the receiving end to improve signal performance will not cause additional interference.

The diversity scheme is one of these approaches. We may use a selective combiner to combine two correlated signals as shown in Fig. 6.17. The performance of other kinds of combiners can be at most 2 dB better than that of selective combiners. However, the selective combining technique is the easiest scheme to use.[8]

Figure 6.17 shows a family of curves representing this selective combination. Each curve has an associated correlation coefficient ρ; when using the diversity scheme, the optimum result is obtained when $\rho = 0$.

We have found that at the cell site the correlation coefficient $\rho \leq 0.7$ should be used[9] for a two-branch space diversity; with this coefficient the separation of two antennas at the cell site meets the requirement of $h/d = 11$, where h is the antenna height and d is the antenna separation.

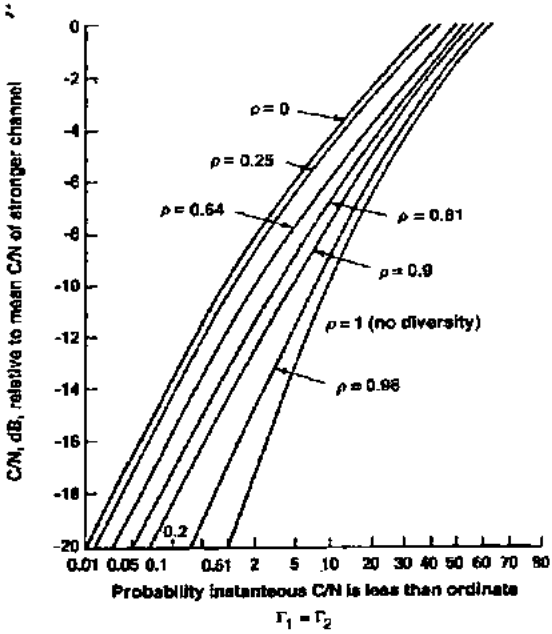

Figure 6.17 Selective combining of two correlated signals.

At the mobile unit we can use $\rho = 0$, which implies that the two roof-mounted antennas of the mobile unit are 0.5λ or more apart. This is verified by the measured data shown in Fig. 6.18.[10]

Now we may estimate the advantage of using diversity. First, let us assume a threshold level of 10 dB below the average power level. Then

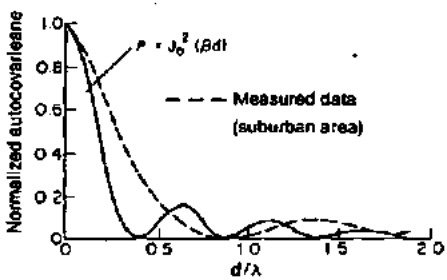

Figure 6.18 Autocorrelation coefficient versus spacing for uniform angular distribution (applied to diversity receiver). (*Reprint after Lee, Ref. 10.*)

we compare the percent of signal below the threshold level both with and without a diversity scheme.

1. *At the mobile unit.* The comparison is between curves $\rho = 0$ and the $\rho = 1$. The signal below the threshold level is 10 percent for no diversity and 1 percent for diversity. If the signal without diversity were 1 percent below the threshold, the power would be increased by 10 dB (see Fig. 6.17). In other words, if the diversity scheme is used, the power can be reduced by 10 dB and the same performance can be obtained as in the nondiversity scheme. With 10 dB less power transmitted at the cell site, cochannel interference can be drastically reduced.

2. *At the cell site.* The comparison is between curves of $\rho = 0.7$ and $\rho = 1$. We use curve $\rho = 0.64$ for a close approximation as shown in Fig. 6.17. The difference is 10 percent of the signal is below threshold level when a nondiversity scheme is used versus 2 percent signal below threshold level when a diversity scheme is used. If the nondiversity signal were 2 percent below the threshold, the power would have to increase by 7 dB (see Fig. 6.17). Therefore, the mobile transmitter (for a cell-site diversity receiver) could undergo a 7-dB reduction in power and attain the same performance as a nondiversity receiver at the cell site. Thus, interference from the mobile transmitters to the cell-site receivers can be drastically reduced.

6.12 Designing a System to Serve a Predefined Area that Experiences Cochannel Interference

A system for a service area wthout cochannel interference can be designed by using the propagation prediction model described in Chap. 4. When cochannel interference does exist, the service in the area will deteriorate to one degree or another, depending on the location of the interference (or interferers). First, let us assume that the ground is flat; then two theoretical equations for designing a system in a given service area can be derived for two different interference cases. Then the same approach can be used to design the systems for a service area where the ground is not flat.

Flat ground

One-interferer case. An interferer (cochannel site) is a distance d away from the serving cell site, and the mobile unit is traveling along the boundary of the serving-cell coverage. When the interferer is inactive, the coverage boundary is at a distance R from the serving site. When

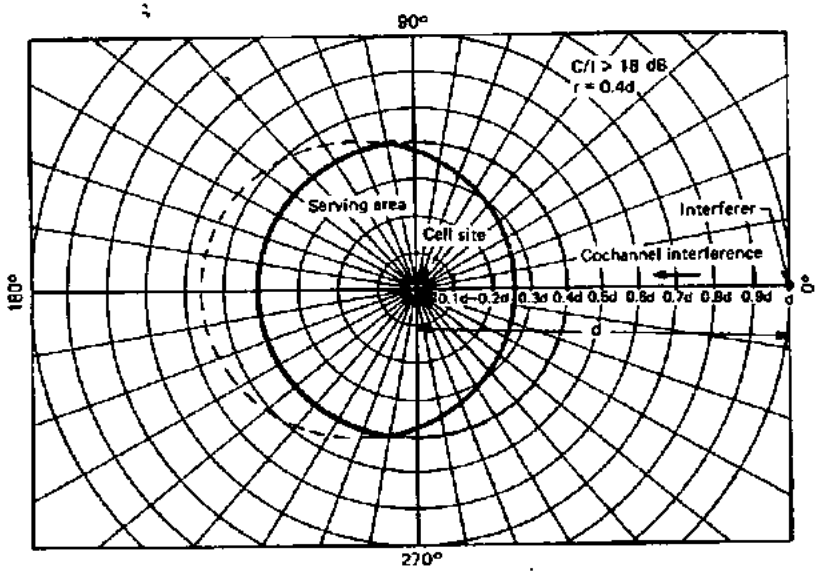

Figure 6.19 Serving area under cochannel interference.

the interferer becomes active, the distance from the serving site to the effective coverage boundary is r, which can be less than R if the interference is either strong or close to the serving site or both. If we use polar coordinates, the serving site is located at (0, 0) with a transmitted power P_0, and the interferer is located at (d, θ_1) with a transmitted power P_1.

The mobile unit is located at $(r, 0)$, where r can be equal to or less than R. Assume the carrier-to-interference ratio requirement is C/I, then

$$\frac{C}{I} \leq \frac{P_0 r^{-4}}{P_1[\sqrt{r^2 + d^2 - 2rd\cos(\theta - \theta_1)}]^{-4}} \qquad r \leq R \qquad (6.12\text{-}1)$$

Let $\theta_1 = 0$ without loss of generality, as shown in Fig. 6.19 as "interferer," and $P_0 = P_1$, then

$$\frac{C}{I} \leq \left(1 + \frac{d^2}{r^2} - \frac{2d}{r}\cos\theta\right)^2 \qquad (6.12\text{-}2)$$

When $r = R$, there is no interference. Then Eq. (6.12-2) becomes

$$\frac{C}{I} \leq \left(1 + \frac{d^2}{R^2} - \frac{2d}{R}\cos\theta\right)^2 \qquad (6.12\text{-}3)$$

Let $\theta = 0$, the strongest interference condition and $C/I = 18$ dB; then Eq. (6.12-3) becomes

$$63 \leq \left(1 - \frac{d}{R}\right)^4$$

or

$$d \geq 3.82R \tag{6.12-4}$$

When $r < d/3.82$, the serving area starts to decrease. Equation (6.12-2) can be converted to rectangular coordinates.

$$\frac{C}{I} \leq \left(1 + \frac{d^2}{x^2 + y^2} - \frac{2dx}{x^2 + y^2}\right)^2$$

or

$$\left(x + \frac{d}{\sqrt{C/I} - 1}\right)^2 + y^2 = d^2\left(\frac{1}{\sqrt{C/I} - 1} + \frac{1}{(\sqrt{C/I} - 1)^2}\right) \tag{6.12-5}$$

where $x^2 + y^2 \leq R^2$, the serving area has its center at $(-d/\sqrt{C/I} - 1, 0)$, and the radius is $d(C/I)^{1/4}/(\sqrt{C/I} - 1)$. An illustration of Eq. (6.12-5) is shown in Fig. 6.19 as the boundary area.

Multiple-interference case. For K_I interferers, Eq. (6.12-1) can be modified as

$$\frac{C}{I} = \frac{P_0 r^{-4}}{\sum_{i=1}^{K_I} P_i \left[\sqrt{r^2 + d^2 - 2rd\cos(\theta - \theta_i)}\right]^{-4}}$$

$$K_I \leq 6, r \leq R \tag{6.12-6}$$

Nonflat ground

The same approach is applied to the propagation model described in Chap. 4 in a real environment for predicting the serving areas.

References

1. W. C. Y. Lee, "Elements of Cellular Mobile Radio Systems," *IEEE Transactions on Vehicular Technology*, Vol. 35, May 1986, pp. 48–56.
2. S. Kozono and M. Sakamoto, "Channel Interference Measurement in Mobile Radio Systems," *Proceedings of the 35th IEEE Vehicular Technology Conference*, Boulder, Colorado, May 21–23, 1985, pp. 60–66.
3. W. C. Y. Lee, *Mobile Communications Design Fundamentals*, Howard W. Sams & Co., 1986, Chap. 4.

4. W. C. Y. Lee, "Cellular Mobile Radiotelephone System Using Tilted Antenna Radiation Pattern," U.S. Patent 4,249,181, February 3, 1981.
5. K. Bullington, "Radio Propagation Fundamentals," *Bell System Technical Journal*, Vol. 36, 1957, pp. 593–626.
6. H. Jasik (Ed.) *Antenna Engineering Handbook*, McGraw-Hill Book Co., 1961, pp. 5–7.
7. A. B. Bailey, *TV and Other Receiving Antenna*, John Francis, Inc., New York, 1950.
8. D. G. Brennan, "Linear Diversity Combining Techniques," *Proceedings of the IRE*, Vol. 47, June 1959, pp. 1075–1102.
9. W. C. Y. Lee, "Mobile Radio Signal Correlation Versus Antenna Height and Spacing," *IEEE Transactions on Vehicular Technology*, Vol. 25, August 1977, pp. 290–292.
10. W. C. Y. Lee, *Mobile Communications Design Fundamentals*, Howard W. Sams & Co., 1986, p. 222.